A Statistical Mechanics Perspective on Glasses and Aging

Francesco Arceri[1], François P. Landes[2],
Ludovic Berthier[3,4] and Giulio Biroli[5]
[1]Department of Physics, University of Oregon,
Eugene, OR, USA
[2]TAU, LRI, Université Paris Sud, CNRS, INRIA,
Université Paris Saclay, Orsay, France
[3]Laboratoire Charles Coulomb (L2C), Université
de Montpellier, CNRS, Montpellier, France
[4]Department of Chemistry, University of
Cambridge, Cambridge, UK
[5]Laboratoire de Physique de l'École normale
supérieure, Université PSL, CNRS, Sorbonne
Université, Université Paris-Diderot, Paris,
France

Article Outline

Glossary

We start with a few concise definitions of the most important concepts discussed in this entry.

Glass transition For molecular liquids, the glass transition denotes a crossover from a viscous liquid to an amorphous solid. Experimentally, the crossover takes place at the glass temperature, T_g, conventionally defined as the temperature where the liquid's viscosity reaches the arbitrary value of 10^{12} Pa.s. The glass transition more generally applies to many different condensed matter systems where a crossover or, less frequently, a true phase transition takes place between an ergodic phase and a frozen, amorphous glassy phase.

Aging In the glass phase, disordered materials are characterized by relaxation times that exceed common observation timescales, so that a material quenched in its glass phase never reaches equilibrium (neither a metastable equilibrium). It exhibits instead an aging behavior during which its physical properties keep evolving with time.

Dynamic heterogeneity Relaxation spectra of dynamical observables, for example, the dynamical structure factor, are very broad in supercooled liquids. This is associated to a spatial distribution of timescales: at any given time, different regions in the liquid relax at different rates. Since the supercooled liquid is ergodic, slow regions eventually become fast, and vice versa. Dynamic heterogeneity refers to the existence of these nontrivial spatiotemporal fluctuations in the local dynamical behavior, a phenomenon observed in virtually all disordered systems with slow dynamics.

Effective temperature An aging material relaxes very slowly, trying (in vain) to reach its equilibrium state. During this process, the system probes states that do not correspond to thermodynamic equilibrium, so that its thermodynamic properties cannot be rigorously defined. Any practical measurement of its temperature becomes a frequency-dependent operation. A "slow" thermometer tuned to the relaxation timescale of the aging system measures an effective temperature corresponding to the ratio between spontaneous fluctuations (correlation) and linear response (susceptibility). This corresponds to a generalized form of the fluctuation-dissipation theorem for off-equilibrium materials.

Frustration Impossibility of simultaneously minimizing all the interaction terms in the energy function of the system. Frustration might arise from quenched disorder (as in the spin glass models), from competing interactions (as in geometrically frustrated magnets), or from competition between a "locally preferred order," and global, for example, geometric, constraints (as in hard spheres packing problems).

Marginal Stability Systems are marginally stable when the number of external inputs controlling their stability is just enough to constrain all their degrees of freedom (think of a table with three legs). Marginally stable systems display an excess of zero-energy modes which makes them highly susceptible to external perturbations, and prone to extensive rearrangements.

Definition of the Subject

Glasses belong to a seemingly well-known state of matter: we easily design glasses with desired mechanical or optical properties on an industrial scale, and they are widely present in our daily life. Yet, a deep microscopic understanding of the glassy state of matter remains a challenge for condensed matter physicists (Angell 1995; Debenedetti and Stillinger 2001; Berthier and Biroli 2011). Glasses share similarities with crystalline solids (they are both mechanically rigid), but also with liquids (they both have similar disordered structures at the molecular level). It is mainly this mixed character that makes them fascinating objects, even to nonscientists.

A glass can be obtained by cooling the temperature of a liquid below its glass temperature, T_g. The quench must be fast enough, such that the more standard first-order phase transition toward the crystalline phase is avoided. The glass "transition" is not a thermodynamic transition at all, since T_g is only empirically defined as the temperature below which the material has become too viscous to flow on a "reasonable" timescale (and it is hard to define the word "reasonable" in any reasonable manner). Therefore, T_g cannot play a

very fundamental role, as a phase transition temperature would. It is simply the temperature below which the material looks solid on the timescale of the observer. When quenched in the glass phase below T_g, liquids slowly evolve toward an equilibrium state they will never reach on experimental timescales. Physical properties are then found to evolve slowly with time in far from equilibrium states, a process known as "aging" (Struik 1977).

Describing theoretically and quantifying experimentally the physical mechanisms responsible for the viscosity increase of liquids approaching the glass transition and for aging phenomena below the glass transition certainly stand as central open challenges in condensed matter physics. Since statistical mechanics aims at understanding the collective behavior of large assemblies of interacting objects, it comes as no surprise that it is a central tool in the glass field. We shall therefore summarize the understanding gained from statistical mechanics perspectives into the problem of glasses and aging.

The subject has quite broad implications. A material is said to be "glassy" when its typical relaxation timescale becomes of the order of, and often much larger than, the typical duration of an experiment or a numerical simulation. Under this generic definition, a large number of systems can be considered as glassy (Young 1998). One can be interested in the physics of liquids (window glasses are then the archetype), in "hard" condensed matter (for instance type II superconductors in the presence of disorder such as high-T_c superconductors), charge density waves or spin glasses, "soft" condensed matter with numerous complex fluids such as colloidal assemblies, emulsions, foams, but also granular materials, proteins, etc. All these materials exhibit, in a part of their phase diagrams, some sort of glassy dynamics characterized by a very rich phenomenology with effects such as aging, hysteresis, creep, memory, effective temperatures, rejuvenation, dynamic heterogeneity, and nonlinear response.

This long list explains why this research field has received increasing attention from physicists in the last four decades. "Glassy" topics now go much beyond the physics of simple liquids (glass

transition physics), and models and concepts developed for one system often find applications elsewhere in physics, from algorithmics to biophysics (Bouchaud et al. 2011). Motivations to study glassy materials are numerous. Glassy materials are everywhere around us and therefore obviously attract interest beyond academic research. At the same time, the glass conundrum provides theoretical physicists with deep fundamental questions since classical tools are sometimes not sufficient to properly account for the glass state. Moreover, numerically simulating the dynamics of microscopically realistic material on timescales that are experimentally relevant remains a difficult challenge, even with modern computers.

Studies on glassy materials constitute an exciting research area where experiments, simulations, and theoretical calculations can meet, and where both applied and fundamental problems are considered. How can one observe, understand, and theoretically describe the rich phenomenology of glassy materials? What are the fundamental quantities and concepts that emerge from these descriptions?

The outline of the entry is as follows. In section "Phenomenology" the phenomenology of glass-forming liquids is discussed. In section "Taxonomy of "Glasses" in Science" different types of glasses are described. We then describe how computer simulations can provide deep insights into the glass problem in section "Numerical Simulations." The issue of dynamic heterogeneity is tackled in section "Dynamic Heterogeneity." The main theoretical perspectives currently available in the field are then summarized in section "Theory of the Glass Transition." The mean-field analysis of the amorphous solid phase is reviewed in section "Mean-Field Theory of the Amorphous Phase." In section "New Computational Methods," we discuss novel developments in computational studies. Aging and off-equilibrium phenomena occupy section "Aging and Off-Equilibrium Dynamics." Finally, issues that seem important for future research are discussed in section "Future Directions."

Phenomenology

Basic Facts

A vast majority of liquids (molecular liquids, polymeric liquids, etc.) form a glass if cooled fast enough in order to avoid the crystallization transition (Angell 1995). Typical values of cooling rate in laboratory experiments are 0.1–100 K/min. The metastable phase reached in this way is called "supercooled liquid." In this regime the typical timescales increase in a dramatic way and they end up to be many orders of magnitudes larger than microscopic timescales at T_g, the glass transition temperature.

For example, around the melting temperature T_m, the typical timescale T_α on which density fluctuations relax is of the order of $\sqrt{ma^2/K_B T}$, which corresponds to few picoseconds (m is the molecular mass, T the temperature, K_b the Boltzmann constant, and a is a typical distance between molecules). At T_g, which as a rule of thumb is about $\frac{2}{3}T_m$, this timescale τ_α has become of the order of 100 s, that is, 14 orders of magnitude larger! This phenomenon is accompanied by a concomitant increase of the shear viscosity η. This can be understood by a simple Maxwell model in which η and τ are related by $\eta = G_\infty \tau_\alpha$, where G_∞ is the instantaneous (elastic) shear modulus which does not vary considerably in the supercooled regime. In fact, viscosities at the glass transition temperature are of the order of 10^{12} Pa.s. In order to grasp how viscous this is, recall that the typical viscosity of water (or wine) at ambient temperature is of the order of 10^{-2} Pa.s. How long would one have to wait to drink a glass of wine with a viscosity 10^{14} times larger?

As a matter of fact, the temperature at which the liquid does not flow anymore and becomes an amorphous solid, called a "glass," is protocol dependent. It depends on the cooling rate and on the patience of the person carrying out the experiment: solidity is a timescale-dependent notion. Pragmatically, T_g is defined as the temperature at which the shear viscosity is equal to 10^{13} Poise (also 10^{12} Pa.s).

The increase of the relaxation timescale of supercooled liquids is remarkable not only because of the large number of decades involved but also because of its temperature dependence. This is vividly demonstrated by plotting the logarithm of the viscosity (or of the relaxation time) as a function of T_g/T, as in Fig. 1. This is called the "Angell" plot (Angell 1995), which is very helpful in classifying supercooled liquids. A liquid is called strong or fragile depending on its position in the Angell plot. Straight lines correspond to "strong" glass-formers and to an Arrhenius behavior. In this case, one can extract from the plot an effective activation energy, suggesting quite a simple mechanism for relaxation, for instance by "breaking" locally a chemical bond. The typical relaxation time is then dominated by the energy barrier to activate this process and, hence, has an Arrhenius behavior. Window glasses fall in this category. (The terminology "strong" and "fragile" is not related to the mechanical properties of the glass but to the evolution of the short-range order close to T_g. Strong liquids, such as SiO_2, have a locally tetrahedric structure which persists both below and above the glass transition contrary to fragile liquids whose short-range amorphous structure disappears rapidly upon heating above T_g.) If one tries to define an effective activation energy for fragile glass-formers using the slope of the curve in Fig. 1, then one finds that this energy scale increases when the temperature decreases, a "super-Arrhenius" behavior. This increase of energy barriers immediately suggests that glass formation is a collective phenomenon for fragile supercooled liquids. Support for this interpretation is provided by the fact that a good fit of the relaxation time or the viscosity is given by the Vogel-Fulcher-Tamman law (VFT):

$$\tau_\alpha = \tau_0 \exp\left[\frac{DT_0}{(T - T_0)}\right], \qquad (1)$$

which suggests a divergence of the relaxation time, and therefore a phase transition of some kind, at a finite temperature T_0. A smaller D in the VFT law corresponds to a more fragile glass. Note that there are other comparably good fits of
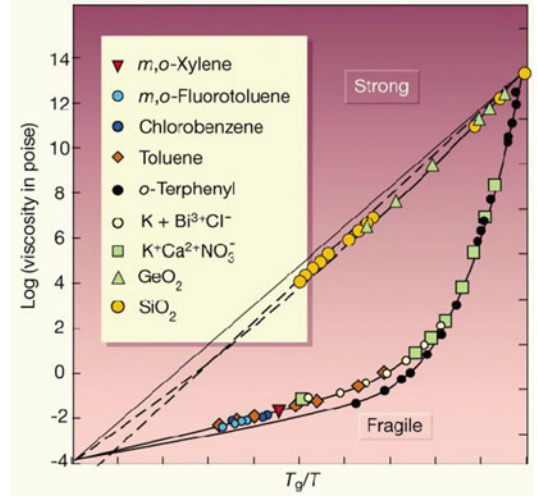
A Statistical Mechanics Perspective on Glasses and Aging, Fig. 1 Arrhenius plot of the viscosity of several glass-forming liquids approaching the glass temperature T_g (Debenedetti and Stillinger 2001). For "strong" glasses, the viscosity increases in an Arrhenius manner as temperature is decreased, $\log \eta \sim E/(K_B T)$, where E is an activation energy and the plot is a straight line, as for silica. For "fragile" liquids, the plot is bent and the effective activation energy increases when T is decreased toward T_g, as for ortho-terphenyl

these curves, such as the Bässler law (Bässler 1987),

$$\tau_\alpha = \tau_0 \exp\left(K\left(\frac{T_*}{T}\right)^2\right), \qquad (2)$$

that only lead to a divergence at zero temperature. Actually, although the relaxation time increases by 14 orders of magnitude, the increase of its logarithm, and therefore of the effective activation energy is very modest, and experimental data do not allow one to unambiguously determine the true underlying functional law without any reasonable doubt. For this and other reasons, physical interpretations in terms of a finite temperature phase transition must always be taken with a grain of salt.

However, there are other experimental facts that shed some light and reinforce this interpretation. Among them is an empirical connection found between kinetic and thermodynamic behaviors. Consider the part of the entropy of liquids,

A Statistical Mechanics Perspective on Glasses and Aging, Table 1 Values of glass transition temperature, VFT singularity and Kauzmann temperatures for four supercooled liquids (Richert and Angell 1998)

Substance	o-terphenyl	2-methyltetra-hydrofuran	n-propanol	3-bromopentane
T_g	246	91	97	108
T_0	202.4	69.6	70.2	82.9
T_K	204.2	69.3	72.2	82.5
T_K/T_0	1.009	0.996	1.028	0.995

S_{exc}, which is in excess compared to the entropy of the corresponding crystal. Once this quantity, normalized by its value at the melting temperature, is plotted as a function of T, a remarkable connection with the dynamics emerges. As for the relaxation time one cannot follow this curve below T_g in thermal equilibrium. However, extrapolating the curve below T_g apparently indicates that the excess entropy vanishes at some finite temperature, called T_K, which is very close to zero for strong glasses and, generically, very close to T_0, the temperature at which a VFT fit diverges. This coincidence is quite remarkable: for materials with glass transition temperatures that vary from 50 K to 1000 K the ratio T_K/T_0 remains close to 1, up to a few percent. Examples reported in Richert and Angell (1998) are provided in Table 1.

The chosen subscript for T_K stands for Kauzmann (1948), who recognized T_K as an important temperature scale for glasses. Kauzmann further claimed that some change of behavior (phase transition, crystal nucleation, etc.) must take place above T_K, because below T_K the entropy of the liquid, a disordered state of matter, becomes less than the entropy of the crystal, an ordered state of matter. The situation that seemed paradoxical at that time is actually not a serious conceptual problem (Berthier and Biroli 2011; Berthier et al. 2019a). There is no general principle that constrains the entropy of the liquid to be larger than that of the crystal. As a matter of fact, the crystallization transition for hard spheres takes place precisely because the crystal becomes the state with the largest entropy at sufficiently high density (Hołyst 2001).

On the other hand, the importance of T_K stands, partially because it is experimentally very close to T_0. Additionally, the quantity S_{exc} which vanishes at T_K is thought to be a proxy for the so-called configurational entropy, S_c, which quantifies the number of metastable states. A popular physical picture due to Goldstein (1969) is that close to T_g the system explores a part of the energy landscape (or configuration space) which is full of minima separated by barriers that increase when temperature decreases. The dynamic evolution in the energy landscape would then consist in a rather short equilibration inside a minimum followed by infrequent "jumps" between different minima. At T_g the barriers between states become so large that the system remains trapped in one minimum, identified as one of the possible microscopic amorphous configurations of a glass. Following this interpretation, one can split the entropy into two parts. A first contribution is due to the fast relaxation inside one minimum and a second one, called the "configurational" entropy, counts the number of metastable states: $S_c = \log N_{\text{metastable}}$. Assuming that the contribution to the entropy due to the "vibrations" around an amorphous glass configuration is not very different from the entropy of the crystal, one finds that $S_{\text{exc}} \approx S_c$. In that case, T_K would correspond to a temperature at which the configurational entropy vanishes. This in turn would lead to a discontinuity (a downward jump) of the specific heat and would truly correspond to a thermodynamic phase transition.

Static and Dynamic Correlation Functions

At this point the reader might have reached the conclusion that the glass transition may not be such a difficult problem: there are experimental indications of a diverging timescale and a concomitant singularity in the thermodynamics. It simply remains to find static correlation functions displaying a diverging correlation length related to the emergence of "amorphous order," which would indeed classify the glass transition as a

standard second-order phase transition. Remarkably, this conclusion remains an open and debated question despite several decades of research. Simple static correlation functions are quite featureless in the supercooled regime, notwithstanding the dramatic changes in the dynamics. A simple static quantity is the structure factor defined by

$$S(q) = \left\langle \frac{1}{N} \delta\rho_{\mathbf{q}} \delta\rho_{-\mathbf{q}} \right\rangle, \qquad (3)$$

where the Fourier component of the density reads

$$\delta\rho_{\mathbf{q}} = \sum_{i=1}^{N} e^{i\mathbf{q}\cdot\mathbf{r}_i} - \frac{N}{V}\delta_{\mathbf{q},0}, \qquad (4)$$

with N the number of particles, V the volume, and $\mathbf{r}_i$ the position of particle i. The structure factor measures the spatial correlations of particle positions, but it does not show any diverging peak in contrast to what happens, for example, at the liquid-gas critical point where there is a divergence at small $\mathbf{q}$. More complicated static correlation functions have been studied (Debenedetti 1996), especially in numerical work, but until now there are no strong indications of a diverging, or at least substantially growing, static lengthscale (Menon and Nagel 1995; Fernández et al. 2006; Cavagna et al. 2007). A snapshot of a supercooled liquid configuration in fact just looks like a glass configuration, despite their widely different dynamic properties (Berthier et al. 2019a). What happens then at the glass transition? Is it a transition or simply a dynamic crossover? A more refined understanding can be gained by studying dynamic correlations or response functions.

A dynamic observable studied in light and neutron scattering experiments is the intermediate scattering function,

$$F(\mathbf{q}, t) = \left\langle \frac{1}{N} \delta\rho_{\mathbf{q}}(t) \delta\rho_{-\mathbf{q}}(0) \right\rangle. \qquad (5)$$

Different $F(\mathbf{q}, t)$ measured by neutron scattering in supercooled glycerol (Wuttke et al. 1996) are shown for different temperatures in Fig. 2. These curves show a first, rather fast, relaxation to a plateau followed by a second, much slower,
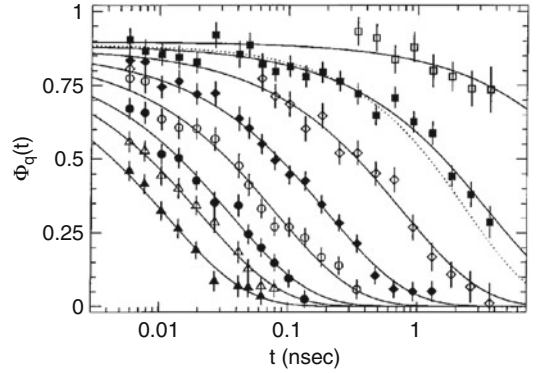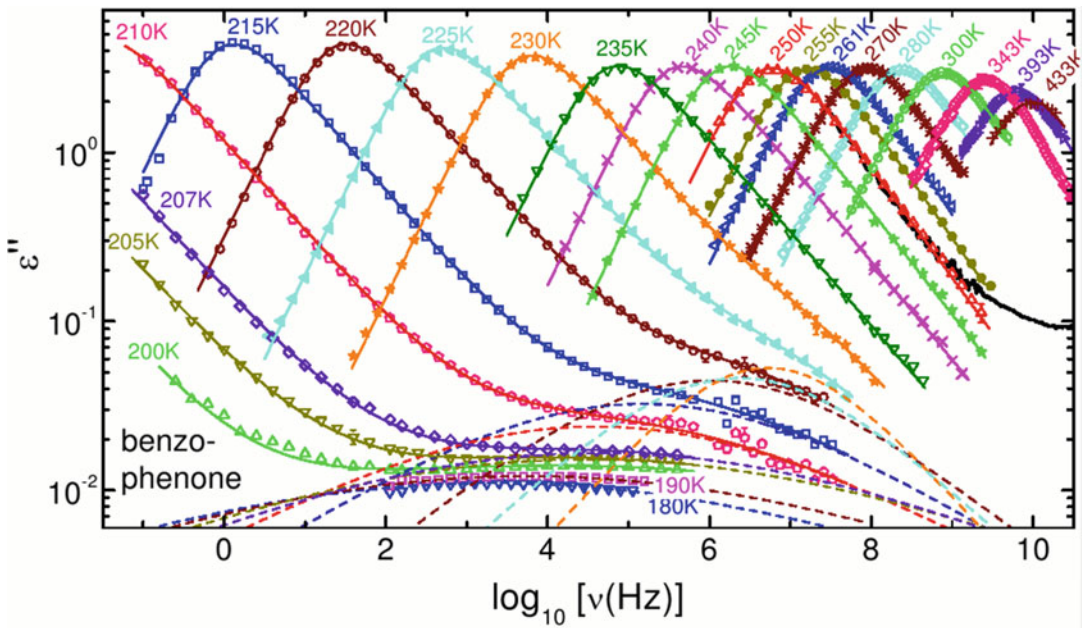

A Statistical Mechanics Perspective on Glasses and Aging, Fig. 2 Temperature evolution of the intermediate scattering function normalized by its value at time equal to zero for supercooled glycerol (Wuttke et al. 1996). Temperatures decrease from 413 K to 270 K from right to left. The solid lines are fit with a stretched exponential with exponent $\beta = 0.7$. The dotted line represents another fit with $\beta = 0.82$

relaxation. The plateau is due to the fraction of density fluctuations that are frozen on intermediate timescales, but eventually relax during the second relaxation. The latter is called "alpha-relaxation," and corresponds to the structural relaxation of the liquid. This plateau is akin to the Edwards-Anderson order parameter q_{EA} defined for spin glasses, which measures the fraction of frozen spin fluctuations (Binder and Kob 2011). Note that q_{EA} continuously increases from zero at the spin glass transition. Instead, for structural glasses, a finite plateau value already appears above any transition.

The intermediate scattering function can be probed only on a relatively small regime of temperatures. In order to track the dynamic slowing down from microscopic to macroscopic timescales, other correlators have been studied. A popular one is obtained from the dielectric susceptibility, which is related by the fluctuation-dissipation theorem to the time correlation of polarization fluctuations. It is generally admitted that different dynamic probes reveal similar temperature dependencies of the relaxation time. The temperature evolution of the imaginary part of the dielectric susceptibility, $\epsilon''(\omega)$, is shown in Fig. 3, which covers a very wide temperature window (Pardo et al. 2007). At high temperature, a good

A Statistical Mechanics Perspective on Glasses and Aging, Fig. 3 Temperature evolution of the dielectric susceptibility of the glass-former benzophenone measured over more than 10 decades of relaxation times (Pardo et al. 2007). Dynamics slows down dramatically as temperature is decreased and relaxation spectra become very broad at low temperature

representation of the data is given by a Debye law, $\epsilon(\omega) = \epsilon(\infty) + \Delta\epsilon/(1 + i\omega\tau_\alpha)$, which corresponds to an exponential relaxation in the time domain. When temperature is decreased, however, the relaxation spectra become very broad and strongly non-Debye. One particularly well-known feature of the spectra is that they are well fitted, in the time domain, for times corresponding to the alpha relaxation with a stretched exponential, $\exp(-(t/\tau_\alpha)^\beta)$. In the Fourier domain, forms such as the Havriliak-Negami law are used, $\epsilon(\omega) = \epsilon(\infty) + \Delta\epsilon/(1 + (i\omega\tau_\alpha)^\alpha)^\gamma$, which generalize the Debye law. The exponents β, α, and γ depend in general on temperature and on the particular dynamic probe chosen, but they capture the fact that relaxation is increasingly non-exponential when T decreases toward T_g. A connection was empirically established between fragility and degree of non-exponentiality, more fragile liquids being characterized by broader relaxation spectra (Debenedetti and Stillinger 2001).

To sum up, there are many remarkable phenomena that take place when a supercooled liquid approaches the glass transition. Striking ones have been presented, but many others have been left out for lack of space (Angell 1995; Debenedetti and Stillinger 2001; Debenedetti 1996; Binder and Kob 2011; Berthier and Ediger 2016). We have discussed physical behaviors, relationships, or empirical correlations observed in a broad class of materials. This is quite remarkable and suggests that there is some physics (and not only chemistry) to the problem of the glass transition, which we see as a collective (critical?) phenomenon which should be relatively independent of microscopic details. This justifies our statistical mechanics perspective on this problem.

Taxonomy of "Glasses" in Science

We now introduce a wider range of systems whose phenomenological behavior is close or related to the one of glass-forming liquids, showing that

glassiness is truly ubiquitous. It does not only appear in many different physical situations but also in more abstract contexts, such as computer science.

Colloidal Glass Transition

Colloidal suspensions consist of large particles suspended in a solvent (Larson 1999). The typical radii of the particles are in the range of $R = 1$–500 nm. The solvent, which is at equilibrium at temperature T, renders the short-time dynamics of the particles Brownian. The microscopic timescale for this diffusion is given by $\tau = R^2/D$, where D is the short-time self-diffusion coefficient. A typical value is of the order of $\tau \sim 1$ ms, which is thus much larger than microscopic timescales for molecular liquids (in the picosecond regime). The interaction potential between particles depends on the systems, and this large tunability makes colloids very attractive objects for technical applications. A particularly relevant case, on which we will focus in the following, is a purely hard sphere potential, which is zero when particles do not overlap and infinite otherwise. In this case the temperature scale becomes an irrelevant number, apart from a trivial rescaling of the microscopic timescale. Colloidal hard sphere systems have been intensively studied (Larson 1999) in experiments, simulations, and theory, varying their density ρ, or their volume fraction $\varphi = \frac{4}{3}\pi R^3 \rho$. Hard spheres display a fluid phase from $\varphi = 0$ to intermediate volume fractions, a freezing-crystallization transition at $\varphi \simeq 0.494$, and a melting transition at $\varphi \simeq 0.545$. Above this latter value the system can be compressed until the close packing point $\varphi \simeq 0.74$, which corresponds to the FCC crystal. Interestingly for our purposes, a small amount of size polydispersity can suppress crystallization. In this case, the system can be "supercompressed" above the freezing transition without nucleating the crystal, at least on experimental timescales. In this regime the relaxation timescale increases very fast (Pusey and VanMegen 1986). At a packing fraction $\varphi_g \simeq 0.58 - 0.60$ it becomes so large compared to typical experimental timescales that the system does not relax anymore: it is frozen. This "colloidal glass transition" is obviously reminiscent of the glass transition of molecular systems. In particular, the location φ_g of the colloidal glass transition is as ill-defined as the glass temperature T_g.

Actually, the phenomena that take place when increasing the volume fraction are analogous to the ones seen in molecular supercooled liquid when decreasing temperature: the relaxation timescales increases very fast and can be fitted (Cheng et al. 2002; Berthier and Witten 2009) by a VFT law in density similar to Eq. (1), dynamical correlation functions display a broad spectrum of timescales and develop a plateau, no static growing correlation length has been found, etc. Also the phenomenon of dynamic heterogeneity that will be addressed in section "Dynamic Heterogeneity" is also observed in colloids (Kegel and van Blaaderen 2000; Weeks et al. 2000). However, it is important to underline a major difference: because the microscopic timescale for colloids is so large, experiments can only track the first five decades of slowing down. A major consequence is that the comparison between the glass and colloidal transitions must be performed by focusing in both cases on the first five decades of the slowing down, which corresponds to relatively high temperatures in molecular liquids (Brambilla et al. 2009). Understanding how much and to what extent the glassiness of colloidal suspensions is related to the one of molecular liquids remains an active domain of research. Recently, by using colloids of smaller size and hence decreasing the microscopic timescale τ, it has been possible to explore a larger range of relaxation times (Hallett et al. 2018). This is a very promising research direction to explore the colloidal glassy regime.

Jamming Transition

Every day life offers many examples of jammed solids: grains and beans poured into a container, foams and emulsions produced by a large shear stress, sand and colloidal particles under very high pressure. Depending on how compressed they are, these materials behave as fluids or solids: a handful of sand will flow from our open hand, while we experience rigidity when closing the fist. Formally, the jamming transition is reached at infinite pressure when all the droplets, bubbles, or colloids are forced to come into enduring kissing

contact with one another (Donev et al. 2004, 2005). All these systems share a fundamental feature: they can be considered athermal in the sense that thermal fluctuations at room temperature are, by far, not able to allow the system to explore its phase space.

As an immediate consequence, the glass and jamming transitions are of a very different nature. The former describes a fluid-to-solid transition in a system controlled by thermal fluctuations, and its location depends on the cooling or compression rate. The latter is a purely geometrical transition happening at $T = 0$ in the absence of any dynamics, but it also corresponds to the change between a viscous liquid to a solid mechanical response (Liu and Nagel 1998). In recent years, the connection between the two phenomena has been elucidated (Charbonneau et al. 2017), and both transitions can be observed under different physical conditions in the hard spheres model.

Granular Glass Transition

Driven granular media represent another family of systems that have recently been studied from the point of view of their glassiness. Grains are macroscopic objects and, as a consequence, are not affected by thermal fluctuations. A granular material is therefore frozen in a given configuration if no energy is injected into the system (Jaeger et al. 1996). However, it can be forced in a steady state by an external drive, such as shearing or tapping. The dynamics in this steady state shows remarkable similarities (and differences) with simple fluids. The physics of granular materials is a very wide subject (Jaeger et al. 1996). In the following we only address briefly what happens to a polydisperse granular fluid at very high packing fractions. As for colloids, the timescales for relaxation or diffusion increase very fast when density is increased, without any noticeable change in structural properties. It is now established (D'Anna and Grémaud 2001; Marty and Dauchot 2005; Keys et al. 2007) that many phenomenological properties of the glass and jamming transitions also occur in granular assemblies. Going beyond the mere analogy and understanding how much colloids and granular materials are related is a very active domain of research.

Active Glasses

Active matter has recently emerged as a new field in physics (Marchetti et al. 2013; Bechinger et al. 2016), fueled by the observation that systems such as a school fish, bacterial colonies, and biological tissues display physical properties and phase transitions which can be described by statistical physics tools, and captured by simplified theoretical models. Physical systems mimicking the behavior of natural systems have also been developed to perform controlled experiments on model systems of active materials. In particular, colloidal particles and macroscopic objects similar to the systems displaying a granular glass transition have also been developed so that these particles can become "active" (Deseigne et al. 2010; Theurkauff et al. 2012; Buttinoni et al. 2013), that is, self-motile objects that can move in the absence of thermal fluctuations, similar to animals, cells, or bacteria.

It is natural to expect that dense assemblies of active particles will undergo some form of dynamic arrest (Henkes et al. 2011; Angelini et al. 2011). As human beings, we are well aware that it becomes difficult to walk very fast in a dense crowd, as observed in the streets of large cities or in subway corridors at peak times. Indeed, there are several indications from experimental observations that a transition from a fluidlike state to an arrested glassy state can be observed in active materials (Angelini et al. 2011; Garcia et al. 2015; Mongera et al. 2018; Klongvessa et al. 2019).

From a conceptual viewpoint, the main difference between these observations and the glass transition observed in molecular and colloidal systems is that the driving force for single particle motion is not of thermal origin, but is instead chemical, mechanical, or biological. This means that any theoretical model for dense active materials must include some sort of nonequilibrium sources of microscopic motion and consequently the glassy phenomena that will be described must necessarily occur far from equilibrium (Berthier and Kurchan 2013). In that sense, the situation is

conceptually not very different from the phenomenon of the granular glass transition discussed in the previous paragraph. The difference between the two essentially lies in the details of the driving motion, which very much resembles a quasi-equilibrium thermal bath in granular glasses (Keys et al. 2007).

Several numerical and theoretical studies of the glass transition in active materials have been recently published, see Berthier et al. (2019b) for a specific review on this topic. In particular, the glassy dynamics of so-called self-propelled particles have received considerable attention (Ni et al. 2013; Berthier 2014; Mandal et al. 2016; Bi et al. 2016; Berthier et al. 2017a; Matoz-Fernandez et al. 2017). In these models, particles interacting with simple pair interactions (similar to the ones studied to model the equilibrium glass transition) are driven by active forces that tend to displace the particles in straight lines over a finite persistence length.

It is now understood that for dense active fluids, due to these nonequilibrium driving forces both the structure and the dynamics are very different from their equilibrium counterparts (Berthier et al. 2019b). It is observed that a large persistence length has a profound influence on the static correlations of the fluid since both density-density (as in Eq. (3)) and velocity-velocity correlation functions develop non trivial nonequilibrium features (Berthier et al. 2017a). As particle crowding is increased, slow dynamics develop and is accompanied by a phenomenology similar to that of equilibrium glassy materials, with motion becoming gradually arrested at large enough density or small enough activity. Dynamic arrest in dense active materials is therefore called a nonequilibrium glass transition (Berthier and Kurchan 2013). Understanding this new class of glassy dynamics is an exciting new direction for research.

Random Pinning Glass Transition
The standard control parameters used to induce a glass transition are temperature and pressure. A new way introduced in the 2000s is "random pinning" (Scheidler et al. 2002; Kim 2003), which consists in freezing the positions of a fraction c of

particles from an equilibrium configuration of a supercooled liquid. Theoretical arguments (Cammarota and Biroli 2012) and numerical simulations (Berthier and Kob 2012; Karmakar and Procaccia 2011) suggested that the dynamics of the remaining free particles slow down and undergo a glass transition by increasing c. The study of the random pinning glass transition has been the focus of several theoretical analyses (Cammarota and Biroli 2013; Krakoviack 2011, 2014; Szamel and Flenner 2013; Franz and Parisi 2013; Cammarota 2013; Franz et al. 2013; Phan and Schweizer 2018; Cammarota and Seoane 2016; Ikeda et al. 2017a) and numerical simulations (Berthier and Kob 2012; Kob and Berthier 2013; Charbonneau and Tarjus 2013; Karmakar and Parisi 2013; Chakrabarty et al. 2015, 2016; Kob and Coslovich 2014; Jack and Fullerton 2013; Fullerton and Jack 2014; Li et al. 2015; Angelani et al. 2018; Ozawa et al. 2018a; Niblett et al. 2018) in the decade 2005–2015. It has also been studied in experiments, in particular in colloidal glasses by optical microscopy (Gokhale et al. 2014, 2016; Ganapathi et al. 2018; Williams et al. 2018).

The interest in the "random-pinning glass transition" has been twofold. First, it represents a new way to test theories of the glass transition. In fact, RFOT theory and MCT (see section "Theory of the Glass Transition") predict that it should have the same properties as the usual glass transition (Cammarota and Biroli 2012; Szamel and Flenner 2013), that is, increasing the pinned fraction c plays the same role as lowering the temperature. This phenomenon was studied and confirmed in Kob and Berthier (2013), where the equilibrium phase diagram of a randomly pinned glass-former was fully characterized. The dynamical behavior is not as well understood. Although it is clear that dynamics dramatically slows down when increasing c, hence the name "random-pinning glass transition," it has proven difficult to disentangle trivial effects due to steric constraints from collective ones. In consequence, numerical simulations could not validate or disprove the competing predictions from dynamical facilitation theories (Jack and Berthier 2012) and RFOT theory (Cammarota and Biroli 2012). The other reason for the random

pinning procedure was to produce configurations equilibrated very close to the glass transition (just after pinning, the remaining unpinned particles are in an equilibrium configuration for the constrained systems (Krakoviack 2010)). This allowed to perform the first computational study of ultrastable glasses (Hocky et al. 2014), see below.

The random pinning procedure has interesting connections, similarities, and differences with other ways to constrain the dynamics of glassy liquids introduced in recent years. Those can be grouped in three main categories: modifications of the Hamiltonian (ε-coupling, see section "Franz-Parisi Potential"), in the dynamical rules (s-ensemble dynamics, see section "s-Ensemble and Large Deviations"), and in the space available to the system (liquids in quenched environments (Thalmann et al. 2000)).

Ultrastable Glasses
Glassy materials are typically prepared by slowly cooling or compressing a dense fluid across the glass transition described above. The glass transition temperature or density is set by the competition between an extrinsic time scale imposed by the experimentalist (for instance the duration of the experiment, or the cooling rate), and an intrinsic timescale of the material, such as the structural relaxation time. The degree of supercooling observed in most glassy materials is then set by the typical duration of an experiment, which corresponds to an intrinsic timescale of about 100 s in molecular liquids.

It has recently become possible to prepare "ultrastable" glasses (Swallen et al. 2007; Ediger 2017), namely glassy materials which reach a degree of supercooling which is equivalent to cooling glasses at rates that are 10^5–10^{10} times slower than usual. Ultrastable glasses are not prepared by cooling bulk liquids across the glass transition, but using a completely different route called physical vapor deposition. In this procedure, the glassy material is prepared directly at the desired temperature (there is no cooling involved) by the slow deposition of individual molecules suspended in a gas phase onto a glassy film whose height increases slowly as more molecules are deposited.

The degree of supercooling that can be achieved by physical vapor deposition is again set by the competition between two timescales (Swallen et al. 2007; Berthier et al. 2017b). The extrinsic timescale is now related to the deposition rate of the molecules, whereas the intrinsic timescale is set by the relaxation time of molecules diffusing at the free surface of the glassy film. It is known that bulk and surface dynamics may differ by many orders of magnitude in glasses (Zhu et al. 2011), because the molecular mobility at a free surface is much less constrained than in the bulk. Therefore, for a similar extrinsic timescale imposed by the experimental setup, a much deeper degree of supercooling is achieved by the vapor deposition process.

Ultrastable glasses prepared using physical vapor deposition are thus expected to behave as extraordinarily slowly cooled supercooled liquids, with a cooling rate or a preparation time that is impractically large. As such, theses glasses have physical properties that can differ rather drastically from ordinary glassy materials. In particular, it was shown that their mechanical, thermodynamic, and kinetic properties differ quantitatively from ordinary glasses, and display specific dynamic phenomena (Kearns et al. 2010; Chen et al. 2013; Pérez-Castañeda et al. 2014; Sepúlveda et al. 2014; Ràfols-Ribé et al. 2018; Vila-Costa et al. 2020). As such, they are currently the subject of intense theoretical investigations as well (Wolynes 2009; Léonard and Harrowell 2010; Lyubimov et al. 2013; Jack and Berthier 2016; Gutiérrez and Garrahan 2016; Fullerton and Berthier 2017; Flenner et al. 2019; Khomenko et al. 2020). The goal is to better understand the deposition process itself, but also to better characterize the physical properties of ultrastable glasses in view of their many potential practical applications. Also, since ultrastable glasses offer a way to access much deeper supercooled states, it can be hoped that they can be used to shed new light on the glass transition phenomenon itself.

Other Glasses in Physics, and Beyond

There are many other physical contexts in which glassiness plays an important role (Young 1998). One of the most famous examples is the field of spin glasses. Real spin glasses are magnetic impurities interacting by quenched random couplings. At low temperatures, their dynamics become extremely slow and they freeze in amorphous spin configuration dubbed a "spin glass" by Anderson. There are many other physical systems, often characterized by quenched disorder, that show glassy behavior, like Coulomb glasses, Bose glasses, etc. In many cases, however, one does expect quite a different physics from structural glasses: the similarity between these systems is therefore only qualitative.

Quite remarkably, glassiness also emerges in other branches of science (Bouchaud et al. 2011). In particular, it has been discovered recently that concepts and techniques developed for glassy systems turn out to apply and be very useful tools in the field of computer science. Problems like combinatorial optimization display phenomena completely analogous to phase transitions, and actually, to glassy phase transitions. A posteriori, this is quite natural, because a typical optimization problem consists in finding a solution in a presence of a large number of constraints. This can be defined, for instance, as a set of N Boolean variables that satisfies M constraints. For N and M very large at fixed $\alpha = M/N$, this problem very much resembles finding a ground state in a statistical mechanics problem with quenched disorder. Indeed one can define an energy function (a Hamiltonian) as the number of unsatisfied constraints, that has to be minimized, as in a $T = 0$ statistical mechanics problem. The connection with glassy systems originates from the fact that in both cases the energy landscape is extremely complicated, full of minima and saddles. The fraction of constraints per degree of freedom, α, plays a role similar to the density in a hard sphere system. For instance, a central problem in optimization, random k-satisfiability, has been shown to undergo a glass transition when α increases, analogous to the one of structural glasses (Krzakala et al. 2007; Antenucci et al. 2019).

Glassiness also plays an important role in machine learning and signal processing. In those cases, one wants to learn a specific task from many examples or retrieve a specific signal from a huge amount of data. This is done in practice by minimizing a cost function. For example, imagine that one is given a tensor $T_{i_1,i_2,i_3} = v_{i_1} v_{i_2} v_{i_3}$, constructed from a vector $v_i (i = 1, \ldots, N)$ of norm $\sqrt{N}$, and that this tensor is corrupted by noise J_{i_1,i_2,i_3}, which for simplicity we take independent and Gaussian for each triple (i_1, i_2, i_3). The problem called tensor PCA, which appears in image and video analysis (Anandkumar et al. 2014), consists in retrieving the signal v_i from the noisy tensor $T_{i_1,i_2,i_3} + J_{i_1,i_2,i_3}$. The simplest procedure to solve this problem is to find the vector x_i minimizing the following cost function:

$$H(\{x_i\}) = \sum_{i_1,i_2,i_3} \left(v_{i_1} v_{i_2} v_{i_3} + J_{i_1,i_2,i_3} - x_{i_1} x_{i_2} x_{i_3} \right)^2.$$

By developing the square, one finds that the cost function H is identical to the one of a 3-spin spherical glass mean-field model with quenched random couplings J_{i_1,i_2,i_3} and a term favoring configurations in the direction of v_i (Richard and Montanari 2014). These two contributions are competing for determining the ground-state properties, the strength of the latter with respect to the former is proportional to the signal-to-noise ratio. This example illustrates one way in which glassiness plays an important role in machine learning: one has to find a signal (the v_i's) buried in a rough landscape (induced by the J_{i_1,i_2,i_3}'s). Practical algorithms, such as gradient descent and its stochastic version, lead to dynamics which are very similar to the ones of physical systems after a quench to low temperature. One of the main questions in this area is characterizing the algorithmic threshold, that is, the critical value of the signal-to-noise ratio such that the original signal can be recovered with some given accuracy. Glassy dynamics plays a central role: it is the main obstacle for recovering the signal, as the dynamics can be lost and trapped in bad minima instead of converging toward the good one correlated with the signal (Mannelli et al. 2020).

Finally, hunting for a signal in a rough landscape (Zdeborová and Krzakala 2016) is not the only context in which glassiness emerged in machine learning in recent years. In fact, more generally, there has been a lot of work aimed at characterizing the landscapes over which optimization dynamics take places in general machine learning problems (from high-dimensional statistics to deep neural networks), and at assessing to which extent glassy dynamics and rough landscapes play a relevant role (Sagun et al. 2014; Baity-Jesi et al. 2019).

Numerical Simulations

Studying the glass transition of molecular liquids at a microscopic level is in principle straightforward since one must answer a very simple question: how do particles move in a liquid close to T_g? It is of course a daunting task to attempt answering this question experimentally because one should then resolve the dynamics of single molecules to be able to follow the trajectories of objects that are a few Angstroms large on timescales of tens or hundreds of seconds, which sounds like eternity when compared to typical molecular dynamics usually lying in the picosecond regime. In recent years, such direct experimental investigations have been developed using time and space resolved techniques such as atomic force microscopy (Russell and Israeloff 2000) or single molecule spectroscopy (Adhikari et al. 2007; Paeng et al. 2015), but this remains a very difficult task.

In numerical simulations, by contrast, the trajectory of each particle in the system can, by construction, be followed at all times. This allows one to quantify easily single particle dynamics, as proved in Fig. 4 where the averaged mean-squared displacement $\Delta(t)$ measured in a simple Lennard-Jones glass-former is shown and is defined as.

$$\Delta(t) = \left\langle \frac{1}{N} \sum_{i=1}^{N} |\mathbf{r}_i(t) - \mathbf{r}_i(0)|^2 \right\rangle, \quad (6)$$

where $\mathbf{r}_i(t)$ represents the position of particle i at time t in a system composed of N particles and the brackets indicate an ensemble average. The particle displacements considerably slow down when T is decreased and the self-diffusion constant decreases by orders of magnitude, mirroring the behavior of the viscosity shown in Fig. 1 for real systems. Moreover, a rich dynamics is observed, with a plateau regime at intermediate timescales, corresponding to an extended time window during which particles vibrate around their initial positions, exactly as in a crystalline solid. The difference with a crystal is of course that this localization is only transient, and all particles eventually escape and diffuse at long times with a diffusion constant D_s, so that $\Delta(t) \sim 6D_s t$ when $t \to \infty$.

In recent years, computer experiments have played an increasingly important role in glass transition studies. It could almost be said that particle trajectories in numerical work have been studied under so many different angles that probably very little remains to be learned from such studies in the regime that is presently accessible using present day computers. Unfortunately, this does not imply complete knowledge of the physics of supercooled liquids. As shown in Fig. 4, it is presently possible to follow the dynamics of a simple glass-forming liquid over more than eight
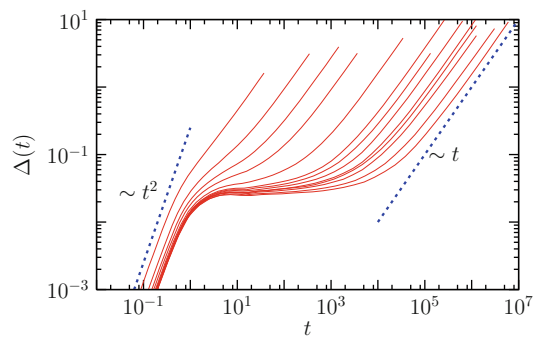
A Statistical Mechanics Perspective on Glasses and Aging, Fig. 4 Mean-squared displacements of individual particles in a simple model of a glass-forming liquid composed of Lennard-Jones particles observed on a wide time window. When temperature decreases (from left to right), the particle displacements become increasingly slow with several distinct time regimes corresponding to (in this order) ballistic, localized, and diffusive regimes

decades of time, and over a temperature window in which average relaxation timescales increase by more than five decades. This might sound impressive, but a quick look at Fig. 1 shows, however, that at the lowest temperatures studied in the computer, the relaxation timescales are still orders of magnitude faster than in experiments performed close to the glass transition temperature. They can be directly compared to experiments performed in this high temperature regime, but this also implies that simulations focus on a relaxation regime that is about eight to ten decades of times faster than in experiments performed close to T_g. Whether numerical works are useful to understand the kinetics of the glass transition itself at all is therefore an open, widely debated, question. We believe that it is now possible to numerically access temperatures which are low enough that many features associated to the glass transition physics can be observed: strong decoupling phenomena, clear deviations from fits to the mode-coupling theory (which are experimentally known to hold only at high temperatures), and crossovers toward truly activated dynamics. In section "New Computational Methods," we discuss recent developments in the field of computational studies that are able to address novel challenges regarding the static properties of supercooled liquids over a broad temperature range.

Classical computer simulations of supercooled liquids usually proceed by solving a cleverly discretized version of Newton's equations for a given potential interaction between particles (Allen and Tildesley 1989). If quantitative agreement with experimental data on an existing specific material is sought, the interaction must be carefully chosen in order to reproduce reality, for instance by combining classical to **ab initio** simulations. From a more fundamental perspective one rather seeks the simplest model that is still able to reproduce qualitatively the phenomenology of real glass-formers, while being considerably simpler to study. The implicit, but quite strong, hypothesis is that molecular details are not needed to explain the behavior of supercooled liquids, so that the glass transition is indeed a topic for statistical mechanics, not for chemistry.
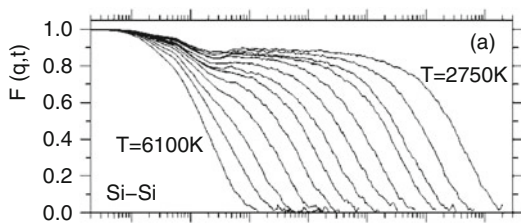
A Statistical Mechanics Perspective on Glasses and Aging, Fig. 5 Intermediate scattering function at wavevector 1.7 Å^{-1} for the *Si* particles at $T = 2750$ K obtained from molecular dynamics simulations of a model for silica (Horbach and Kob 2001)

A considerable amount of work has therefore been dedicated to studying models such as hard spheres, soft spheres, or Lennard-Jones particles. More realistic materials are also studied focusing for instance on the physics of network forming materials, multicomponent ones, anisotropic particles, or molecules with internal degrees of freedom. Connections to experimental work can be made by computing quantities that are experimentally accessible such as the intermediate scattering function, static structure factors, $S(\mathbf{q})$, or thermodynamic quantities such as specific heat or configurational entropy, which are directly obtained from particle trajectories and can be measured in experiments as well. As an example we show in Fig. 5 the intermediate scattering function $F(\mathbf{q}, t)$ obtained from a molecular dynamics simulation of a classical model for SiO_2 as a function of time for different temperatures (Horbach and Kob 2001).

An important role is played by simulations also because a large variety of dynamic and static quantities can be simultaneously measured in a single model system. As we shall discuss below, there are scores of different theoretical approaches to describe the physics of glass-formers, and sometimes they have their own set of predictions that can be readily tested by numerical work. Indeed, quite a large amount of numerical papers have been dedicated to testing in detail the predictions formulated by the mode-coupling theory of the glass transition, as reviewed in Götze (1999). Here, computer simulations are particularly well-suited as the theory specifically

addresses the relatively high temperature window that is studied in computer simulations.

While Newtonian dynamics is mainly used in numerical work on supercooled liquids, a most appropriate choice for these materials, it can be interesting to consider alternative dynamics that are not deterministic, or which do not conserve the energy. In colloidal glasses and physical gels, for instance, particles undergo Brownian motion arising from collisions with molecules in the solvent, and a stochastic dynamics is more appropriate. Theoretical considerations might also suggest the study of different sorts of dynamics for a given interaction between particles, for instance, to assess the role of conservation laws and structural information. Of course, if a given dynamics satisfies detailed balance with respect to the Boltzmann distribution, all structural quantities remain unchanged, but the resulting dynamical behavior might be very different. Several papers (Gleim et al. 1998; Szamel and Flenner 2004; Berthier and Kob 2007) have studied in detail the influence of the chosen microscopic dynamics on the dynamical behavior in glass-formers using either stochastic dynamics (where a friction term and a random noise are added to Newton's equations, the amplitude of both terms being related by a fluctuation-dissipation theorem), Brownian dynamics (in which there are no momenta, and positions evolve with Langevin dynamics), or Monte-Carlo dynamics (where the potential energy between two configurations is used to accept or reject a trial move). Quite surprisingly, the equivalence between these three types of stochastic dynamics and the originally studied Newtonian dynamics was established at the level of the averaged dynamical behavior (Gleim et al. 1998; Szamel and Flenner 2004; Berthier and Kob 2007), except at very short times where obvious differences are indeed expected. This strongly suggests that an explanation for the appearance of slow dynamics in these materials originates from their amorphous structure. However, important differences were found when dynamic fluctuations were considered (Berthier and Kob 2007; Berthier et al. 2007a, b), even in the long-time regime comprising the structural relaxation.

Another crucial advantage of molecular simulations is illustrated in Fig. 6. This figure shows a spatial map of single particle displacements recorded during the simulation of a binary soft sphere system in two dimensions (Hurley and Harrowell 1995). This type of measurement, out of reach of most experimental techniques that study the liquid state, reveals that dynamics might be very different from one particle to another. More importantly, Fig. 6 also unambiguously reveals the existence of spatial correlations between these dynamic fluctuations. The presence of nontrivial spatiotemporal fluctuations in supercooled liquids is now called "dynamic heterogeneity" (Ediger 2000), as we now discuss.

Dynamic Heterogeneity

Existence of Spatiotemporal Dynamic Fluctuations

A new facet of the relaxational behavior of supercooled liquids has emerged in the last two decades thanks to a considerable experimental and theoretical effort. It is called "dynamic heterogeneity" (DH), and now plays a central role in modern descriptions of glassy liquids (Ediger 2000; Berthier et al. 2011a). As anticipated in the previous section, the phenomenon of dynamic heterogeneity is related to the spatiotemporal fluctuations of the dynamics. Initial motivations stemmed from the search of an explanation for the non-exponential nature of relaxation processes in supercooled liquids, related to the existence of a broad relaxation spectrum. Two natural but fundamentally different explanations can be put forward. (1) The relaxation is locally exponential, but the typical relaxation timescale varies spatially. Hence, global correlation or response functions become non-exponential upon spatial averaging over this spatial distribution of relaxation times. (2) The relaxation is complicated and inherently non-exponential, even locally. Experimental and theoretical works (Ediger 2000) suggest that both mechanisms are likely at play, but definitely conclude that relaxation is spatially heterogeneous, with regions that are faster and slower than the average. Since supercooled

A Statistical Mechanics Perspective on Glasses and Aging, Fig. 6 Spatial map of single particle displacements in the simulation of a binary mixture of soft spheres in two dimensions (Hurley and Harrowell 1995). Arrows show the displacement of each particle in a trajectory of length about 10 times the structural relaxation time. The map reveals the existence of particles with different mobilities during relaxation, but also the existence of spatial correlations between these dynamic fluctuations
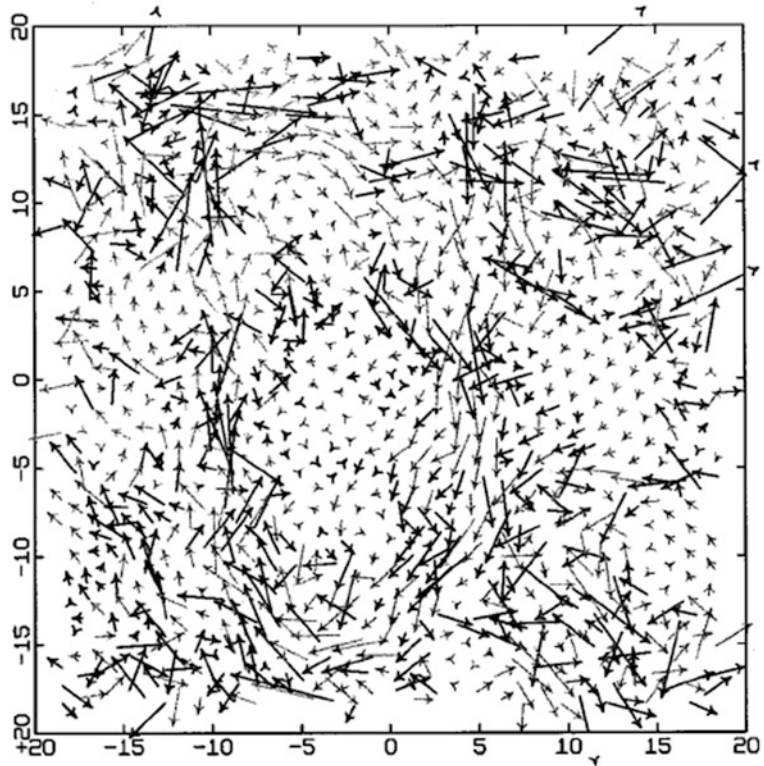
liquids are ergodic materials, a slow region will eventually become fast, and vice versa. A physical characterization of DH entails the determination of the typical lifetime of the heterogeneities, as well as their typical lengthscale.

A clear and more direct confirmation of the heterogeneous character of the dynamics also stems from simulation studies. For example, whereas the simulated average mean-squared displacements are smooth functions of time, time signals for individual particles clearly exhibit specific features that are not observed unless dynamics is resolved both in space and time. These features are displayed in Fig. 7. What do we see? We mainly observe that particle trajectories are not smooth but rather composed of a succession of long periods of time where particles simply vibrate around well-defined locations, separated by rapid "jumps." Vibrations were previously inferred from the plateau observed at intermediate times in the mean-squared displacements of Fig. 4, but the existence of jumps that are clearly

statistically widely distributed in time cannot be guessed from averaged quantities only. The fluctuations in Fig. 7 suggest, and direct measurements confirm, the importance played by fluctuations around the averaged dynamical behavior.

A simple type of such fluctuations has been studied in much detail. When looking at Fig. 7, it is indeed natural to ask, for any given time, what is the distribution of particle displacements. This is quantified by the self-part of the van-Hove function defined as

$$G_s(\mathbf{r}, t) = \left\langle \frac{1}{N} \sum_{i=1}^{N} \delta(\mathbf{r} - [\mathbf{r}_i(t) - \mathbf{r}_i(0)]) \right\rangle. \quad (7)$$

For an isotropic Gaussian diffusive process, one gets $G_s(\mathbf{r}, t) = \exp(-|\mathbf{r}|^2/(4D_s t))/(4\pi D_s t)^{3/2}$. Simulations reveal instead strong deviations from Gaussian behavior on the timescales relevant for structural relaxation (Kob et al. 1997). In particular they reveal "fat" tails in the distributions that
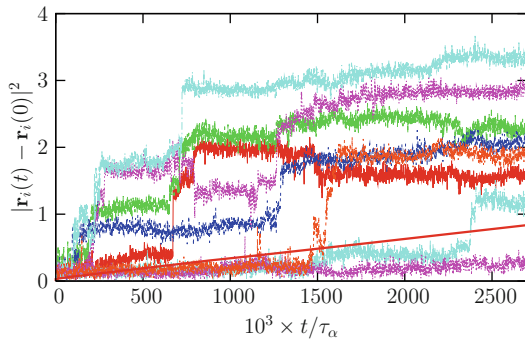
A Statistical Mechanics Perspective on Glasses and Aging, Fig. 7 Time resolved squared displacements of individual particles in a simple model of a glass-forming liquid composed of Lennard-Jones particles. The average is shown as a smooth full line. Trajectories are composed of long periods of time during which particles vibrate around well-defined positions, separated by rapid jumps that are widely distributed in time, underlying the importance of dynamic fluctuations

are much wider than expected from the Gaussian approximation. These tails are in fact better described by an exponential decay rather than a Gaussian one, in a wide time window comprising the structural relaxation, such that $G_s(\mathbf{r}, t) \sim \exp(-|\mathbf{r}|/\lambda(t))$ (Chaudhuri et al. 2007). Thus, they reflect the existence of a population of particles that moves distinctively further than the rest and appears therefore to be much more mobile. This observation implies that relaxation in a viscous liquid qualitatively differs from that of a normal liquid where diffusion is close to Gaussian, and that a nontrivial single particle displacements statistics exists.

A long series of questions immediately follows this seemingly simple observation. Answering them has been the main occupation of many workers in this field over the last decade. What are the particles in the tails effectively doing? Why are they faster than the rest? Are they located randomly in space or do they cluster? What is the geometry, time, and temperature evolution of the clusters? Are these spatial fluctuations correlated to geometric or thermodynamic properties of the liquids? Do similar correlations occur in all glassy materials? Can one predict these fluctuations theoretically? Can one understand glassy

phenomenology using fluctuation-based arguments? Can these fluctuations be detected experimentally?

Another influential phenomenon that was related early on to the existence of DH is the decoupling of self-diffusion (D_s) and viscosity (η). In the high temperature liquid self-diffusion and viscosity are related by the Stokes-Einstein relation (Hansen and McDonald 1990), $D_s \eta / T =$ const. For a large particle moving in a fluid the constant is equal to $1/(6\pi R)$ where R is the particle radius. Physically, the Stokes-Einstein relation means that two different measures of the relaxation time R^2/D_s and $\eta R^3/T$ lead to the same timescale up to a constant factor. In supercooled liquids this phenomenological law breaks down, as shown in Fig. 8 for ortho-terphenyl (Mapes et al. 2006). It is commonly found that D_s^{-1} does not increase as fast as η so that, at T_g, the product $D_s \eta$ has increased by 2–3 orders of magnitude as compared to its Stokes-Einstein value. This phenomenon, although less spectacular than the overall change of viscosity, is a significant indication that different ways to measure relaxation times lead to different answers and thus is a strong hint of the existence of a distribution of relaxation timescales.

Indeed, a natural explanation of this effect is that different observables probe the underlying distribution of relaxation times in different ways (Ediger 2000). For example, the self-diffusion coefficient of tracer particles is dominated by the more mobile particles whereas the viscosity or other measures of structural relaxation probe the timescale needed for every particle to move. An unrealistic but instructive example is a model where there is a small, non-percolative subset of particles that are blocked forever, coexisting with a majority of mobile particles. In this case, the structure never relaxes but the self-diffusion coefficient is nonzero because of the mobile particles. Of course, in reality all particles move, eventually, but this shows how different observables are likely to probe different moments of the distribution of timescales, as explicitly shown within several theoretical frameworks (Tarjus and Kivelson 1995; Jung et al. 2004).

A Statistical Mechanics Perspective on Glasses and Aging,
Fig. 8 Decoupling between viscosity (full line) and self-diffusion coefficient (symbols) in supercooled ortho-terphenyl (Mapes et al. 2006). The dashed line shows a fit with a "fractional" Stokes-Einstein relation, $D_s \sim (T/\eta)^\zeta$ with $\zeta \sim 0.82$
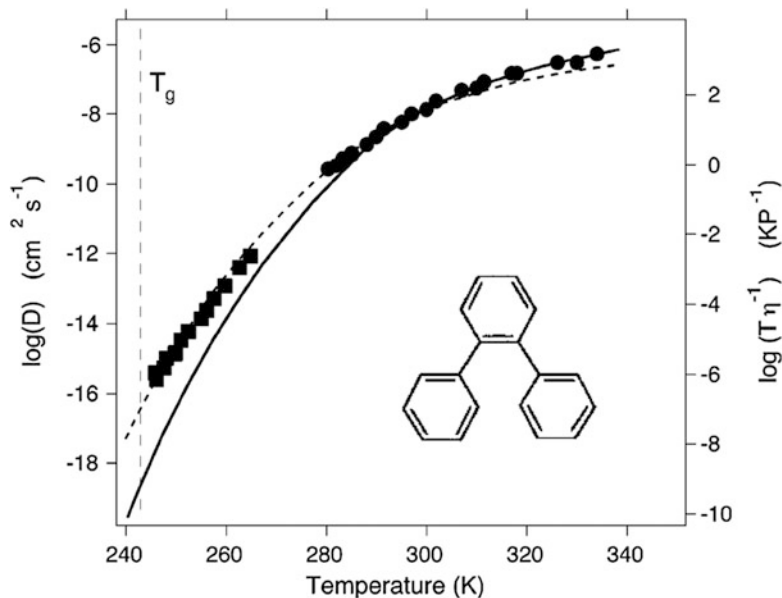
The phenomena described above, although certainly an indication of spatiotemporal fluctuations, do not allow one to study how these fluctuations are correlated in space. This is however a fundamental issue both from the experimental and theoretical points of view. How large are the regions that are faster or slower than the average? How does their size depend on temperature? Are these regions compact or fractal? These important questions were first addressed in pioneering works using four-dimensional NMR (Reinsberg et al. 2001), or by directly probing fluctuations at the nanoscopic scale using microscopy techniques. In particular, Vidal Russel and Israeloff using Atomic Force Microscopy techniques (Russell and Israeloff 2000) measured the polarization fluctuations in a volume of size of few tens of nanometers in a supercooled polymeric liquid (PVAc) close to T_g. In this spatially resolved measurement, the hope is to probe a small enough number of dynamically correlated regions, and detect their dynamics. Indeed, the signal shown in Fig. 9 shows a dynamics which is very intermittent in time, switching between periods with intense activity and other periods with no dynamics at all, suggesting that extended regions of space indeed transiently behave as fast or slow regions. A much smoother signal would be measured if such dynamically correlated "domains" were not present. Spatially resolved and NMR experiments are quite difficult. They give undisputed information about the typical lifetime of the DH, but their determination of a dynamic correlation lengthscale is rather indirect and/or performed on a small number of liquids in a small temperature window. Nevertheless, the outcome is that a nontrivial dynamic correlation length emerges at the glass transition, where it reaches a value of the order of 5–10 molecule diameters (Ediger 2000).

Multipoint Correlation Functions

More recently, substantial progress in characterizing spatiotemporal dynamical fluctuations was obtained from theoretical (Berthier et al. 2007a, b; Franz and Parisi 2000; Toninelli et al. 2005) and numerical results (Hurley and Harrowell 1995; Yamamoto and Onuki 1998; Franz et al. 1999; Bennemann et al. 1999; Lačević et al. 2003; Berthier 2004). In particular, it is now understood that dynamical fluctuations can be measured and characterized through the use of four-point correlation functions. These multipoint functions can be seen as a generalization of the spin glass susceptibility measuring the extent of amorphous long-range order in spin glasses. In this subsection, we
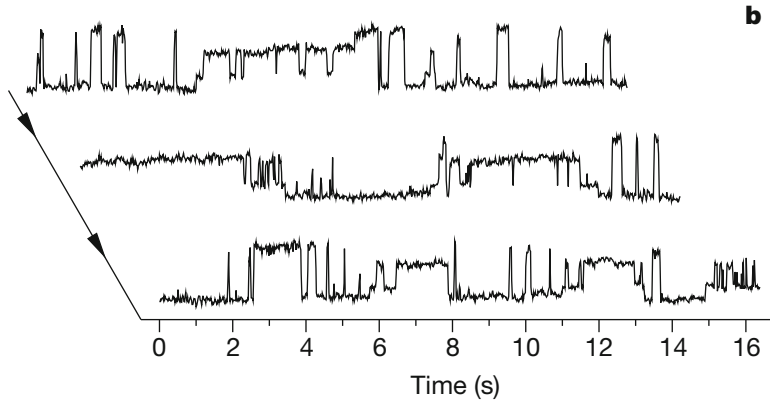
A Statistical Mechanics Perspective on Glasses and Aging, Fig. 9 Time series of polarization in the AFM experiment performed by Vidal Russell and Israeloff ([2000](#)) on PVAc at $T = 300$ K. The signal intermittently switches between periods with fast or slow dynamics, suggesting that extended regions of space indeed transiently behave as fast and slow regions

introduce these correlation functions and summarize the main results obtained using them.

Standard experimental probes of the averaged dynamics of liquids give access to the time-dependent autocorrelation function of the spontaneous fluctuations of some observable $O(t)$, $F(t) = \langle \delta O(0)\delta O(t) \rangle$, where $\delta O(t) = O(t) - \langle O \rangle$ represents the instantaneous value of the deviation of $O(t)$ from its ensemble average $\langle O \rangle$ at time t. One can think of $F(t)$ as being the average of a two-point quantity, $C(0, t) = \delta O(0)\delta O(t)$, characterizing the dynamics. A standard example corresponds to O being equal to the Fourier transform of the density field. In this case $F(t)$ is the dynamical structure factor as in Eq. ([5](#)). More generally, a correlation function $F(t)$ measures the global relaxation in the system. Intuitively, in a system with important dynamic correlations, the fluctuations of $C(0, t)$ are stronger. Quantitative information on the amplitude of those fluctuations is provided by the variance

$$\chi_4(t) = N\left\langle \delta C(0,t)^2 \right\rangle, \qquad (8)$$

where $\delta C(0, t) = C(0, t) - F(t)$, and N is the total number of particles in the system. The associated spatial correlations show up more clearly when considering a "local" probe of the dynamics, like for instance an orientational correlation function measured by dielectric or light scattering experiments, which can be expressed as

$$C(0,t) = \frac{1}{V}\int d^3r\, c(\mathbf{r};0,t), \qquad (9)$$

where V is the volume of the sample and $c(\mathbf{r}; 0, t)$ characterizes the dynamics between times 0 and t around point $\mathbf{r}$. For example, in the abovementioned case of orientational correlations, $c(\mathbf{r};0,t) \propto \frac{V}{N}\sum_{i,j=1}^{N}\delta(\mathbf{r} - \mathbf{r}_i)Y(\Omega_i(0))Y(\Omega_j(t))$, where Ω_i denotes the angles describing the orientation of molecule i, $\mathbf{r}_i(0)$ is the position of that molecule at time 0, and $Y(\Omega)$ is some appropriate rotation matrix element. Here, the "locality" of the probe comes from the fact that it is dominated by the self-term involving the same molecule at times 0 and t, or by the contribution coming from neighboring molecules. The dynamic susceptibility $\chi_4(t)$ can thus be rewritten as

$$\chi_4(t) = \rho\int d^3r G_4(\mathbf{r};0,t), \qquad (10)$$

where

$$G_4(\mathbf{r};0,t) = \langle \delta c(\mathbf{0};0,t)\delta c(\mathbf{r};0,t) \rangle, \qquad (11)$$
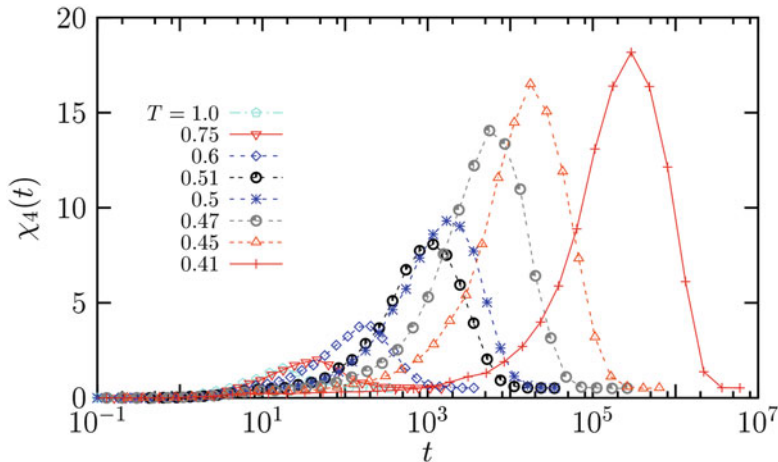
A Statistical Mechanics Perspective on Glasses and Aging, Fig. 10 Time dependence of $\chi_4(t)$, quantifying the spontaneous fluctuations of the intermediate scattering function in a Lennard-Jones supercooled liquid. For each temperature, $\chi_4(t)$ has a maximum, which shifts to larger times and has a larger value when T is decreased, revealing the increasing lengthscale of dynamic heterogeneity in supercooled liquids approaching the glass transition

and translational invariance has been taken into account ($\rho = N/V$ denotes the mean density). The above equations show that $\chi_4(t)$ measures the extent of spatial correlation between dynamical events at times 0 and t at different points, that is, the spatial extent of dynamically heterogeneous regions over a time span t.

The function $\chi_4(t)$ has been measured by molecular dynamics, Brownian and Monte Carlo simulations in different liquids (Franz et al. 1999; Bennemann et al. 1999; Lačević et al. 2003; Berthier 2004, 2007a; Gebremichael et al. 2004). An example is shown in Fig. 10 for a Lennard-Jones liquid. The qualitative behavior is similar in all cases (Berthier et al. 2007a; Franz and Parisi 2000; Toninelli et al. 2005): as a function of time $\chi_4(t)$ first increases, it has a peak on a timescale that tracks the structural relaxation timescale and then it decreases. (The decrease at long times constitutes a major difference with spin glasses. In a spin glass, χ_4 would be a monotonically increasing function of time whose longtime limit coincides with the static spin glass susceptibility. Physically, the difference is that spin glasses develop long-range static amorphous order while structural glasses do not or, at least, in a different and more subtle way.) Thus the peak value measures the volume on which the structural

relaxation processes are correlated. It is found to increase when the temperature decreases and the dynamics slows down. By measuring directly $G_4(\mathbf{r}; 0, t)$ it has also been checked that the increase of the peak of $\chi_4(t)$ corresponds, as expected, to a growing dynamic lengthscale ξ (Berthier et al. 2007a; Bennemann et al. 1999; Lačević et al. 2003; Berthier 2004), although these measurements are much harder in computer simulations, because very large systems need to be simulated to determine ξ unambiguously. Note that if the dynamically correlated regions were compact, the peak of χ_4 would be proportional to ξ^3 in three dimensions, directly relating χ_4 measurements to that of the relevant lengthscale of DH.

These results are also relevant because many theories of the glass transition assume or predict, in a way or another, that the dynamics slows down because there are increasingly large regions on which particles have to relax in a correlated or cooperative way. However, this lengthscale remained elusive for a long time. Measures of the spatial extent of dynamic heterogeneity, in particular $\chi_4(t)$ and $G_4(\mathbf{r}; 0, t)$, seem to provide the long-sought evidence of this phenomenon. This in turn suggests that the glass transition is indeed a critical phenomenon characterized by

growing timescales and lengthscales. A clear and conclusive understanding of the relationship between the lengthscale obtained from $G_4(\mathbf{r}; 0, t)$ and the relaxation timescale is still the focus of an intense research activity.

One major issue is that obtaining information on the behavior of $\chi_4(t)$ and $G_4(\mathbf{r}; 0, t)$ from experiments is difficult. Such measurements are necessary because numerical simulations can only be performed rather far from T_g, see section "Numerical Simulations." Up to now, direct experimental measurements of $\chi_4(t)$ have been restricted to colloidal (Weeks et al. 2007) and granular materials (Keys et al. 2007; Dauchot et al. 2005) close to the jamming transition, because dynamics is more easily spatially resolved in those cases. Unfortunately, similar measurements are currently not available in molecular liquids.

Recently, an approach based on fluctuation-dissipation relations and rigorous inequalities has been developed in order to overcome this difficulty (Berthier et al. 2005, 2007a; b; Dalle-Ferrier et al. 2007). The main idea is to obtain a rigorous lower bound on $\chi_4(t)$ using the Cauchy-Schwarz inequality $\langle \delta H(0)\delta C(0, t)\rangle^2 \leq \langle \delta H(0)^2\rangle \langle \delta C(0, t)^2\rangle$, where $H(t)$ denotes the enthalpy at time t. By using fluctuation-dissipation relations the previous inequality can be rewritten as (Berthier et al. 2005)

$$\chi_4(t) \geq \frac{k_B T^2}{c_P}[\chi_T(t)]^2, \qquad (12)$$

where the multipoint response function $\chi_T(t)$ is defined by

$$\chi_T(t) = \left.\frac{\partial F(t)}{\partial T}\right|_{N,P} = \frac{N}{k_B T^2}\langle \delta H(0)\delta C(0,t)\rangle. \qquad (13)$$

In this way, the experimentally accessible response $\chi_T(t)$ which quantifies the sensitivity of average correlation functions $F(t)$ to an infinitesimal temperature change, can be used in Eq. (12) to yield a lower bound on $\chi_4(t)$. Moreover, detailed numerical simulations and theoretical arguments (Berthier et al. 2007a, b) strongly

suggest that the right hand side of (12) actually provides a good estimation of $\chi_4(t)$, not just a lower bound.

Using this method, Dalle-Ferrier et al. (2007) have been able to obtain the evolution of the peak value of χ_4 for many different glass-formers in the entire supercooled regime. In Fig. 11 we show some of these results as a function of the relaxation timescale. The value on the y-axis, the peak of χ_4, is a proxy for the number of molecules, $N_{\mathrm{corr},4}$ that have to evolve in a correlated way in order to relax the structure of the liquid. Note that χ_4 is expected to be equal to $N_{\mathrm{corr},4}$ only up to a proportionality constant that is not known from experiments, which probably explains why the high temperature values of $N_{\mathrm{corr},4}$ are smaller than one. Figure 11 also indicates that $N_{\mathrm{corr},4}$ grows faster when T_α is not very large, close to the onset of slow dynamics, and a power law relationship between $N_{\mathrm{corr},4}$ and T_α fits this regime well $(\tau_\alpha/\tau_0 < 10^4)$. The growth of $N_{\mathrm{corr},4}$ becomes much slower closer to T_g. A change of six decades in time corresponds to a mere increase of a factor about 4 of $N_{\mathrm{corr},4}$, suggesting logarithmic rather than power law growth of dynamic correlations. This is in agreement with several theories of the glass transition which are based on activated dynamic scaling (Xia and Wolynes 2000; Garrahan and Chandler 2003; Tarjus et al. 2005).

Understanding quantitatively this relation between timescales and lengthscales is one of the main recent topics addressed in theories of the glass transition, see section "Theory of the Glass Transition." Furthermore, numerical works are also devoted to characterizing better the geometry of the dynamically heterogeneous regions (Donati et al. 1998; Appignanesi et al. 2006; Kob et al. 2012).

Nonlinear Response Function

Diverging responses are characteristic signatures of phase transitions. Linear static responses measuring the change in the order parameter due to external fields diverge at second-order phase transitions (Chaikin et al. 1995). By using fluctuation-dissipation relations one can show that such divergence is intimately related to the divergence of the correlation length emerging in two point-
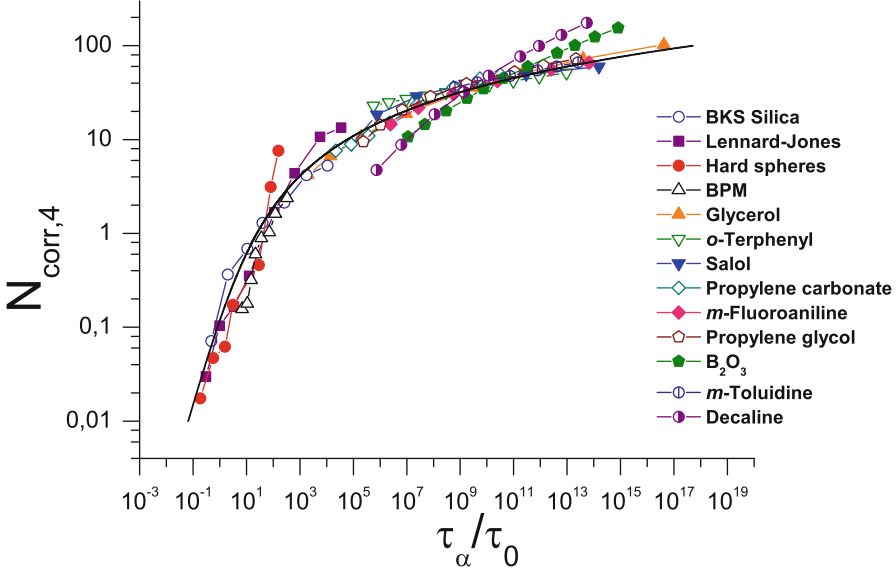
A Statistical Mechanics Perspective on Glasses and Aging, Fig. 11 Universal dynamic scaling relation between number of dynamically correlated particles, $N_{\text{corr},4}$, and relaxation timescale, τ_α, for a number of glass-formers (Dalle-Ferrier et al. 2007), determined using Eq. (12)

functions. Spin-glasses, the archetypal example of disordered systems, display a diverging static magnetic nonlinear cubic response (Binder and Young 1986; Baity-Jesi et al. 2013). In Bouchaud and Biroli (2005) it was argued that the counterpart of these phenomena for supercooled liquids can be found in nonlinear dynamical susceptibilities, which should grow approaching the glass transition, thus providing a complementary way (compared to χ_4) to reveal its collective nature. In experiments on molecular liquids, nonlinear dielectric susceptibility is a natural probe to unveil this phenomenon.

The simplest explanation (Albert et al. 2016) for this scenario is based on the assumption that $N_{\text{corr}} = (\ell/a)^{d_f}$ molecules are amorphously ordered over the lengthscale ℓ, where a is the molecular size and d_f is the fractal dimension of the ordered clusters. In consequence, their dipoles, which are oriented in apparently random positions, are essentially locked together during a time τ_α. In the presence of an external electric field E oscillating at frequency $\omega \geq \tau_\alpha^{-1}$, the dipolar degrees of freedom of these molecules contribute to the polarization per unit volume as

$$p = \mu_{\text{dip}} \frac{\sqrt{(\ell/a)^{d_f}}}{(\ell/a)^d} F\left(\frac{\mu_{\text{dip}} E \sqrt{(\ell/a)^{d_f}}}{kT}\right) \quad (14)$$

where μ_{dip} is an elementary dipole moment, F is an odd scaling function, and $d = 3$ the dimension of space. This states that randomly locked dipoles have an overall moment $\sqrt{\tilde{N}_{\text{corr}}}$, and that we should compare the thermal energy with the energy of this "super-dipole" in a field.

Expanding Eq. 14 in powers of E, one finds the "glassy" contribution to p:

$$\frac{p}{\mu_{dip}} = F'(0)\left(\frac{\ell}{a}\right)^{d_f-d}\left(\frac{\mu_{dip} E}{kT}\right) +$$
$$+ \frac{1}{3!}F^{(3)}(0)\left(\frac{\ell}{a}\right)^{2d_f-d}\left(\frac{\mu_{dip} E}{kT}\right)^3 + \quad (15)$$
$$+ \frac{1}{5!}F^{(5)}(0)\left(\frac{\ell}{a}\right)^{3d_f-d}\left(\frac{\mu_{dip} E}{kT}\right)^5 + \cdots$$

Because $d_f \leq d$, the first term, contributing to the usual linear dielectric susceptibility, $\chi_1(\omega)$, cannot grow as ℓ increases. This simple theoretical argument explains why spatial glassy correlations

does not show up in $\chi_1(\omega)$, in experiments. The second term, contributing to the third-order dielectric susceptibility $\chi_3(\omega)$, does grow with ℓ provided $d_f > d/2$. Several theories indeed suggest that ordered domains are compact, $d_f = d$ (Tarjus et al. 2005; Wolynes and Lubchenko 2012). The third term leads to the fifth-order susceptibility $\chi_5(\omega)$, which should diverge as $\ell^{3d_f - d}$ (higher n-order susceptibilities diverge as $\ell^{(n+1)d_f/2 - d}$. This line of arguments shows that measuring non-linear susceptibilities is a way to probe and characterize the collective dynamical behavior associated to glassy dynamics.

This challenge was taken up in the series of works (Albert et al. 2016; Crauste-Thibierge et al. 2010; Bauer et al. 2013; Brun et al. 2012). The main outcomes of these experiments have been: (i) to show that indeed a growth of the nonlinear responses goes along with the glass transition, (ii) to measure in a new way the number of correlated molecules close to T_g, (iii) to estimate that $d_f \simeq d$ (for $d = 3$). As an example, we reproduce the results of (Albert et al. 2016) in Fig. 12, which shows the increase of the fifth-order susceptibility with temperature (panel A), its humped shape in frequency (panel B), and the stronger singularity of the fifth-order susceptibility compared to the third-order one (panel C), as expected for a collective phenomenon.

Another set of experiments on nonlinear responses was performed in colloids: nonlinear mechanical susceptibilities were probed approaching the colloidal glass transition (Seyboldt et al. 2016) and shown to grow approaching it. Differently from the dielectric case, third-harmonic shear responses have a peak at a frequency associated to the β-relaxation, and not to the α-relaxation. The reason is related to the fact that a very slow shear-strain does not affect the relaxation time-scale, whereas an external electric field (even a static one) does, see Seyboldt et al. (2016).

Finally, a word about theories. Given that the growth of nonlinear dynamical susceptibility is a relatively newly established fact in the glass-physics arena, one can wonder how the different theoretical framework developed to explain the glass transitions cope with it. Thermodynamic theories based on the increases of some kind of medium range order naturally do, as explained above. Mode-Coupling-Theory also predicts diverging dynamical nonlinear susceptibility at the MCT transition (Seyboldt et al. 2016; Tarzia et al. 2010). Purely local theory are instead at odds. Dynamical facilitation theory was argued to be compatible with such findings in Speck (2019), even though the general arguments put forward in Albert et al. (2016) indicate the opposite conclusion.

Theory of the Glass Transition

We now present some theoretical approaches to the glass transition. It is impossible to cover all of them in a brief review, simply because there are way too many of them, perhaps the clearest indication that the glass transition remains an open problem. We choose to present approaches that are keystones and have a solid statistical mechanics basis. Loosely speaking, they have a Hamiltonian, can be simulated numerically, or studied analytically with statistical mechanics tools. Of course, the choice of Hamiltonians is crucial and contains very important assumptions about the nature of the glass transition. All these approaches have given rise to unexpected results. One finds more in them than what was supposed at the beginning, which leads to new, testable predictions. Furthermore, with models that are precise enough, one can test (and hopefully falsify!) these approaches by working out all their predictions in great detail, and comparing the outcome to actual data. This is not possible with "physical pictures," or simpler approaches of the problem which we therefore do not discuss.

Before going into the models, we would like to state the few important questions that theoreticians face.

- Why do the relaxation time and the viscosity increase when T_g is approached? Why is this growth super-Arrhenius?
- Can one understand and describe quantitatively the average dynamical behavior of supercooled liquids, in particular broad
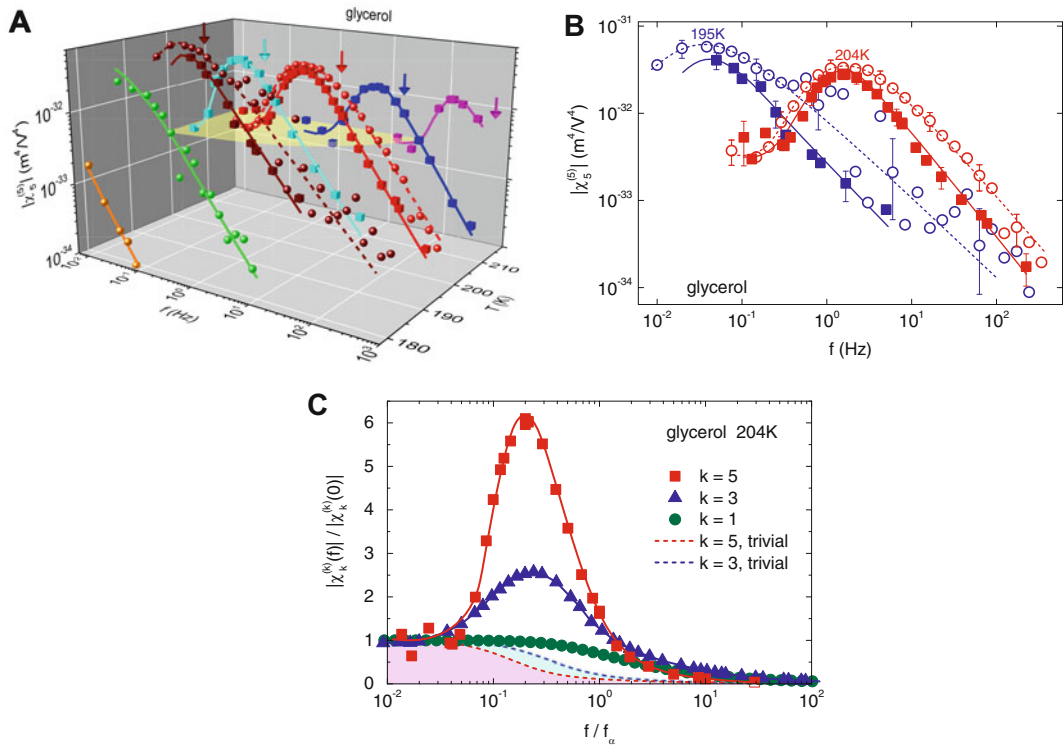
A Statistical Mechanics Perspective on Glasses and Aging, Fig. 12 Modulus of the fifth-order susceptibility in supercooled glycerol as a function of frequency (from Albert et al. (2016)). (**a**) The susceptibilities $\chi_5^{(5)}$ reported are obtained directly by monitoring the response of the sample at 5ω, when applying an electric field E at angular frequency ω. Two independent setups were used. Lines are guides for the eyes. (**b**) Projection onto the susceptibility-frequency plane of the data of panel A at 204 K and at 195 K. (**c**) Comparison of the fifth-order, cubic, and linear susceptibilities. Symbols, with line to guide the eyes. The higher the order k, the stronger the hump of $|\chi_k^{(k)}|$

relaxation spectra, non-exponential behavior, and their evolution with fragility?

- Is there a relation between kinetics and thermodynamics (like $T_0 \simeq T_K$), and why?
- Can one understand and describe quantitatively the spatiotemporal fluctuations of the dynamics? How and why are these fluctuations related to the dynamic slowing down?
- Is the glass transition a collective phenomenon? If yes, of which kind? Is there a finite temperature or zero temperature ideal glass transition?
- Is the slowing down of the dynamics driven by the growth of amorphous order and a static length? Or is its origin purely dynamic?
- Is there a geometric, real space explanation for the dynamic slowing down that takes into account molecular degrees of freedom?

The glass transition appears as a kind of "intermediate coupling" problem, since for instance typical growing lengthscales are found to be at most a few tens of particles large close to T_g. It would therefore be difficult to recognize the correct theory even if one bumped into it. To obtain quantitative, testable predictions, one must therefore be able to work out also preasymptotic effects. This is particularly difficult, especially in cases where the asymptotic theory itself has not satisfactorily been worked out. As a consequence, at this time, theories can only be judged by their overall predictive power and their theoretical consistency.

Random First-Order Transition Theory

Mean-Field Models and a Zest of Replica Theory
In the last three decades, three independent lines of research, Adam-Gibbs theory (Adam and Gibbs 1965), mode-coupling theory (Götze 1999), and spin glass theory (Mézard et al. 1987), have merged to produce a theoretical ensemble that now goes under the name of Random First-Order Transition theory (RFOT), a terminology introduced by Kirkpatrick, Thirumalai, and Wolynes (Kirkpatrick and Thirumalai 1987; Kirkpatrick and Wolynes 1987a) who played a major role in this unification. Instead of following the rambling development of history, we summarize it in a more modern and unified way.

A key ingredient of RFOT theory is the existence of a chaotic or complex free energy landscape with a specific evolution with temperature and/or density. Analyzing it in a controlled way for three-dimensional interacting particles is an impossible task. This can be achieved, however, in simplified models or using mean-field approximations that have therefore played a crucial role in the development of RFOT theory.

A first concrete example is given by "lattice glass models" (Biroli and Mézard 2001). These are models of hard particles sitting on a lattice. The Hamiltonian is infinite either if there is more than one particle on a site or if the number of occupied neighbors of an occupied site is larger than a parameter m, but is zero otherwise. Tuning the parameter m, or changing the type of lattice, in particular its connectivity, yields different models. Lattice glasses are constructed as simple statmech models to study the glassiness of hard sphere systems. The constraint on the number of occupied neighbors mimics the geometric frustration (Nelson 2002) encountered when trying to pack hard spheres in three dimensions. Numerical simulations show that their phenomenological glassy behavior is indeed analogous to the one of supercooled liquids (Darst et al. 2010; Seif and Grigera 2016; Nishikawa and Hukushima 2020). Other models with a finite energy are closer to molecular glass-formers, and can also be constructed (McCullagh et al. 2005). These models can be solved exactly on a Bethe lattice, which reveals a rich physical behavior (Rivoire et al. 2004). (In order to have a well-defined thermodynamics, Bethe lattices are generated as random graphs with fixed connectivity, also called random regular graphs.) In particular their free energy landscape can be analyzed in full details and turns out to have the properties that are also found in several "generalized spin glasses." Probably the most studied example of such spin glasses is the p-spin model, defined by the Hamiltonian (Gross and Mézard 1984)

$$H = - \sum_{i_1, ..., i_p} J_{i_1,...,i_p} S_{i_1} ... S_{i_p}, \qquad (16)$$

where the S_i's are N Ising or spherical spins, $p > 2$ is the number of interacting spins in a single term of the sum, and $J_{i_1,...,i_p}$ quenched random couplings extracted from a distribution which, with no loss of generality, can be taken as the Gaussian distribution with zero mean and variance $p!/(2N^{p-1})$. In this model, the couplings $J_{i_1,...,i_p}$ play the role of self-induced disorder in glasses, and promote a glass phase at low temperature.

All these models can be analyzed using the so-called replica theory (Mézard et al. 1987). Given its importance in setting the foundations of the theory of glasses at the mean-field level, we now present its main technical steps. To keep the discussion as simple as possible, we focus on p-spin models. Note that the theory holds for more complex models but it is technically more involved. The starting point is the computation of the free-energy which is obtained as an average over the distribution of couplings:

$$F = \lim_{N \to \infty} - \frac{1}{\beta N} \overline{\log Z_J}, \qquad (17)$$

where $\overline{\cdots}$ represents the average over the disorder. Performing this average is possible thanks to the replica trick

$$\overline{\log Z_J} = \lim_{n \to 0} \frac{1}{n} \log \overline{Z^n}, \qquad (18)$$

where n is the index of replicas, that is, clones of the same system with different couplings $J_{i_1,...,i_p}$

extracted from the same distribution. The use of the replica trick may seem purely mathematical, yet it has a profound physical sense. If the system is ergodic, averages of thermodynamical observables for two replicas of the same system (with identical disorder) coincide, whereas they differ if ergodicity is broken. We can define the overlaps between two replicas a, b as Q_{ab}, which defines the $n \times n$ overlap matrix:

$$Q_{ab} = \frac{1}{N} \sum_{i=1}^{N} S_i^a S_i^b, \qquad (19)$$

where the product between spins represents a dot product for spherical spins (Castellani and Cavagna 2005). After some computations, the free energy can be expressed as a function of Q_{ab}, which therefore plays the role of the order parameter. In the ergodic phase one expects symmetry between replicas (if additional symmetries are broken, then one can have ergodicity breaking also in the RS phase), and the so-called replica-symmetric (RS) parameterization of Q_{ab} is adopted: all the off-diagonal elements of Q_{ab} are equal to $q_0 < 1$ and the diagonal elements are $Q_{aa} = 1$. The parameterization that corresponds to the glass phase, when ergodicity is broken, is the so-called one-step replica symmetry breaking (1RSB) solution. Here, the overlap matrix is divided into blocks of dimension $m \times m$; elements belonging to blocks far from the diagonal are equal to q_0, while off-diagonal elements of blocks along the diagonal are equal to q_1 with $1 > q_1 > q_0$. On the diagonal $Q_{aa} = 1$. This parameterization encodes the existence of many thermodynamically equivalent basins, hence two replicas can either fall in the same basin and have overlap q_1, or fall in two different basins and have overlap q_0. The crucial simplification introduced by the mean-field approximation is that barriers between basins have a free energy cost which grows exponentially with N, so that truly metastable states can be defined in the thermodynamic limit (Cavagna 2009). At high temperature (or low density) the RS solution has a lower free energy. Below the ideal glass transition temperature the 1RSB solution instead becomes dominant.

Liquids and Glasses in Infinite Dimensions

A major theoretical breakthrough of the last years is the analysis of the glass transition for interacting particle systems in the limit of infinite dimensions (Kurchan et al. 2012, 2013; Charbonneau et al. 2014a, b; Parisi et al. 2020). The starting point approach is the definition of a pair interaction potential with a proper scaling with dimension d to ensure a nontrivial thermodynamic limit:

$$v(r) = \widetilde{v} [d(r/\ell - 1)] \qquad (20)$$

where ℓ defines the range of the interaction. Many different potentials used to model glasses can be written in this way by using a suitable function $\widetilde{v}(x)$, such as hard spheres, Lennard-Jones, Yukawa, square-well, harmonic, and Weeks-Chandler-Andersen potentials (Parisi et al. 2020). In the limit of infinite space dimension, $d \to \infty$, and using the scaling above, the thermodynamics and the dynamics of liquids and glasses can be analyzed exactly. (For large d the crystalline phase does not intervene. In fact, the amorphous and crystalline solid phases are well separated in configuration space and issues related to finite dimensions, such as the crystallization of monodisperse particles, are suppressed (Skoge et al. 2006; van Meel et al. 2009).) The resulting theory is qualitatively very similar to the one obtained from the simple models discussed in the previous section (both for the statics, in terms of replica formalism, and for the dynamics, in terms of self-consistent Langevin equations).

In fact, all these models belong to the universality class of 1RSB systems (Charbonneau et al. 2014b), with a free-energy landscape evolving as in the sketch in Fig. 13. At low densities or high enough temperatures, they all describe an ergodic liquid phase, analogous to the paramagnetic phase of a spin glass. Under cooling or application of an external pressure, the free energy breaks up into many different minima which eventually trap the dynamics, and the system enters the glass phase, as described further below.

The merit of the infinite dimensional theory is that it offers quantitative results and applies directly to microscopic models of liquids and glasses. Moreover, it directly reveals the nature

A Statistical Mechanics Perspective on Glasses and Aging,
Fig. 13 Sketch of the evolution of free-energy landscape of hard spheres across the glass transition. In the liquid phase (**a**) at low packing fractions $\varphi < \varphi_g$, every portion of the phase space is accessible. For $\varphi < \varphi_g$ the system is in the glass phase (**b**) and remains trapped in one of the many equivalent basins

$\varphi < \varphi_g$

$\varphi > \varphi_g$
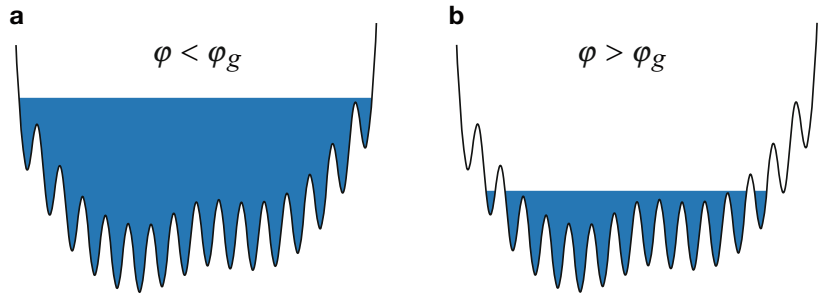
of "mean-field" theories and approximations, such as the diagrammatic liquid theory and Mode-Coupling Theory. Last but not least, it establishes once and for all that the 1RSB phase and associated physics and phase transition is the correct and universal mean-field theory of glass-forming models.

Random First-Order Transitions

We now discuss the physics associated to the 1RSB phase transition, and more generally to RFOT. The free energy landscape of glassy systems is "rugged," as shown in Fig. 13. It is characterized by many minima and saddle points of various orders. Actually, the number of stationary points is so large that in order to count them one has to introduce an entropy, called configurational entropy or complexity, $s_c = \frac{1}{N} \log \mathcal{N}(f)$, where $\mathcal{N}(f)$ is the number of stationary points with a given free energy density f. The (real space) density profile corresponding to one given minimum is amorphous and lacks any type of periodic long-range order, and different minima are very different from one another. Defining a similarity measure between them, an "overlap" Q (see Eq. (39) below for a precise definition), one typically finds that two minima with the same free energy f have zero overlap. The typical shape of the configurational entropy as a function of f is shown in Fig. 14.

At high temperature, there is typically a single minimum, the high temperature liquid state. There is a temperature below which an exponentially large (in the system size) number of minima appear. Within mean-field models, corresponding to Bethe lattices, completely connected lattices, and interacting particles for $d \to \infty$ these minima correspond to macroscopic physical states analogous to the periodic minimum corresponding to the crystal. (There is of course no crystal state in disordered systems such as in Eq. (16). In the case of lattice glass models, there is a crystal phase but it can disappear depending whether the Bethe lattice is a Cayley tree or a random regular graph.) Once the system is in one of these states it remains trapped there forever, since the barriers separating states diverge with the system size. However, when transposed to finite dimensional systems, these states become metastable and have a finite lifetime. As a consequence, in order to compute thermodynamic properties, one has to sum over all of them using the Boltzmann weight $\exp(-\beta N f_\alpha)$ for each state α (Monasson 1995):

$$Z = \sum_\alpha e^{-\beta N f_\alpha} = \int df \exp\left[N s_c(f; T)\right] e^{-\beta N f},$$

(21)

where $\beta = 1/(K_B T)$. Evaluating this sum by saddle point method yields three regimes. At high temperature, $T > T_{MCT}$, the liquid corresponding to a flat density profile dominates the sum. The landscape is simple and has a single minimum. This is followed by an intermediate temperature regime, $T_K < T < T_{MCT}$, where the sum is dominated by all terms with free energy density satisfying

$$\left. \frac{\partial s_c(f, T)}{\partial f} \right|_{f=f^*} = \beta. \qquad (22)$$

There are many of them, the logarithm of their number being given by $N s_c(f^*, T)$, see Fig. 14 for a graphical solution of Eq. (22). Upon decreasing the temperature, $s_c(f^*, T)$ decreases until a temperature, T_K, below which the sum in Eq. (21) becomes dominated by only few terms corresponding to states with free energy density f_K given by $s_c(f_K, T) = 0$, see Fig. 14. The entropy in the intermediate temperature range above T_K has two contributions: the one counting the number of minima, given by s_c, and the intra-state entropy, s_{in}, counting the number of configurations inside each state. At T_K, the configurational entropy vanishes, $s_c(T_K) = 0$. As a consequence the specific heat undergoes a jump toward a
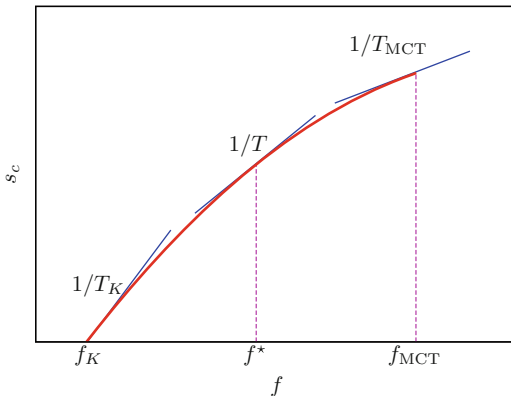
A Statistical Mechanics Perspective on Glasses and Aging, Fig. 14 Typical shape of the configurational entropy, sc, as a function of free energy density, f in the range $T_k < T < T_{MCT}$ for random first-order landscapes. A graphical solution of Eq. (22) is obtained by finding the value of f at which the slope of the curve is $1/T$. Note that s_c is also a function of temperature, so this curve changes with T

smaller value across T_K, an exact realization of the "entropy vanishing" mechanism conjectured by Kauzmann (1948).

Let us discuss the dynamical behavior which results from the above analysis. We have already mentioned that relaxation processes do not occur below T_{MCT} because states have an infinite lifetime. The stability of these states can be analyzed by computing the free energy Hessian in the minima (Castellani and Cavagna 2005). One finds that states become more fragile when $T \to T_{MCT}^-$ are marginally stable at $T = T_{MCT}$, unstable for $T > T_{MCT}$. The relaxation dynamics of these models can be analyzed exactly (Barrat et al. 2004; Maimbourg et al. 2016). Coming from high temperature, the dynamics slows down and the relaxation time diverges at T_{MCT} in a power law manner,

$$\tau_\alpha \sim \frac{1}{(T - T_{MCT})^\gamma}, \qquad (23)$$

where γ is a critical exponent. The physical reason is the incipient stable states that appear close to T_{MCT}. The closer the temperature is to T_{MCT}, the longer it takes to find an unstable direction to relax.

Amazingly, the dynamical transition that appears upon approaching T_{MCT} in random first-order landscapes is completely analogous to the one predicted for supercooled liquids by the Mode-Coupling Theory (MCT) of the glass transition, and developed independently by Leuthesser, Bengtzelius, Götze, Sjolander, and coworkers (Götze 1999). Actually, MCT can be considered as an approximation which becomes controlled and exact for these mean-field models. Originally, MCT was developed using projector operator formalism (Leutheusser 1984; Bengtzelius et al. 1984) and field-theory methods (Das and Mazenko 1986) to yield closed integro-differential equations for the dynamical structure factor in supercooled liquids. These approaches were recently generalized (Biroli and Bouchaud 2004; Biroli et al. 2006) to deal with dynamic heterogeneity and make predictions for the multi-point susceptibilities and correlation functions discussed in section "Dynamic Heterogeneity."

Within MCT, the relaxation timescale diverges in a power law fashion at T_{MCT}, as in Eq. (23). This divergence is accompanied by critical behavior that appears both in space (long range spatial dynamic correlations), and in time (time-dependent power laws).

Comparing Eqs. (1) and (23) makes it clear that MCT cannot be used to describe viscosity data close to T_g since it does not predict activated behavior. It is recognized that an MCT transition at T_{MCT} does not occur in real materials, so that T_{MCT} is, at best, a dynamical crossover. A central advantage of MCT compared to many other theories is that it can yield quantitative predictions from microscopic input obtained for a particular material. As such it has been applied to scores of different systems, with predictions that can be directly confronted to experimental or numerical measurements. A major drawback is the freedom offered by the "crossover" nature of the MCT transition, so that "negative" results can often be attributed to corrections to asymptotic predictions rather than deficiencies of the theory itself. Nevertheless, MCT has proven to be useful and continues to be developed, applied, and generalized to study many different physical situations (Götze 1999), including aging systems and nonlinear rheology of glassy materials (Berthier et al. 2000; Miyazaki and Reichman 2002; Fuchs and Cates 2002), see also section "Aging and Off-Equilibrium Dynamics."

What happens below T_{MCT} in a finite dimensional system if the relaxation time does not diverge as predicted in Eq. (23)? Why is the transition avoided? In fact, the plethora of states that one finds in mean-field are expected to become (at best) metastable in finite dimension, with a finite lifetime, even below T_{MCT}. What is their typical life time and how these metastable states are related to the structural relaxation are issues that still await for a complete microscopic analysis.

There exist, however, phenomenological arguments (Xia and Wolynes 2000; Kirkpatrick et al. 1989; Bouchaud and Biroli 2004), backed by microscopic computations (Dzero et al. 2005; Franz 2006) that yield a possible solution dubbed "mosaic state" by Kirkpatrick, Thirumalai, and Wolynes (1989). Schematically, the mosaic picture states that, in the regime $T_K < T < T_{MCT}$, the liquid is composed of domains of linear size ξ. Inside each domain, the system is in one of the mean-field states. The length of the domains is fixed by a competition between energy and configurational entropy. A state in a finite but large region of linear size l can be selected by appropriate boundary conditions that decrease its free energy by an amount which scales as Υl^θ with $\theta \leq 2$. On the other hand, the system can gain entropy, which scales as $s_c l^3$, if it visits the other numerous states. Entropy obviously gains on large lengthscales, the crossover length ξ being obtained by balancing the two terms,

$$\xi = \left(\frac{\Upsilon}{Ts_c(T)} \right)^{1/(3-\theta)}. \qquad (24)$$

In this scenario, the configurational entropy on scales smaller than ξ is too small to stir the configurations efficiently and win over the dynamically generated pinning field due to the environment, while ergodicity is restored at larger scale. Hence, the relaxation time of the system is the relaxation time, $\tau(\xi)$, of finite size regions. Barriers are finite, unlike in the mean-field treatment. Smaller length scales are faster but unable to decorrelate, whereas larger scales are orders of magnitude slower. Assuming thermal activation over energy barriers which are supposed to grow with size as ξ^ψ, one finally predicts, using Eq. (24), that (Bouchaud and Biroli 2004)

$$\log \left(\frac{\tau_\alpha}{\tau_0} \right) = c \frac{\Upsilon}{k_B T} \left(\frac{\Upsilon}{Ts_c(T)} \right)^{\psi/(3-\theta)}, \qquad (25)$$

where c is a constant.

The above argument is rather generic and therefore not very predictive. There exist microscopic computations (Dzero et al. 2005; Franz 2006; Biroli and Cammarota 2017) aimed at putting these phenomenological arguments on a firmer basis and computing the exponents θ and ψ. The results are not yet fully conclusive because they involve replica calculations with some assumptions, but they do confirm the

phenomenological scenario presented above and suggest that $\theta = 2$. Some other phenomenological arguments suggest the value of $\theta = 3/2$ (Kirkpatrick et al. 1989). There are no computation available for ψ, only the suggestion that $\psi = 0$ (Kirkpatrick et al. 1989).

Note that using the value $\theta = 3/2$ with $\theta = \psi$ simplifies Eq. (25) into a form that is well-known experimentally and relates $\log \tau_\alpha$ directly to $1/S_c$, which is the celebrated Adam-Gibbs relation (Adam and Gibbs 1965) between relaxation time and configurational entropy that is in rather good quantitative agreement with many experimental results (Angell 1997; Hodge 1997; Johari 2000; Ozawa et al. 2019). The Random First-Order Transition theory can be considered, therefore, as a microscopic theory that reformulates and generalizes the Adam-Gibbs mechanism. Furthermore, using the fact that the configurational entropy vanishes linearly at T_K, a VFT divergence of the relaxation time as in Eq. (1) is predicted, with the identification that

$$T_0 = T_K. \tag{26}$$

The equality (26) between two temperatures that are commonly used in the description of experimental data certainly constitutes a central achievement of RFOT theory since it accounts for the empirical relation found between the kinetics and the thermodynamics of supercooled liquids. Furthermore RFOT theory naturally contains MCT, which can be used to describe the first decades of the dynamical slowing down, while the spin glass side of RFOT theory qualitatively explains the dynamics in terms of the peculiar features of the free energy landscape that have been detailed above. Dynamics first slows down because there appear incipient metastable states, and once these metastable states are formed, the dynamics becomes dominated by the thermally activated barrier crossing from one metastable state to another, which is consistent with the relation between dynamical correlation length and timescale discussed in section "Dynamic Heterogeneity." Quite importantly, microscopic computations of T_{MCT} and T_0 for realistic models of

liquids are possible (Parisi et al. 2020; Mézard and Parisi 1999).

Probably the most serious weakness of the RFOT theory construction is that the theory, although worked out in full details within mean-field models or the large dimensionality limit, is based for finite dimensions on asymptotic results valid, for example, for $T \to T_K$. The application of RFOT theory to temperatures accessible in experiments (hence not very close to T_K) requires additional phenomenological assumptions. Moreover, the dynamical processes leading to the VFT law are not understood completely. Although the ultimate consequences of the theory are sometimes in very good agreement with experiments, as Eq. (26), direct tests of the mosaic state picture are rare and difficult (Cavagna et al. 2007; Ozawa and Berthier 2017).

Heterogeneous Disorder and Mapping to the Random, Field Ising Model

The study of second-order phase transitions shows that field theory provides a natural framework to go beyond mean-field theory (Chaikin et al. 1995). With this in mind, researchers in glass physics have also gone down this route in recent years. One of their main achievements has been to identify fluctuations that are neglected by mean-field theory and play a very important role in shaping the physical behavior of supercooled liquids. These fluctuations have been related to the notion of "self-induced disorder" in Franz et al. (2011). In the following, we may prefer the name "self-induced heterogeneity" to make the distinction with the "self-induced disorder" discussed in section "Franz-Parisi Potential." (This terminology was suggested to us by Jean-Philippe Bouchaud.) The main idea is that when observing equilibrium relaxation from time t to time $t + \tau_\alpha$, the state of the system at time t is spatially heterogeneous: for instance it can have higher density in one region and lower density in another. Actually, theoretical analysis shows (Stevenson et al. 2008; Biroli et al. 2018a, b) that even key mean-field quantities, such as the configurational entropy, are heterogeneously distributed in space. Since the amount of slowing down is directly linked to those quantities

(at least within RFOT theory), these static fluctuations induce strong dynamical fluctuations, leading in particular to dynamical heterogeneities (Franz et al. 2011). From the theoretical point of view, they play a key role in changing properties of the MCT transition and the ideal glass transition. In fact, even though the MCT transition is like a spinodal instability within mean-field theory (Kirkpatrick and Wolynes 1987b), one finds that once these fluctuations are included, MCT enters the universality class of a disordered spinodal, like, for example, the spinodal of the Random Field-Ising Model (Franz et al. 2011). Using results obtained on this problem, this connection implies that even in the absence of activated hopping, the MCT transition changes nature in any finite dimension: it is either wiped out by non-perturbative fluctuations (Rizzo 2016) or it becomes dominated by rare and non-perturbative events, as happens for the spinodal of the RFIM (Nandi et al. 2016). One nevertheless expects that the higher the spatial dimension, the more obvious an echo of the MCT mean-field transition should persist (Maimbourg et al. 2016; Biroli and Bouchaud 2012; Berthier et al. 2020).

Finally, the role of heterogeneous disorder on the ideal glass transition has been investigated in Stevenson et al. (2008) and Biroli et al. (2018a, b). The main outcome of these studies is an effective model for the glass transition that takes the form of an RFIM with extra long-range anti-ferromagnetic and multi-body interactions. These new couplings depress the ideal glass transition temperature but do not lead to qualitative changes. The strength of the disorder is, however, crucial: a strong enough disorder (a system-dependent feature) can destroy the ideal glass transition, as may happen for the RFIM. Another relation with the RFIM was also found in Biroli and Bouchaud (2012), where it was shown that amorphous interfaces between rearranging regions behave statistically as the ones of domain walls in the RFIM.

Let us conclude with a word of caution: not everything is understood about self-induced heterogeneity. Since the disorder is strongly linked to the state of the system, it is also to a large extent renewed after a time τ_α, thus it evolves and at the same time it affects the dynamics, that is, it is not truly quenched. This is a first difficulty in assessing precisely its role for glassy relaxation (Berthier et al. 2019c). A second one is that although for static properties, such as configurational entropy or the Franz-Parisi potential, one can establish a mapping to the RFIM, for the dynamics the situation is more intricate and no mapping has been found up to now. (The difficulty is that the mapping to the RFIM proceeds by relating the overlap (for glasses) to the magnetization (for the RFIM). There are no natural dynamical equations for the overlap, and in the only cases where those have been established – the β-regime of MCT – these proved to be quite complex and different from the corresponding equations for the magnetization of the RFIM.)

Renormalization Group for the Glass Transition
In parallel with the efforts described in the previous section, developing a renormalization group (RG) analysis of the glass transition has been a new important theoretical activity in the last decade. Different methods have been used, and were applied on lattice disordered models and replica lattice field theories which display a glass transition. Given that the ideal glass transition has a mixed character, intermediate between first- and second-order phase transition, usual perturbative RG techniques developed for continuous phase transitions do not work. Therefore researchers had to focus on non-perturbative methods. In Castellana et al. (2010) the hierarchical Dyson RG method was employed to analyze the Random Energy Model in finite dimension. The authors found an ideal glass phase transition similar to the one taking place within mean-field but with a nonanalytical behavior of the free-energy at T_K, leading in particular to a specific heat exponent different from one, as assumed within RFOT theory. The real-space properties, correlation length and energy barrier, and the nature of the fixed-point were first studied in Yeo and Moore (2012) and Cammarota et al. (2011) by Migdal-Kadanoff RG. A complete and more advanced analysis was performed in Angelini and Biroli (2017), in which it was shown that the ideal glass transition is associated to a so-called zero temperature fixed

point (Fisher 1986). The main implication is that the correlation length and the typical energy barrier have power law divergences with nontrivial exponents, hence implying a super-Arrhenius behavior. However, such a fixed point was found only in dimensions higher than three. In consequence, this RG treatment predicts that in three dimensions the glass transition is actually an avoided phase transition (Kivelson et al. 1995): glassy behavior is still driven by the RG fixed point present in higher dimension, but the correlation length and the timescale do not truly diverge (arguably an irrelevant fact since one cannot approach the transition close enough, but an important conceptual one).

The RG approaches we reviewed above offer a new perspective on the nature of the glass transition. They provide important guidelines for more controlled non-perturbative RG treatments. Ideally, one would like to tackle directly interacting particle systems in the continuum and use methods that have been proved to be precise and reliable in previous studies, such as the one developed by Wetterich (Berges et al. 2002). This is a formidable challenge as those techniques do not seem to be able to handle the kind of rare and localized non-perturbative events that are relevant for glassy dynamics (Rulquin et al. 2016).

Free Volume, Defects, and Facilitated Models

Lattice Gases

In this subsection we motivate and briefly summarize studies of a different family of statistical mechanics models that turns out to yield a rich variety of physical behaviors. Their starting points are physical assumptions that might seem similar to the models described in section "Random First-Order Transition Theory," but the outcome yields a different physical explanation of the glass transition. Although the two theoretical approaches cannot be simultaneously correct, they both have been influential and very instructive in order to develop a theoretical understanding of glassy phenomena.

As in section "Random First-Order Transition Theory," we first consider hard sphere systems. We follow the lattice gas description introduced

by Kob and Andersen (1993), and work on a three-dimensional cubic lattice. As in a hard sphere system, we assume no interaction between particles beyond the hard-core constraint that the occupation number n_i at site i is at most equal to 1,

$$H[\{n_i\}] = 0, n_i = 0, 1. \qquad (27)$$

In contrast to the lattice glass model, all configurations respecting the hard-core constraint are allowed and are equally probable. Geometric frustration is instead introduced at the level of the kinetic rules, which are defined as constrained local moves. Namely, a particle can jump to a nearest neighbor site only if that site is empty (to satisfy the hard-core constraint), but, additionally, only if the sites occupied before and after the move have less than m neighbors, m being an adjustable parameter, which Kob and Andersen choose as $m = 4$ for $d = 3$ ($m = 6$ corresponds to the unconstrained lattice gas). The model captures the idea that if the liquid if locally very dense, no movement is possible while regions with low density move more easily.

Of course, such kinetically constrained lattice gases have been studied in various spatial dimensions, for different values of m, for different constraints, or even different lattice geometries (Ritort and Sollich 2003). These models capture the idea of a "cage" effect in a strict sense, meaning that a particle with a dense neighbor shell cannot diffuse. Although the cage seems a purely local concept, it turns out that diffusion in constrained lattice gases arises from cooperative rearrangements, so that slow dynamics can be directly shown to be driven by the growth of dynamic lengthscales for these cooperative moves (Franz et al. 2002; Toninelli et al. 2004; Pan et al. 2005). This strongly suggests that such cooperative moves most probably have a role in the dynamics of real liquids.

Free Volume, Dynamic Criticality

In the lattice gas picture, the connection with the liquid is not obvious because it is the density ("free volume") rather than the temperature that controls the dynamics. Thermal models with similar features can in fact be defined along the

following lines. In a liquid, low temperature implies a very small probability to find a location with enough free volume to move. The idea of a small concentration of "hot spots" is in fact reminiscent of another picture of the glass transition based on the idea of "defects" which is captured by the defect model proposed by Glarum ([1960]) in the 1960s, where relaxation proceeds via the diffusion of a low concentration of independent defects. In the mid-1980s, using both ideas of kinetic constraints and rare defects, Fredrickson and Andersen defined a family of kinetic Ising models for the glass transition (Fredrickson and Andersen [1984]). They studied an assembly of noninteracting spins,

$$H[\{n_i\}] = \sum_{i=1}^{N} n_i, n_i = 0, 1, \qquad (28)$$

where $n_i = 1$ represents the defects, whose concentration becomes exponentially small at low temperature, $\langle n_i \rangle \approx \exp(-1/T)$. As for the Kob-Andersen lattice gas, the nontrivial ingredient lies in the chosen rates for the kinetic transitions between states. The kinetic rules stipulate that a transition at site i can happen with a usual Glauber rate, but only if site i is surrounded by at least k defects ($k = 0$ corresponds to the unconstrained limit). Again, one can easily imagine studying such models in different spatial dimensions, on different lattices, and with slightly different kinetic rules, yielding a large number of possible behaviors (Ritort and Sollich [2003]; Léonard et al. [2007]). The similarity between those spin facilitated models and the kinetically constrained lattice gases is striking. Altogether, they form a large family of models generically called kinetically constrained models (KCMs) (Ritort and Sollich [2003]).

The connection between KCMs and the much older concept of free volume is obvious from our presentation. Free volume models are among the most widely used models to analyze experimental data, especially in polymeric systems. They have been thoroughly reviewed before (Debenedetti [1996]; Cohen and Grest [1982]), and the main prediction is that dynamic slowing down occurs because

the free volume available to each particle, v_f, vanishes at some temperature T_0 as $v_f \approx \alpha(T - T_0)$. Statistical arguments then relate relaxation timescales to free volume assuming that a movement is possible if locally there is "enough" available free volume, more than a typical value v_0. This is clearly reminiscent of the above idea of a kinetic constraint for local moves in lattice gases. An appealing VFT divergence is then predicted:

$$\frac{\tau_\alpha}{\tau_0} \sim \exp\left(\gamma \frac{v_0}{v_f}\right) \tilde{\exp}\left(\frac{\gamma v_0/\alpha}{|T - T_0|^\mu}\right), \qquad (29)$$

where γ is a numerical factor and $\mu = 1$. Predictions such as Eq. ([29]) justify the wide use of free volume approaches, despite the many (justified) criticisms that have been raised.

Initially it was suggested that KCMs would similarly display finite temperature or finite density dynamic transitions similar to the one predicted by the mode-coupling theory of supercooled liquids (Fredrickson and Andersen [1984]), but it was soon realized (Fredrickson and Brawer [1986]; Butler and Harrowell [1991]) that most KCMs do not display such singularity, and timescales in fact only diverge in the limit of zero temperature ($T = 0$) or maximal density ($\rho = 1$). Models displaying a $T_c > 0$ or $\rho_c < 1$ transition have also been introduced and analyzed (Toninelli et al. [2006]). They provide a microscopic realization, based on well-defined statistical mechanics models, of the glass transition predicted by free volume arguments. Their relaxation timescale diverges with a VFT-like form but with an exponent $\mu \simeq 0.64$. Understanding their universality classes or the degree of generality of the mechanism leading to the transition is still an open problem (Elmatad et al. [2009], [2010]; Elmatad and Keys [2012]); the most recent results on this front come from mathematical physicists who have been able to classify many of the different possible behaviors on the basis of the microscopic dynamical rules (Hartarsky et al. [2019a], [b]; Martinelli et al. [2019a], [b]).

Extensive studies have shown that KCMs have a macroscopic behavior which resembles the phenomenology of supercooled liquids, displaying in

particular an Arrhenius or super-Arrhenius increase of relaxation timescales upon decreasing temperature, and non-exponential relaxation functions at equilibrium (Ritort and Sollich 2003). Early studies also demonstrated that, when suddenly quenched to very low temperatures, the subsequent nonequilibrium aging dynamics of these models compares well with experimental observations on the aging of liquids (Fredrickson and Brawer 1986). The diverse definitions of such models suggest a broad variety of different behaviors. This feature is both positive and negative: on the one hand one can explore various scenarios to describe glass transition phenomena, but on the other hand, one would like to be able to decide what particular model should be used to get a quantitative description for a particular liquid. It is not straightforward to perform microscopic predictions using the framework of KCMs, since there is no direct observable parameter to use as input of the theory (unlike $g(r)$, for MCT). An operative definition of KCMs' defects was provided (see next section and Keys et al. (2011, 2013)); however, this does not allow to directly choose which KCM (which rules) are appropriate for a given liquid.

Despite this caveat, it is quite useful to use KCMs as theoretical tools to define concepts and obtain new ideas. It is precisely in this perspective that interest in KCMs has increased, in large part since it was realized that their dynamics is spatially heterogeneous (Franz et al. 2002; Butler and Harrowell 1991; Garrahan and Chandler 2002), a central feature of supercooled liquids dynamics. In particular, virtually all the aspects related to dynamic heterogeneity mentioned in section "Dynamic Heterogeneity" can be investigated and rationalized, at least qualitatively, in terms of KCMs. The dynamics of these systems can be understood by considering where "relaxation" happens and then propagate, which is dictated by the underlying defect motion (Ritort and Sollich 2003). Depending on the particular model, defects can diffuse or have a more complicated motion. Furthermore, they can be point-like or "cooperative" (formed by point-like defects moving in a cooperative way). A site can relax only when it is visited by a defect. As a consequence, the heterogeneous character of the dynamics is entirely encoded in the defect configuration and defect motion (Garrahan and Chandler 2002). For instance, a snapshot similar to Fig. 6 in a KCM shows clusters which have relaxed within the time interval t (Whitelam et al. 2005; Berthier and Garrahan 2005). These are formed by all sites visited by a defect between 0 and t. The other sites are instead frozen in their initial state. In these models the dynamics slows down because the defect concentration decreases. As a consequence, in the regime of slow dynamics there are few defects and strong dynamic heterogeneity. Detailed numerical and analytical studies have indeed shown that in these systems, non-exponential relaxation patterns do stem from a spatial, heterogeneous distribution of timescales, directly connected to a distribution of dynamic lengthscales (Toninelli et al. 2004, 2006; Pan et al. 2005; Garrahan and Chandler 2002; Whitelam et al. 2005; Jack et al. 2006a). Decoupling phenomena also appear naturally in KCMs and can be shown to be very direct, quantifiable, consequences of the dynamic heterogeneity (Jung et al. 2004), which also deeply affects the process of self-diffusion in a system close to its glass transition (Berthier et al. 2004). More fundamentally, multipoint susceptibilities and multipoint spatial correlation functions such as the ones defined in Eqs. (8) and (11) can be studied in much greater detail than in molecular systems, relating their evolution to time and length scales (Berthier et al. 2007b; Toninelli et al. 2005; Pan et al. 2005; Chandler et al. 2006; Whitelam et al. 2004). This type of scaling behavior has been observed close to $T = 0$ and $\rho = 1$ in spin models and lattice gases without a transition. (Acritical (diérent) behavior is expected and predicted for models having a transition (Toninelli et al. 2006).) Different theoretical approaches have shown that these particular points of the phase diagram correspond to genuine critical points where timescales and dynamic lengthscales diverge with well-defined critical laws (Jack et al. 2006a; Whitelam et al. 2004). Such "dynamic criticality" implies the existence of universal scaling behavior in the physics of supercooled liquids, of the type reported for instance in Fig. 11.

Defects: Connection with Hamiltonian Dynamics Models

A central criticism about the free volume approach, that is equally relevant for KCMs, concerns the identification, at the molecular level, of the vacancies (in lattice gases), mobility defects (in spin facilitated models), or of the free volume itself. The attempts to provide reasonable coarse-graining from molecular models with continuous degrees of freedom to lattice models with kinetic rules have been, for a very long time, quite limited and not fully convincing (Gebremichael et al. 2004; Downton and Kennett 2007).

For molecular models, this issue was first attacked in 2010, with a definition of the cumulated dynamical activity K, an extensive quantity characterizing the frequency of state changes (from excited to non-excited and vice versa) (Elmatad et al. 2010; Hedges et al. 2009). This definition was made more concrete and studied in models of supercooled liquids in Keys et al. (2011), where an appropriate functional is explicitly designed as a recorder of excitations (or defects). Defects or excitations are not to be mistaken with displacements. Indeed, some locations providing opportunities for structural reorganization do coincide with defects, and their presence can be inferred by observing nontrivial particle displacements associated with transitions between relatively long-lived configurations. Displacements instead refer to dynamical moves in short segments of a trajectory, while defects refer to underlying configurations. The explicit definition of defects has since been used to estimate the role of facilitation in glassy dynamics, to provide a microscopic validation of KCMs (Keys et al. 2015; Isobe et al. 2016), to explain dynamical heterogeneities in glassy materials, or to compute the dynamical facilitation volume (Elmatad and Keys 2012).

The conceptual proof that kinetic rules emerge effectively and induce a slow dynamics has been obtained for simple lattice spin models (Garrahan 2002), with a dynamics that directly maps onto constrained models. A deeper study of this kind of model was performed more recently (Turner et al. 2015). Several examples are available but here we only mention the simple case of the bidimensional plaquette model defined by a Hamiltonian of a p-spin type on a square lattice of linear size L,

$$H = -J \sum_{i=1}^{L-1} \sum_{j=1}^{L-1} S_{i,j} S_{i+1,j} S_{i,j+1} S_{i+1,j+1}, \quad (30)$$

where $S_{i,j} = \pm 1$ is an Ising variable lying at node (i, j) of the lattice. Contrary to KCMs, the Hamiltonian in Eq. (30) contains genuine interactions, which are no less (or no more) physical than p-spin models discussed in section "Random First-Order Transition Theory." Interestingly the dynamics of this system is (trivially) mapped onto that of a KCM by analyzing its behavior in terms of plaquette variables, $p_{i,j} = S_{i,j} S_{i+1,j} S_{i,j+1} S_{i+1,j+1}$, such that the Hamiltonian becomes a non-interacting one, $H = -J \sum_{i,j} p_{i,j}$, as in Eq. (28). More interestingly, the analogy also applies to the dynamics (Garrahan 2002). The fundamental moves are spin-flips, but when a single spin is flipped the states of the four plaquettes surrounding that spin change. Considering the different types of moves, one quickly realizes that excited plaquettes, $p_{i,j} = +1$, act as sources of mobility, since the energetic barriers to spin flips are smaller in those regions. This observation allows to identify the excited plaquettes as defects, by analogy with KCMs. Spatially heterogeneous dynamics, diverging lengthscales accompanying diverging timescales and scaling behavior sufficiently close to $T = 0$ can be established by further analysis (Jack et al. 2005), providing a simple but concrete example of how an interacting many body system might effectively behave as a model with kinetic constraints. (This type of plaquette models and other spin models were introduced originally (Lipowski et al. 2000; Sethna et al. 1991) to show how ultraslow glassy dynamics can emerge because of growing free energy barriers.)

Connection with Other Perspectives

An essential drawback of facilitated models is that among the microscopic "details" thrown away to arrive at simple statmech models such as the ones in Eqs. (27) and (28), information on the thermodynamical behavior of the liquids has totally disappeared. In particular, a possible coincidence

between VFT and Kauzmann temperatures, To and T_K is not expected, nor can the dynamics be deeply connected to thermodynamics, as in Adam-Gibbs relations. The thermodynamical behavior of KCMs appears different from the one of real glass-formers close to T_g (Biroli et al. 2005). This is probably the point where KCMs and RFOT approaches differ most obviously. Even though the dynamics of KCMs shares similarities with systems characterized with a complex energy landscape (Berthier and Garrahan 2003; Whitelam and Garrahan 2004), thermodynamical behaviors are widely different in both cases, as has been recently highlighted in Jack and Garrahan (2005) by focusing on the concrete examples of plaquette models such as in Eq. (30).

Finally, when KCMs were first defined, they were argued to display a dynamical transition of a very similar nature to the one predicted by MCT (Fredrickson and Andersen 1984). Although the claim has been proven wrong, it bears some truth: both approaches basically focus on the kinetic aspects of the glass transition and they both predict the existence of some dynamic criticality with diverging lengthscales and timescales. (Most KCMs do not have a finite temperature dynamical transition and the ones displaying a transition have critical properties diérent from MCT.) This similarity is even deeper, since a modecoupling singularity is present when (some) KCMs are studied on the Bethe lattice (Toninelli et al. 2004), but is "avoided" when more realistic lattice geometries are considered (Berthier et al. 2012).

Geometric Frustration, Avoided Criticality, and Locally Preferred Structures

In all of the above models, "real space" was present in the sense that special attention was paid to different lengthscales characterizing the physics of the models that were discussed. However, apart from the "packing models" with hard-core interactions, no or very little attention was paid to the geometric structure of local arrangements in molecular liquids close to a glass transition. This slight oversight is generally justified using concepts such as "universality" or "simplicity," meaning that one studies complex phenomena using simple models, a typically statistical

mechanics perspective. However, important questions remain: what is the liquid structure within mosaic states? How do different states differ? What is the geometric origin of the defects invoked in KCMs? Are they similar to defects found in crystalline materials (disclinations, dislocations, vacancies, etc.)? Some lines of research attempt to provide answers to these questions, making heavy use of the concept of geometric frustration.

Geometric Frustration

Broadly speaking, frustration refers to the impossibility of simultaneously minimizing all the interaction terms in the energy function of a system. Frustration might arise from quenched disorder (as in the spin glass models described above), but liquids have no quenched randomness. In liquids, instead, frustration has a purely geometrical origin. It is attributed to a competition between a short-range tendency for the extension of a "locally preferred order," and global constraints that prevent the periodic tiling of space with this local structure.

This can be illustrated by considering once more the packing problem of spheres in three dimensions. In that case, locally the preferred cluster of spheres is an icosahedron. However, the fivefold rotational symmetry characteristic of icosahedral order is not compatible with translational symmetry, and formation of a periodic icosahedral crystal is impossible (Frank 1952). The geometric frustration that affects spheres in three dimensional Euclidean space can be relieved in curved space (Nelson 2002). In Euclidian space, the system possesses topological defects (disclination lines), as the result of forcing the ideal icosahedral ordering into a "flat" space. Nelson and coworkers developed a solid theoretical framework based on this picture to suggest that the slowing down of supercooled liquids is due to the slow wandering of these topological defects (Nelson 2002), but their treatment remains too abstract to obtain quantitative, explicit results. Further theoretical work extended the integral-equation approach to calculate the pair correlation function in hyperbolic geometry, making it easier to compare predictions and simulation data

(Sausset et al. 2009). MCT was also re-derived in curved space (on a sphere), showing that it still cannot capture quantitatively the transition (Vest et al. 2014, 2015). Explicit numerical results were also obtained recently (Turci et al. 2017a), showing a clear first-order like transition from liquid to ordered solid in an appropriately curved space, becoming avoided as Euclidean space is retrieved.

Coulomb Frustrated Theories

The picture of sphere packing disrupted by frustration has been further developed in simple statistical models characterized by geometric frustration, in a pure statistical mechanics approach (Tarjus et al. 2005). To build such a model, one must be able to identify, then capture, the physics of geometric frustration. Considering a locally ordered domain of linear size L, Kivelson et al. (1995) suggest that the corresponding free energy scales as

$$F(L,T) = \sigma(T)L^2 = \phi(T)L^3 + s(T)L^5. \quad (31)$$

The first two terms express the tendency of growing locally preferred order and represent respectively the energy cost of having an interface between two phases and a bulk free energy gain inside the domain. Geometric frustration is encoded in the third term which represents the strain free energy resulting from frustration. The remarkable feature of Eq. (31) is the super-extensive scaling of the energy cost due to frustration which opposes the growth of local order. The elements in Eq. (31) can then be directly incorporated into ferromagnetic models where "magnetization" represents the local order, ferromagnetic interactions represent the tendency to local ordering, and Coulombic antiferromagnetic interactions represent the opposite effect, coming from the frustration. The following Hamiltonian possesses these minimal ingredients:

$$H = -J\sum_{\langle i,j \rangle} \mathbf{S}_i \cdot \mathbf{S}_j + K\sum_{i \neq j} \frac{\mathbf{S}_i \cdot \mathbf{S}_j}{|\mathbf{x}_i - \mathbf{x}_j|}, \quad (32)$$

where the spin $\mathbf{S}_i$ occupies the site i at position $\mathbf{x}_i$. Such Coulomb frustrated models have been studied in great detail, using various approximations to study models for various space and spin dimensions (Tarjus et al. 2005).

The general picture is that the ferromagnetic transition occurring at $T = T_c^0$ in the pure model with no frustration ($K = 0$) is either severely displaced to lower temperatures for $K > 0$, sometimes with a genuine discontinuity at $K \to 0$, yielding the concept of "avoided criticality." For the simple case of Ising spins in $d = 3$, the situation is different since the second-order transition becomes first-order between a paramagnetic phase and a spatially modulated phase (stripes). For $K > 0$ and $T < T_c^0$ the system is described as a "mosaic" of domains corresponding to some local order, the size of which increases (but does not diverge!) when T decreases. Tarjus, Kivelson, and coworkers clearly demonstrated that such a structuration into mesoscopic domains allows one to understand most of the fundamental phenomena occurring in supercooled liquids (Tarjus et al. 2005). Their picture as a whole is very appealing because it directly addresses the physics in terms of the "real space," and the presence of domains of course connects to ideas such as cooperativity, dynamic heterogeneity, and spatial fluctuations, which directly explains, at least qualitatively, non-exponential relaxation, decoupling phenomena, or super-Arrhenius increase of the viscosity. However, as for the RFOT mosaic picture, direct confirmations of this scenario are rare (Coslovich and Pastore 2007), or difficult to obtain.

Locally Preferred Structures

Going back to the geometric structure of local arrangements in real space, a line of research has emerged that is based upon some kind of local order (Coslovich 2011; Royall and Williams 2015; Malins et al. 2013a, b). Icosahedral order was initially shown to be linked to the dynamics of some binary mixtures. But more generally, for simple enough glass-formers, a broader variety of locally ordered structures can be defined (Royall and Williams 2015), such as, for example, defective icosahedron (Royall and Kob 2017). A vast body of literature has shown that these locally preferred structures (LPS) seem to correlate with

structural relaxation. Using trajectory path sampling (see section "*s-Ensemble and Large Deviations*"), it was found that LPS and dynamic activity play equivalent roles, and are therefore strongly correlated (Turci et al. 2017b, 2018). The increased number of LPS has also been linked to hindered crystallization (Turci et al. 2019). These multiple effects suggest the LPS impacts the dynamics in various ways.

For several systems in $d = 2, 3$, simple local order parameters measuring the distance from sterically favored structures (sixfold symmetry, angles, and closeness to local tetrahedron) have been spatially coarse-grained (Tong and Tanaka 2018), thus revealing a clear structure-dynamics relationship. The interpretation in Tong and Tanaka (2018) is that these LPS represent an indirect measurement of the true amorphous order. The very simple and widespread tetrahedral order has been observed in a variety of materials (Shi and Tanaka 2019). The LPS-dynamics correlation has also been confirmed recently in experiments on colloids (Hallett et al. 2018; Pinchaipat et al. 2017), providing further evidence of the important role of LPS in glassy behavior.

Despite these important advances, the concrete application of LPS-based techniques on any particular realistic glass-forming material is hindered by the lack of a universal operative definition of the LPS. For relatively simple systems, an operative scheme was designed to automatically find these LPS (Royall and Williams 2015; Mossa and Tarjus 2006).

A natural alternative to this tedious exercise is the use of modern machine learning techniques. In particular, one may consider the unsupervised learning task of grouping together similar local structures (this is called clustering). Once clusters (corresponding to automatically found LPS) are found, any local environment may be assigned to its most similar group (LPS), but without the burden of defining the LPS's one by one (Ronhovde et al. 2011, 2012; Paret et al. 2020; Boattini et al. 2020).

Mean-Field Theory of the Amorphous Phase

The phase transition between liquid and glass is not the only interesting phenomenon characterizing the phase diagram of glassy materials. Since the transition occurs at finite pressure and temperature, glasses can be further compressed or cooled within the glass phase itself (Kurchan et al. 2012, 2013; Biroli and Urbani 2018; Rainone and Urbani 2016; Rainone et al. 2015; Scalliet et al. 2019a). How do physical properties of glasses change in this context? In mean-field theory, this question has been widely investigated by using the hard spheres glass model (Parisi and Slanina 2000; Parisi and Zamponi 2010), a favorite canonical example of a glass-former system because of its analytical simplicity. Eventually, by compressing a hard sphere glass, the system undergoes the jamming transition in the limit of infinite pressure (Donev et al. 2004). In this section, we briefly survey recent progress in the development of an analytic theory of the glass phase in the large d limit, with a particular emphasis on hard spheres (Parisi et al. 2020).

Mean-Field Glassy Phase Diagrams

When a glass-forming liquid undergoes the glass transition, it becomes confined into a single free energy minimum and the timescale to explore different minima becomes infinite. It is formally possible to define thermodynamic properties by restricting the available statistical configurations to a single free energy minimum. This can be enforced in the replica formalism by considering two copies of the system and constraining the distance between them (Charbonneau et al. 2017). First, an equilibrium reference configuration $\underline{Y}$ at $\left(T_g, \widehat{\varphi}_g\right)$ is introduced, where $\widehat{\varphi}$ is the scaled packing fraction $\widehat{\varphi} = 2^d \varphi / d$. Second, a copy of the equilibrium configuration $\underline{X}(t)$ is created and evolved in time. Let us define now the mean-squared displacement (MSD) between the two copies as $\overline{\langle \Delta(X, Y) \rangle} = \Delta_r$. The properties of $\underline{X}(t)$ are sampled in a restricted region of phase space close to the equilibrium configuration.

Within this state following construction, the system at $\left(T_g, \widehat{\varphi}_g\right)$ with initial configuration $\underline{Y}$ can be adiabatically followed anywhere in the glass phase diagram.

Concretely, for the glass state selected by $\underline{Y}$ and followed until $(T, \widehat{\varphi})$, we can write the restricted partition function as:

$$Z[T, \widehat{\varphi}|\underline{Y}, \Delta_r] = \int d\underline{X} e^{-\beta V(\underline{X})} \delta(\Delta_r - \Delta(\underline{X}, \underline{Y})), \tag{33}$$

where $V(\underline{X})$ is the potential energy of the configuration $\underline{X}$, and the delta function enforces the restricted average. In order to obtain the glass free energy, we need to compute its average over the chosen reference configuration $\underline{Y}$, which acts as a source of quenched disorder:

$$f_g\left(T, \widehat{\varphi}|T_g, \widehat{\varphi}_g, \Delta_t\right) = -\frac{T}{N} \int \frac{d\underline{Y}}{Z\left[T_g, \widehat{\varphi}_g\right]} e - \beta_g V(\underline{Y})$$
$$\times \ln Z[T, \widehat{\varphi}|\underline{Y}, \Delta_r] \tag{34}$$

where $Z\left[T_g, \widehat{\varphi}_g\right] = \int dY \exp^{-\beta_g V(\underline{Y})}$ is the partition function at $\left(T_g, \widehat{\varphi}_g\right)$. Mathematically, the quenched disorder is handled using the replica method. We then introduce $(n + 1)$ replicas of the original system, with the initial glass at $\left(T_g, \widehat{\varphi}_g\right)$ being the master replica, while the n other slave replicas describe the glass at $(T, \widehat{\varphi})$. The glass free energy is finally expressed in terms of the average MSD between the slave replicas and the master replica Δ_r, and the average distance between the slave replicas Δ. At this step, we assume that the symmetry between slave replicas is not broken, which corresponds to the 1RSB ansatz described in section "Random First-Order Transition Theory."

By choosing the state point at $(T, \widehat{\varphi}) = \left(T_g, \widehat{\varphi}_g\right)$, the recursive equations for Δ and Δ_r have to satisfy $1/\widehat{\varphi} = \mathcal{F}_\beta(\Delta)$, where $\mathcal{F}_\beta(\Delta)$ is a positive function which vanishes for both $\Delta \to \infty$ and $\Delta \to 0$, with an absolute maximum in between. This equation can then be satisfied only if

$$\frac{1}{\widehat{\varphi}_d} \leq \max_\Delta \mathcal{F}_\beta(\Delta). \tag{35}$$

This condition occurs for volume fractions larger than a critical value $\widehat{\varphi}_d\left(\beta_g\right)$, which corresponds to the dynamical glass transition.

We can explore the glass phase following the glass prepared at the glass transition $\left(T_g, \widehat{\varphi}_g\right)$ at different temperatures and packing fractions. At low T and high $\widehat{\varphi}$ one eventually meets another phase transition (Kurchan et al. 2013), where the 1RSB assumption fails (Mézard et al. 1987) and the more complex full-replica symmetry breaking (fullRSB) solution is necessary to compute the glass free energy, the so-called Gardner phase transition (Gardner 1985; Berthier et al. 2019d). Here, the fullRSB solution corresponds to a hierarchical organization of the distances between the slave replicas and the glass becomes marginally stable (Rainone and Urbani 2016; Franz et al. 2017). The emergence of a complex free energy landscape gives rise to nontrivial dynamical processes (Scalliet and Berthier 2019; Liao and Berthier 2019; Scalliet et al. 2019b). A pictorial representation of the Gardner transition is shown in Fig. 15.

It is worth noting that the derivation sketched above is completely general and can be used for any glassy pair potential mentioned in section "Random First-Order Transition Theory." In the following we will apply this formalism to the hard spheres model, for which several implications from the mean field picture have been successfully tested numerically (Charbonneau et al. 2014b; Berthier et al. 2016a). Here, the relevant state parameter is the scaled reduced pressure $\widehat{p} = \beta P/\rho d$. We refer to Biroli and Urbani (2016, 2018), Berthier et al. (2019d), and Scalliet et al. (2017, 2019a, b) for more results regarding systems made of soft potentials.

Starting from an equilibrated hard sphere liquid configuration at $\widehat{\varphi}_g$, we can apply the state following formalism to explore the hard sphere

A Statistical Mechanics Perspective on Glasses and Aging, Fig. 15 (a) Sketch of the free energy structure deep in the hard sphere glass phase, where each basin breaks down in sub-basins corresponding to secondary relaxations. At the Gardner transition in (b), the sub-basins become fractal and ergodicity is broken
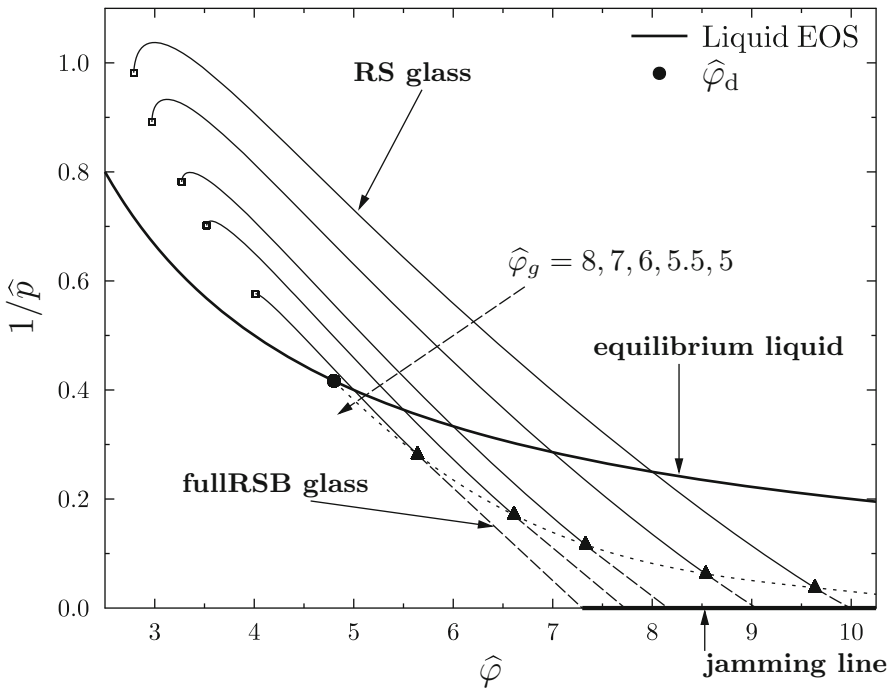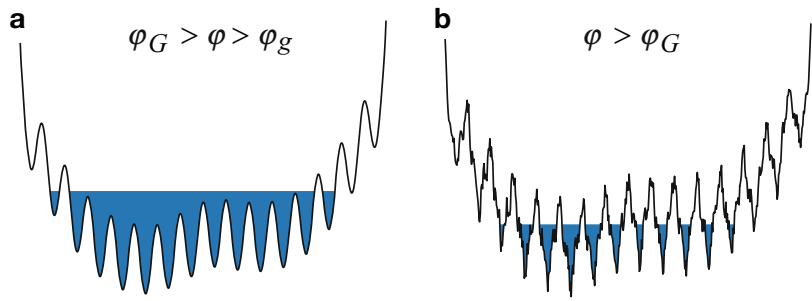
A Statistical Mechanics Perspective on Glasses and Aging, Fig. 16 Phase diagram of hard spheres in the inverse reduced pressure – reduced peaking fraction $(1/\widehat{p}, \widehat{\varphi})$ plane. The glass transition is marked by a full circle. The glass equations of state are reported as full lines in the region where the replica symmetric solution is stable.

The Gardner transition is marked by triangles, beyond which the fullRSB solution is stable (dashed lines). Tice glass equations of state end at the jamming transition. Upon decompression, glasses are stabile until a spinodal instability arises (open squares)

phase diagram in Fig. 16. The reduced pressure can lie computed from the equation of state of an infinite dimensional hard sphere liquid $\widehat{p}\,\widetilde{\widehat{\varphi}}/2$,

derived from a Virial expansion of the free energy (Maimbourg et al. 2016). Starting from $\widehat{\varphi}_g$ and decompressing the system, the glass eventually

undergoes a melting transition: the 1RSB solution becomes unstable and the glass melts into the liquid via a spinodal instability (Kurchan et al. 2013). Upon compression instead, the glass enters deeper into the glass phase and remains dynamically arrested. Numerically, this has been proven by measuring Δ as the long-time limit of the MSD $\Delta(t)$ between the system at time t and the initial configuration at $t = 0$. The order parameter of the transition Δ_r is instead computed as the long-time limit of the distance $\Delta ab(t)$ between two copies A and B of the same initial system evolved with different initial velocities:

$$\Delta_{AB} = \left\langle \frac{1}{N} \sum_{i=1}^{N} \left| \mathbf{r}_i^A - \mathbf{r}_i^B \right|^2 \right\rangle. \qquad (36)$$

Upon further compression, the glass eventually undergoes the Gardner transition at a finite pressure $\widehat{p}_G$. Here, the relation between Δ_r and Δ breaks down and $\Delta(t)$ is characterized by a logarithmic growth in time, suggesting the emergence of a complex free energy landscape (Berthier et al. 2016a). The copies A and B cannot occupy the same sub-basin and are no longer able to explore the entire metabasin. Due to the fractal nature of the free energy landscape, the excitations required to move around the fractal states correspond to soft modes (Scalliet et al. 2019b). The correlation length of these modes can be estimated by measuring the dynamical susceptibility, computed as the variance of Δ_{AB}, which indeed shows a divergence at the Gardner transition (Berthier et al. 2016a).

Compressing further within the Gardner phase, the pressure eventually diverges as the system reaches its jamming density $\widehat{\varphi}_J$, which depends explicitly on the selected initial condition $\left(T_g, \widehat{\varphi}_g\right)$. In particular, there exists a range of jamming points, or a "jamming line" (Chaudhuri et al. 2010), whose extension increases with d (Kurchan et al. 2012).

Jamming

During the last two decades, a large research effort has shed light on the critical behavior characterizing the jamming transition (Liu and Nagel 2010). Jamming can be seen from two different perspectives. An assembly of Brownian hard spheres under compression becomes rigid at a finite density, at which point the pressure diverges. On the other hand, athermal packings of soft repulsive spheres reach the jamming point under decompression when the pressure vanishes. In both situations, each particle is constrained by enduring contacts with the neighbor particles and the system is rigid. In particular, at jamming the average number of contacts per particle Z reaches the critical value $Z_c = 2d$, which represents the lower limit for mechanical stability (O'Hern et al. 2002) (Maxwell's criterion for rigidity). From the hard spheres side, Z jumps from zero to Z_c at the transition, while from the soft spheres side, as the pressure decreases toward zero the excess number of contacts scales as (Ohern et al. 2003; Durian 1995):

$$\Delta Z = Z - Z_c \tilde{\Delta} \varphi^{1/2}, \qquad (37)$$

where $\Delta \varphi = \varphi - \varphi_J$ is the amount of compression above the jamming threshold. A connection between hard and soft spheres at jamming is observed in the pair correlation function (Donev et al. 2005; Ohern et al. 2003), confirming that allowed configurations of hard and soft spheres are identical at jamming.

When $\Delta Z = 0$ the system is isostatic, that is, there are just enough contacts to ensure mechanical stability and the system is marginally stable: breaking a bond between contacts can lead to an excitation that causes a collective motion throughout the whole system (Wyart 2012). Not surprisingly, this critical behavior fits well into the free energy picture of marginal glasses reported above.

Marginality in athermal jammed solids can be explained in real space by the so-called cutting argument (Wyart et al. 2005). Imagine removing the contacts between a subsystem of linear size l and the rest of the system. If we slightly compress the system, this cutting will lead to a

competition between the overall excess contacts ΔZ created by the compression, and the missing contacts at the boundary of the subsystem. If the total number of contacts is below the isostatic value $N_{iso} = NZ/2$, then there are modes with no energetic cost, that is, soft modes. The number of soft modes N_{soft} then corresponds to the difference between the number of contacts at the boundary, proportional to l^{d-1}, and the number of extra contacts created by the compression, which scales as $\Delta Z l^d$. There is then a critical length $l^* \sim \Delta \varphi^{-1/2}$ for which the system looks isostatic and for $l = l^*$, soft modes correlate over the whole subsystem. These extended anomalous modes correspond to random excitations over all the system, profoundly different from acoustic modes proper of crystalline solids.

Other anomalies of jammed solids are observed in the scaling of the elastic moduli near the transition. These critical behaviors have been successfully described within a force network picture, for which en effective medium theory has been developed (Wyart 2010; Degiuli et al. 2015). In particular, a jammed soft sphere configuration can be mapped onto a network of springs with elastic contacts k_{eff}, computed as second derivatives of the pairwise interaction between particles. The resulting scaling behaviors for the bulk modulus $B \sim k_{\text{eff}}$ and the shear modulus $G \sim k_{\text{eff}} \Delta \varphi^{1/2}$ suggest that the Poisson ratio $G/B \sim \Delta \varphi^{1/2}$ vanishes at the jamming transition (Ohern et al. 2003). This criticality reflects on the frequency of normal modes which is directly related to the elastic moduli ($B(\omega)$, $G(\omega)$) by the dispersion relation $\omega^* = ck^*$, where $k^* \sim 1/l^*$ and c is the speed of sound. Since sound propagates either longitudinally (B) or transversely (G), two different length scales can be defined: the longitudinal length scale $l^* \sim \Delta \varphi^{-1/2}$, which matches the cutting length scaling behavior and is indeed attributed to extended soft modes, and the transverse length scale which follows the scaling $l_t \sim \Delta \varphi^{-1/4}$.

Other critical scaling laws have been predicted both by replica mean field calculations and effective medium theory for a spring network, with good consistency with numerical results in finite dimensions. In particular, the distributions of interparticle voids and interparticle forces follow universal power laws (Charbonneau et al. 2012, 2015; DeGiuli et al. 2014; Lerner et al. 2013). Contact forces can be either extended or localized, with distributions defined by power law exponents θ_e and θ_l, respectively. Extended forces are predicted from the infinite dimensional exact solution, whereas the localized forces likely result from the presence of localized defects, such as rattling particles, which only exist in finite dimensions. Remarkably, the numerical value of the critical exponents associated to scaling laws near jamming can be predicted analytically in the mean-field approach (Charbonneau et al. 2014a, b; Parisi et al. 2020), and their value is confirmed by numerical simulations in dimensions $d \geq 2$.

The influence of temperature on the jamming criticality has also been studied (Degiuli et al. 2015; Ikeda et al. 2013). These works show that above jamming there exists a region in the plane $T - \varphi$ where the harmonic approximation of the soft sphere potential holds, and the vibrational spectrum converges to its zero temperature limit, provided that $T < T^*(\varphi)$. The value of $T^*(\varphi)$ decreases with $\Delta \varphi \to 0$ with a trivial scaling exponent. A similar result holds below jamming for hard sphere glasses (Brito and Wyart 2009). For $T > T^*(\varphi)$, the harmonic approximation breaks down, defining an anharmonic critical regime, controlled by nonanalyticities in the interparticle potential. Physically, strong anharmonicites stem from the constant breaking and reformation of particle contacts in the presence of thermal fluctuations (Schreck et al. 2011).

Vibrational Properties

The anomalous thermal properties of low temperature glasses can be related to the structure of the free energy landscape of glassy states. Amorphous solids behave very differently from crystalline solids. In terms of heat capacity and thermal conductivity, crystals are dominated by phononic excitations with a low-frequency density of states (DOS) $D(\omega)$ given by the Debye scaling law $D(\omega) \sim \omega^{d-1}$. Instead, the thermal properties of glasses are dominated by an excess of vibrational modes referred to as the boson peak and by an anomalous low-frequency scaling of $D(\omega)$. This excess of anomalous vibrations reflects, within

mean-field theory, the existence of multiple free energy barriers in glassy states. In fact, when the glass enters the Gardner phase, the system becomes marginal and even infinitesimal perturbations lead to excitations that can bring the system to a different glassy state.

The mean-field theory of glasses has been explored using soft spheres in the jamming limit (Franz et al. 2015). The theory predicts the low-frequency scaling of the vibrational density of states (vDOS) to be $D(\omega) \sim \omega^2$ in any dimension (Parisi and Zamponi 2010; Wyart 2010; Berthier et al. 2011b), quite differently from the Debye scaling. The same result was previously obtained within the effective medium theory (DeGiuli et al. 2014).

Numerically, the nature of the low-frequency vibrational spectrum has been widely studied using soft spheres packings close to jamming. Early studies suggested the existence of the $D(\omega) \sim \omega^2$ scaling (Charbonneau et al. 2014b; Franz et al. 2015) for a wide range of dimensions d, reinforcing the relevance of the mean-field description for finite dimensional systems (Charbonneau et al. 2016a). The modes giving rise to this scaling form have been found to be extended anomalous modes. A more recent study established that the ω^2 scaling is only observed over a finite frequency range, which seems to increase systematically with the space dimension d, which is consistent with a pure quadratic scaling when $d = \infty$. However, for any finite d, the density of states eventually obeys Debye scaling for sufficiently low frequencies.

Finally, recent numerical works show that for frequencies lower than the boson peak, an additional family of soft modes due to marginal instabilities can be observed (Mizuno et al. 2017; Lerner et al. 2016). As Fig. 17 shows, the vibrational density of these additional modes scales as ω^4. A spatial analysis of such modes shows that they correspond to quasi-localized modes, which are again absent from the large d analytic description.

Rheology

Once the glass is created, it can be adiabatically cooled or compressed, but it can also be deformed by applying an external mechanical constraint. The rheology of amorphous solids is a very broad research field. Here, we present recent results in this field obtained using the mean field glass theory, including implications regarding elasticity, yielding, and shear jamming (Rainone and Urbani 2016; Rainone et al. 2015; Biroli and Urbani 2016; Yoshino and Zamponi 2014).

We report results obtained from the same state following formalism applied to study the amorphous phase along a compression in the $d \to \infty$ limit. If the master replica $\underline{Y}$ is in the dynamically arrested region, the system reacts elastically to a small applied strain γ. We can then obtain the stress-strain curve as a function of the state point $(T, \widehat{\varphi})$ of the slave replica $\underline{X}$. The stress for an elastic medium increases linearly with strain, which defines the shear modulus $\widehat{\mu} = \frac{d\widehat{\sigma}}{d\gamma}$ computed at zero strain, where stress and shear modulus are scaled such that the $d \to \infty$ limit remains finite. In the small strain limit one finds

$$\widehat{\mu} = \frac{1}{\Delta} \tag{38}$$

where Δ is the long time limit of the MSD. The MSD $\Delta(\underline{X}, \underline{Y})$ is the superposition of an affine component due to the strain, and of a non-affine contribution defined by the particular shear protocol. At the glass transition, the shear modulus jumps from a zero value (liquid state) to a finite value at $\widehat{\varphi}_d$ (glass state). In finite dimensions, this sharp discontinuity becomes a crossover (Parisi et al. 2020).

When the system is confined within a glass state, it is able to sustain a shear strain on a time scale which corresponds to the diverging time scale for which the dynamics becomes diffusive. One can then follow adiabatically the slave replica until a state point $(T, \widehat{\varphi})$ and study the linear response to shear for the different phases of the glass. This corresponds to exploring the strain vs volume fraction phase diagram of the system. Upon decompression, the shear modulus decreases and displays a square root singularity at the melting spinodal point (Parisi et al. 2020; Rainone et al. 2015).
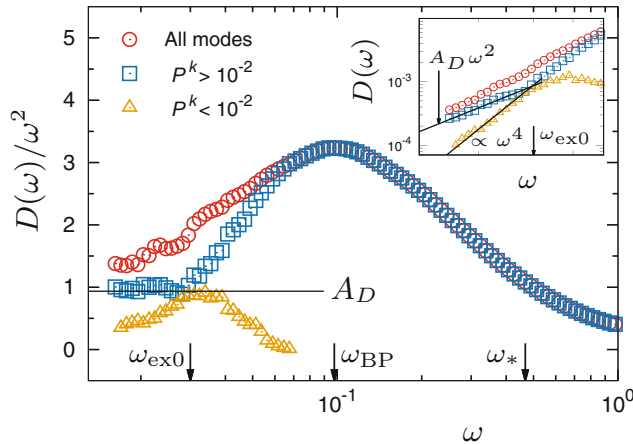
A Statistical Mechanics Perspective on Glasses and Aging, Fig. 17 Adapted from (Mizuno et al. 2017). Vibrational density of states of jammed harmonic soft spheres scaled by the Debye law ω^{d-1} in $d = 3$. Modes with index k are classified as extended (blue) or localized (yellow) by their participation ratio P^k. Below the boson peak frequency ω_{BP}, the density of states is the superposition of anomalous extended modes eventually obeying Debye scaling, and a population of quasi-localized modes scaling as ω^4, as confirmed in the inset

Increasing the strain and/or the volume fraction, the glass phase may undergo a Gardner transition and transform into a marginal glass, for which all nonlinear elastic moduli diverge and standard elasticity theory does not hold anymore (Biroli and Urbani 2016). As for a simple compression without shear, the boundary of the Gardner phase transition explicitly depends on the selected glass state.

Once the Gardner phase is entered, upon further compression or strain, two kinds of transition may occur in hard sphere glasses. First, the shear modulus may increase and eventually diverge when a jamming point is reached. At zero strain, this is the ordinary jamming transition. In that case, the power law scaling of the MSD directly implies a similar behavior for the shear modulus. In the presence of a finite strain, this corresponds to the phenomenon of shear jamming, observed in the context of granular materials (Urbani and Zamponi 2017; Peters et al. 2016).

A second type of instability can occur when increasing the strain of a hard sphere glass. Here, the shear stress reaches a maximum followed by a spinodal instability where the fullRSB solution for Δ and Δ_r is no longer stable. The spinodal point $\gamma_Y\left(\widehat{\varphi}_g\right)$ corresponds to the glass yielding transition (Urbani and Zamponi 2017; Parisi et al.

2017). The yielding transition in glasses has been studied for a variety of models and under different physical conditions (Lin et al. 2014; Ozawa et al. 2018b). In particular, it has been suggested that the yielding transition belongs to the same universality class as the RFIM, that is, a spinodal transition with disorder.

New Computational Methods

In the last decade, a number of new numerical techniques have allowed to attack the challenges presented in the above theoretical sections. These techniques typically make use of tools that go beyond the realm of standard computer simulations to either sample phase space more efficiently or access information and observables that are not directly stored in particle trajectories.

The Swap Monte-Carlo Method
To sample deeply supercooled states in equilibrium, one needs to run computer simulations over a duration that scales with the equilibrium structural relaxation time τ_α. Because τ_α grows rapidly as the system approaches the glass transition, ordinary computer simulations are limited to a

A Statistical Mechanics Perspective on Glasses and Aging, Fig. 18 From (Ninarello et al. 2017). Relaxation times for standard (open symbols) and swap (closed symbols) Monte Carlo dynamics. The standard dynamics is fitted with the VFT, parabolic, and Arrhenius laws, which are then used to estimate the location of the experimental glass temperature T_g (vertical dashed lines). The swap dynamics efficiently equilibrates the system at temperatures below T_g
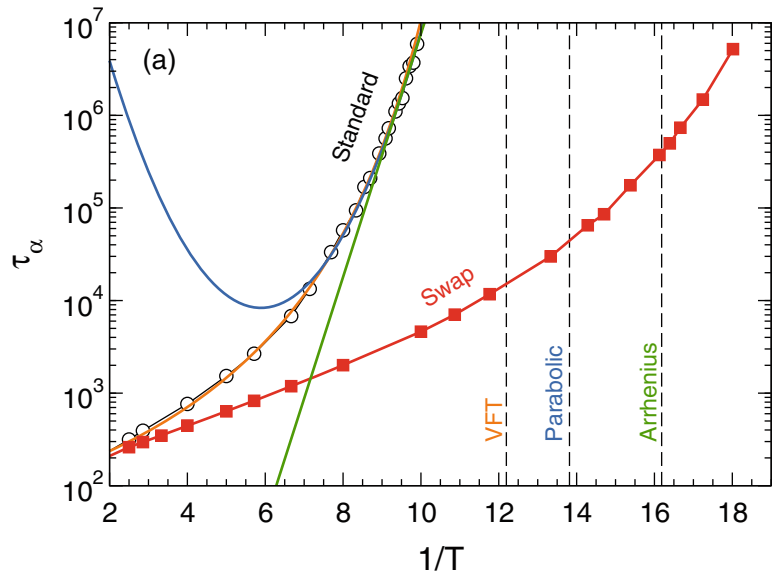
rather high temperature regime much above the experimental glass transition T_g.

The swap Monte Carlo algorithm is an efficient way to produce equilibrium configurations of a supercooled liquid on the computer (Berthier et al. 2016b; Ninarello et al. 2017). Here, "efficient" means that the equilibration time of the swap Monte Carlo algorithm increases much less than τ_α as temperature decreases. Actually, it was shown that for several three-dimensional model systems, the equilibration speedup can be larger than a factor 10^{11}, as illustrated in Fig. 18. For this particular model of soft spheres, the swap algorithm continues to reach thermal equilibrium below the experimental glass transition T_g.

The swap algorithm was introduced long ago (Gazzillo and Pastore 1989), and it was first used in the context of the glass transition by Grigera and Parisi (2001). Its ability to reach equilibrium at extremely low temperatures was established more recently (Berthier et al. 2016b; Ninarello et al. 2017; Ninarello 2017). By comparison with ordinary computer simulations, the swap Monte Carlo algorithm introduces unphysical particle moves, where the identity of a pair of randomly chosen particles is exchanged. Provided the swap moves are constructed to satisfy detailed balance, the algorithm is guaranteed to reach thermal equilibrium. The swap Monte Carlo

algorithm can be implemented in a molecular dynamics setting, replacing the swap moves by an exchange between the system and a reservoir of particles (Brito et al. 2018; Kapteijns et al. 2019; Berthier et al. 2019e). Typically, increasing the frequency of swap moves speeds up the dynamics but there are practical limits to the maximal allowed frequency (Berthier et al. 2019e). The swap algorithm was shown to work well from $d = 2$ up to at least $d = 8$ dimensions (Berthier et al. 2019f).

A decisive step to increase the efficiency of the swap Monte Carlo algorithm was the development of models for supercooled liquids that were tailored to increase the swap efficiency. However, and perhaps more importantly, many models that were previously thought to be good glass-formers were in fact crystallizing very easily when swap was employed. Thus, a key step was also the development of more robust glass-forming models, using size polydispersity and nonadditive interaction parameters to prevent structural ordering (Ninarello et al. 2017; Parmar et al. 2020).

In summary, the swap Monte Carlo algorithm easily and rapidly produces a large number of independent equilibrium configurations of a glass-former over a very broad range of temperatures, from the high temperature liquid, down to the mode-coupling crossover, and even below the experimental glass transition temperature. The

latter regime can be explored experimentally only using physical vapor deposition, see section "Ultrastable Glasses." Therefore, many physical properties of glassy materials can now be measured over a temperature regime that is extremely broad, and may be compared directly to experiments with no extrapolation. This has led to an important activity to address several problems related to glassy materials: the Gardner transition in finite dimensional glass-formers (Liao and Berthier 2019; Scalliet et al. 2019b; Berthier et al. 2016a), the link between glass and jamming transitions (Berthier et al. 2016b; Coslovich et al. 2018), the measurement of the configurational entropy in deeply supercooled liquids (Ozawa et al. 2018c; Berthier et al. 2019g), the analysis of point-to-set lengthscales (Berthier et al. 2017c; Yaida et al. 2016) and of the Franz-Parisi potential (Berthier et al. 2017c; Guiselin et al. 2020), the evolution of several important properties of glasses with the glass preparation (Khomenko et al. 2020; Wang et al. 2019a; Wang et al. 2019b), and the physics of ultrastable glasses (Berthier et al. 2017b; Flenner et al. 2019).

In addition, the demonstration that a very simple algorithm can speed up the equilibration dynamics of supercooled liquids can be seen as an interesting physical result in itself. If such a result appears quite natural in the context of kinetic facilitation (Wyart and Cates 2017; Gutiérrez et al. 2019), it is more challenging (but possible) to interpret in the context of the random first-order transition theory (Berthier et al. 2019c; Ikeda et al. 2017b; Szamel 2018), where dynamics becomes highly collective at very low temperatures.

Franz-Parisi Potential

In seminal work (Franz and Parisi 1997; Franz and Parisi 1998), Franz and Parisi introduced a quantity now called the Franz-Parisi potential, $V(Q)$. This quantity plays the role of a Landau free energy for mean-field phase transitions, in the sense that it expresses the free energy cost of the order parameter fluctuations at the mean-field level.

For spin glass models, where the approach was first introduced, the overlap Q represents indeed the spin glass order parameter. It quantifies the degree of similarity between two configurations C_0 and C_1. For liquids with continuous degrees of freedom, a practical definition of the overlap reads:

$$Q = \frac{1}{N} \sum_{i=1}^{N} \sum_{j=1}^{N} \Theta \left(a - |\mathbf{r}_i^{C_0} - \mathbf{r}_j^{C_1}| \right), \qquad (39)$$

where $\mathbf{r}_i^{C_0}$ represents the position of particle i in configuration C_0. The overlap is close to unity when the two configurations C_0 and C_1 have similar density profiles, up to thermal vibrations of spatial extension a (typically, one takes a as a small fraction of the particle diameter, $a \sim 0.2\sigma$).

The Franz-Parisi potential $V(Q)$ efficiently captures all the features associated to a random first-order transition. It can be defined from the probability distribution function $P(Q)$ of the overlap as $V(Q) = -(T/N) \log P(Q)$. In particular, $V(Q)$ is characterized by a single minimum near $Q = 0$ at high temperature, but develops within mean-field theory a secondary minimum at a finite $Q > 0$ when T decreases toward the Kauzmann transition, indicating that the glass phase is metastable with respect to the liquid. The free energy difference between the glass and the liquid phases in this regime is given by $TS_c(T)$, where $S_c(T)$ is the configurational entropy. Physically, this means that localizing the system in a single free energy minimum in the liquid phase comes with a free energy cost of entropic nature.

In addition, Franz and Parisi introduced a field ε conjugate to the overlap Q:

$$H_{FP}[C_1] = H[C_1] - \varepsilon Q[C_0, C_1]. \qquad (40)$$

This allowed them to explore an extended phase diagram by changing both T and ε (Cardenas et al. 1999; Donati et al. 2002). In this plane, the Kauzmann transition at $(T = T_K, \varepsilon = 0)$ extends as a first-order transition line, which ends at a second-order critical point at a position $(T_c > T_K, \varepsilon_c)$. More recent work taking into account finite dimensional fluctuations suggest that this critical point should exist also in finite dimensions, and should be in the same universality class of the random field Ising model (Biroli et al. 2014).

The Franz-Parisi potential and the extended phase diagram have been studied numerically in finite dimensional models in recent years (Turner et al. 2015; Berthier et al. 2017c; Guiselin et al. 2020; Cardenas et al. 1999; Berthier 2013; Biroli et al. 2016; Berthier and Jack 2015; Jack and Garrahan 2016; Parisi and Seoane 2014). Taken together, these studies confirm the existence of both a first-order transition line and a second-order RFIM critical point in finite dimensional glass-formers.

A second important outcome of the Franz-Parisi potential is the possibility to directly estimate a configurational entropy for equilibrium glass-formers using the free energy difference between the liquid and metastable glass phase (Berthier et al. 2017c; Berthier and Coslovich 2014). This definition of the configurational entropy is conceptually closer to its mean-field definition, and does not rely on an explicit definition of metastable states for a finite dimensional system (Berthier et al. 2019a).

Point-to-Set Lengthscale
As mentioned in section "Static and Dynamic Correlation Functions," assessing and measuring a growing static length scale is crucial to the glass problem. Standard probes used for second-order phase transitions, such as 2-point and 4-point correlation functions, do not seem to provide any useful evidence. A possible explanation is that these correlation functions do not carry enough information to capture the relevant structural order, also termed amorphous order, and that one has to use higher-order correlation functions (see also section "Jamming Transition"). The point-to-set correlation function $C(R)$ is effectively an n-point correlation function, where n is the number of particles comprised in a sphere of radius R (the "set"), which can indeed be a large number.

The justification is that in order to probe amorphous order one has to proceed as in standard phase transitions: fix a suitable boundary condition and study whether it enforces a given arrangement of particles in the bulk of the system. For simple cases, such as the ferromagnetic Ising model, it is clear what type of boundary conditions are needed (all spins up or all spins down).

However, for supercooled liquids this is a much harder task. The problem can be circumvented by using equilibrated configurations and freezing all particles outside a cavity of radius R. This provides the boundary conditions sought for: if the system is indeed ordering, then using cavities drawn from different equilibrium configurations will give access to different sets of appropriate boundary conditions. This method was first proposed theoretically in the context of RFOT theory (Bouchaud and Biroli 2004; Montanari and Semerjian 2006) and signal processing (Mézard and Montanari 2006), and was transformed into a concrete numerical procedure in Cavagna et al. (2007) and Biroli et al. (2008). In the last decades, measurements of the point-to-set length were progressively refined (Berthier and Kob 2012; Berthier et al. 2016c, 2017c; Yaida et al. 2016; Cavagna et al. 2012; Charbonneau et al. 2016b).

Let us describe the main steps and mention some important obstacles that had to be overcome. Firstly, one needs a collection of well-equilibrated configurations $\mathcal{C}_0$ to start with. This is not supposed to be the hardest part, but for very low temperatures, methods such as the swap Monte Carlo algorithm are necessary.

Secondly, for each sample $\mathcal{C}_0$ one freezes all particles outside a cavity of radius R, then let the particles inside ergodically visit the remaining phase space, and record the configurations $\mathcal{C}_1$ that are sampled. For small cavities, large activation barriers make conventional molecular dynamics simulations ineffective, but this problem can be solved using parallel tempering techniques (Berthier et al. 2016c), in addition to swap Monte Carlo (Cavagna et al. 2012). It is crucial to check that a complete sampling of the restricted configurational space has been reached inside the cavity, and careful tests have been devised to this end (Cavagna et al. 2012).

Thirdly, one needs to measure the overlap distribution $P(Q)$ between the quenched reference configuration $\mathcal{C}_0$ and the equilibrium samples $\mathcal{C}_1$. This is very similar to the Franz-Parisi construction, except for the local nature of the constraint. There are two possibilities. One is that the cavity is so small that only one state (one configuration, up to vibrations) can be visited, so that the peak of

$P(Q)$ is in the high-overlap range. The other is that the cavity is sufficiently large for many different states to be accessible. In that case, $P(Q)$ has a peak at low Q. In between the two cases, there is a critical value of the radius, $R \sim \xi_{PTS}$, which corresponds to the crossover, with a bimodal $P(Q)$. Since finite size cavities cannot be self-averaging, one needs to repeat the overlap measurements for many independent quenched configurations C_0, and then perform an average over these realizations of the disorder. Indeed, for $R \sim \xi_{PTS}$, large sample-to-sample variations of $P(Q)$ are observed.

There are a number of subtleties and extensions related to the overlap function that we now describe. A first subtlety is that an appropriate measure of the overlap needs to focus on the center of the spherical cavity, since boundaries always have a high overlap, and this makes the results difficult to interpret (Biroli et al. 2008). Moreover, the overlap needs to be a smooth function of the distance between configurations, and step functions are too singular to average over. A second subtlety is that for some liquids, the simple positional information does not adequately cover all the structural information. In that case, the conventional overlap needs to be completed with additional coordinates overlap, for example, bond angles. This was used in Yaida et al. (2016) to show that hexatic order could be captured by the point-to-set correlations (see also Russo and Tanaka (2015)).

Let us also mention a few extensions of the method that have been proposed. In Cavagna et al. (2012), the authors proposed to relax the frozen configuration constraint by letting the outside atoms vibrate, so long as they maintain a large overlap with the initial configuration: they called this reference state "frozen state" (as opposed to frozen configuration). A second type of extension is to study various confinement geometries, as in Berthier and Kob (2012), Kob et al. (2012), Cavagna et al. (2012), and Li et al. (2014), where it was shown that the geometry of confinement needs to be carefully considered.

Thanks to the computational progress outlined above, several important results were established in the last decade. Among them: (i) clear evidence that the slowing down of the dynamics is
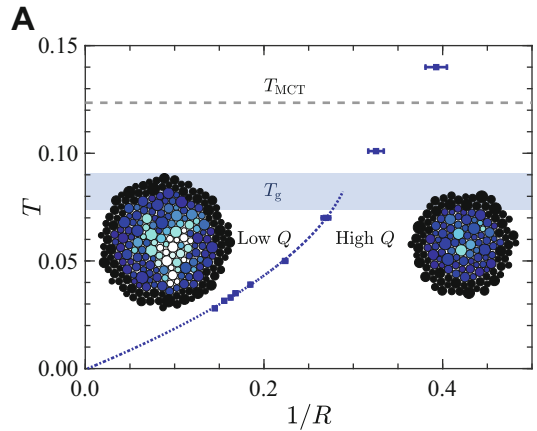
A Statistical Mechanics Perspective on Glasses and Aging, Fig. 19 From Berthier et al. (2019g). Evolution of the inverse point to set length, denoted here as $1/R$ with the temperature T. A clear growth of the point to set length up to $\xi_{PTS} \approx 6.5$ is observed. Cavities smaller (larger) than ξ_{PTS} have a large (small) overlap with the reference configuration, as illustrated in the snapshots, where the particle shade encodes the overlap value

accompanied by the growth of the point-to-set length (even though a mild one), (ii) established relation between point-to-set and configurational entropy: the former appears to be inversely proportional to the other (Berthier et al. 2019a), thus directly linking the growth of amorphous order to the decrease in number of metastable states – a tenet of RFOT theory, (iii) clear difference between two-dimensional and three-dimensional behavior: two-dimensional glass-formers display a point-to-set that appears to diverges at zero temperature, as shown in Fig. 19, thus indicating a $T_K = 0$ Kauzman transition temperature (Berthier et al. 2019g). This is in sharp contrast with the results in three dimensions, where the extrapolated T_K is larger than zero.

s-Ensemble and Large Deviations
The Franz-Parisi potential is an example of a large deviation analysis. The idea behind it is that fluctuations in the overlap field play an important role for the glass transition, analog to the magnetization field in a ferromagnet. In order to investigate such fluctuations, one can then study the large deviation function (the free-energy) associated to the spatial average of the field (the order parameter). This is the usual route followed in

thermodynamic analyses of second-order phase transitions. The s-ensemble is the dynamical counterpart of such a procedure. One modifies the dynamical rules, in order to be in a particular subset of the "dynamical states," to probe the tendency of the original system to explore these states. This idea originates both from theoretical considerations on the large deviations of activity (rare events) predicted in KCMs (Garrahan et al. 2007, 2009) and from considerations on efficient simulation schemes (for rare events as well) that apply more generally (Noe et al. 2009). In practice, the s-ensemble dynamics is a particular instance of transition path sampling, where the quantity of interest is a measure of the activity of a multi-particles trajectory $\{x_i(t)\}_{i=1,\dots,N}$, cumulated over time

$$K[x(t)] = \frac{1}{Nt_{obs}} \sum_{t \in [t_0, t_0+t_{obs}]} \sum_{i \in [1,N]} (x_i(t+\Delta t) - x_i(t))^2 \quad (41)$$

where Δt (resp. t_{obs}) is chosen to be of the order of a few ballistic times (resp. a few relaxation times). In the s-ensemble, the actual relaxation time then becomes larger than t_{obs}. Here we follow the notations used in (Hedges et al. 2009), where this biasing method was first applied to structural glasses (for its initial introduction in KCMs, see Elmatad et al. (2010), and Garrahan et al. (2007, 2009)). The method is called s-ensemble because the probability of a trajectory $x(t)$ is $P_0[x(t)]e^{-sK[x(t)]}$, where $P_0[x(t)]$ is the probability for the unperturbed system. This amounts to defining a "thermodynamics of trajectories" which are biased (and classified) depending on their activity; s is the biasing field. In order to numerically simulate and probe such a measure, one can perform Monte-Carlo sampling in trajectory space. This method is actually so efficient at finding low-energy states that special attention must be paid to crystallization (Hedges et al. 2009).

One of the most important results obtained by the s-ensemble method is a direct evidence of a first-order phase transition between an active phase (for low s) and an inactive phase (for large s) in supercooled liquids: see Fig. 20. In the $s - T$ plane this corresponds to a first-order transition line $s^*(T)$

which ends in a critical point at high temperature (Elmatad et al. 2010; Hedges et al. 2009). Although the method focuses on the dynamical properties, inactive states do exhibit interesting structural features. They are more stable than equilibrium samples (Jack et al. 2011): mechanically, in terms of their lower number of low-energy modes (depletion of $D(\omega)$), and thermodynamically, in terms of a longer lived "melting" transient from the glass to the liquid state. This suggests that inactive states correspond to very stable glassy state, that is, nonequilibrium glassy states with low fictive temperatures.

The foundation of the s-ensemble relies on the dynamical behavior of KCMs. For the East model scenario it was shown (Keys et al. 2015) that configurations obtained by (i) the s-ensemble, (ii) finite-rate cooling, and (iii) quenching and longtime aging are all equivalent. This provides a concrete example where glassiness is directly related to the phase transition unveiled by the s-ensemble. Let us conclude by noticing that even systems having an RFOT display such a phase transition, the difference being that the line $s^*(T)$ reaches $s^* = 0$ for $T = T_K$ and not for $T = 0$ as for KCMs (Jack and Garrahan 2010). This shows that the s-ensemble is actually a general construction, which transforms the physics of metastability observed in supercooled liquids in well-defined phase transitions in the extended ensemble comprising space and time.

Machine Learning Developments

We have mentioned the possible use of (unsupervised) Machine Learning (ML) in section "Geometric Frustration, Avoided Criticality, and Locally Preferred Structures" for automatic identification of LPS in supercooled liquids (see also Ronhovde et al. (2011, 2012), Paret et al. (2020), and Boattini et al. (2020)). Another set of ML techniques to be used is supervised learning: automatically defining fluid- or solid-like structures (features in ML language) by labeling them for a training set of local environments which are observed to be locally fluid-or solid-like. The general idea developed in Schoenholz (2018) is to train a neural network (or other fitting model) to "predict" the current degree of mobility or "instantaneous activity" from
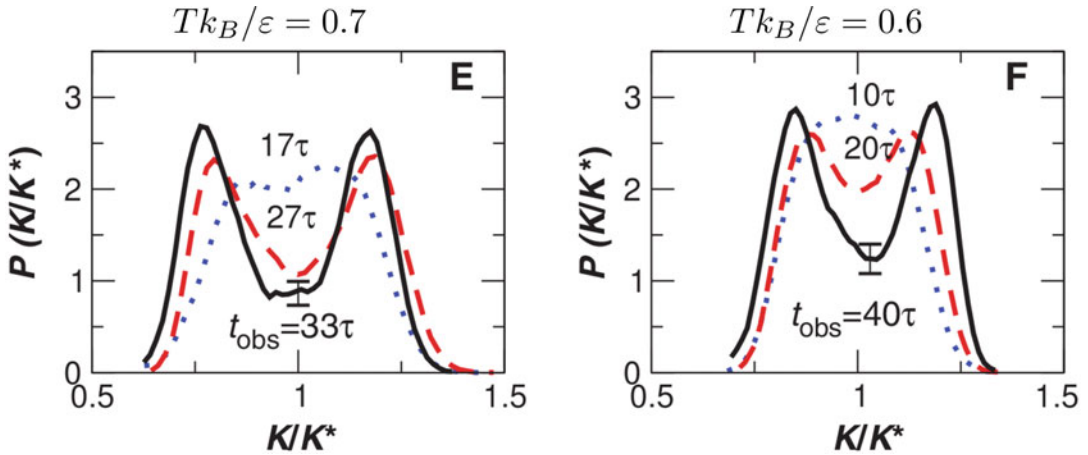
A Statistical Mechanics Perspective on Glasses and Aging, Fig. 20 From Hedges et al. (2009). Coexistence of the active (large K) and inactive (small K) phases, as evidenced from s-ensemble biased simulations. As temperature is reduced, the distribution becomes increasingly bimodal, as expected when approaching a first-order phase transition

the knowledge of structure only. This may be cast as finding the function f such that $f\left(\left\{\vec{r}\right\}\right)(i,t) = y_{\text{precl}} \approx y_{\text{true}}(i,t)$, where $\left\{\vec{r}\right\}(i,t)$ is the structure of the neighborhood of particle i at time t, and $y_{\text{true}}(i, t)$ (the label) is a measure of the dynamical activity for particle i at time t. Concretely, the target label y_{true} has to encode some notion of local, instantaneous mobility (Candelier et al. 2009, 2010a, b), while the local structure may be defined, for example, by the (local, instantaneous) density pair correlation function $g(r)$, with the possible addition of angular variables (Cubuk et al. 2016; Schoenholz et al. 2016). This technique has been applied with success, showing how much structure correlates with dynamics in supercooled liquids (Schoenholz et al. 2016; Landes et al. 2020), disordered solids (Cubuk et al. 2016; Schoenholz et al. 2015, 2016; Landes et al. 2020; Cubuk et al. 2015), for the plasticity of amorphous materials (Ivancic et al. 2017; Cubuk et al. 2017), and in polycrystalline materials (Sharp et al. 2018).

The problem of the interpretation, which is one of the major issues with statistical learning in general, remains open: how to make use of predictions emerging from hundred-parameters models? This issue is transverse to most ML applications and is currently under active scrutiny. In terms of basic science, the conclusion of Liu and collaborators is that the predicted y_{pred} provides a new observable, called the softness field (Schoenholz et al. 2015), which plays a key role for the dynamics.

We conclude mentioning a very recent work which introduced a new ML technique in the glass physics arena. The authors of (Bapst et al. 2020) focused on the problem of predicting long-time dynamics (more precisely, the propensity field (Widmer-Cooper and Harrowell 2006)) from knowledge of structure alone, by leveraging on recent progress in graph neural networks. The results are impressive: the ability to predict the propensity map is substantially better than existing numerical physics-based methods and the ML techniques described above, thus establishing a promising new way to study glassy dynamics.

Aging and Off-Equilibrium Dynamics

Why Aging?

We have dedicated most of the above discussion to properties of materials approaching the glass transition at thermal equilibrium. We discussed a rich phenomenology and serious challenges for both our numerical and analytical capabilities to account for these phenomena. For most people,

however, glasses are interesting below the glass transition, so deep in the glass phase that the material seems to be frozen forever in a seemingly arrested amorphous state, endowed with enough mechanical stability for a glass to retain, say, the liquid it contains (preferably a nice red wine). Does this mean that there is no interesting physics in the glass state?

The answer is clearly "no." There is still life (and physics) below the glass transition. We recall that for molecular glasses, T_g is defined as the temperature below which relaxation is too slow to occur within an experimental timescale. Much below T_g, therefore, the equilibrium relaxation timescale is so astronomically large that thermal equilibrium is out of reach. One enters therefore the realm of off-equilibrium dynamics. A full physical understanding of the nonequilibrium glassy state remains a central challenge (Young 1998; Barrat et al. 2004).

A first consequence of studying materials in a time window smaller than equilibrium relaxation timescales is that the system can, in principle, remember its complete history, a most unwanted experimental situation since all details of the experimental protocol may then matter. The simplest protocol to study aging phenomena in the glass phase is quite brutal (Struik 1977): take a system equilibrated above the glass transition and suddenly quench it at a low temperature at a "waiting time" $t_w = 0$ which corresponds to the beginning of the experiment. For $t_w > 0$ the system is left unperturbed at constant temperature where it tries to slowly reach thermal equilibrium, even though it has no hope to ever get there. Aging means that the system never forgets the time t_w spent in the glass phase, its "age." The evolution of one time quantities, for example, the energy, as a function of time is not a good evidence of aging. In order to show that the system never equilibrates, two time quantities such as density-density or spin-spin correlation functions are much more useful. A typical example is presented in Fig. 21 where the self-part of the intermediate function in Eq. (5) is shown for a Lennard-Jones molecular liquid at low temperature. Immediately after the quench, the system exhibits a relatively fast relaxation: particles still

move substantially. However, when the age increases, dynamics slow down and relaxation becomes much slower. When t_w becomes very large, relaxation becomes too slow to be followed in the considered time window and the system seems frozen on that particular timescale: it has become a glass. A striking feature conveyed by these data is that an aging system not only remains out-of-equilibrium for all practical purposes, but its typical relaxation time is in fact set by its age t_w. In simple cases, the effective relaxation time after waiting a time t_w scales at t_w itself, which means that since equilibration timescales have diverged, t_w is the only remaining relevant timescale in the problem.

A popular interpretation of this phenomenon is given by considering trap models (Bouchaud 1992). In this picture, reminiscent of the Goldstein view of the glass transition mentioned above (Goldstein 1969), the system is described as a single particle evolving in a complex energy landscape with a broad distribution of trap depths – a paradigmatic mean-field approach. Aging in this perspective arises because the system visits traps that become deeper when t_w increases, corresponding to more and more stable states. It therefore takes more and more time for the system to escape, and the dynamics slow down with time, as observed in Fig. 21. This implies that any physical property of the glass becomes an age-dependent quantity in aging protocols, and more generally becomes dependent on how the glass was prepared. One can easily imagine using this property to tune mechanical or optical characteristics of a material by simply changing the way it is prepared, like how fast it is cooled to the glassy state (recall our discussion of ultrastable glasses in section "Ultrastable Glasses").

A real space alternative picture was promoted in particular in the context of spin glass studies, based on the ideas of scaling and renormalization (Bray and Moore 1984; van Hemmen and Morgenstern 1987; Fisher and Huse 1986). The physical picture is that of a coarsening process, where the system develops long-range order by growing extended domains of lengthscale $\ell(t_w)$. On lengthscales less than $\ell(t_w)$, the system has had the time to order since the quench at $t_w = 0$. The
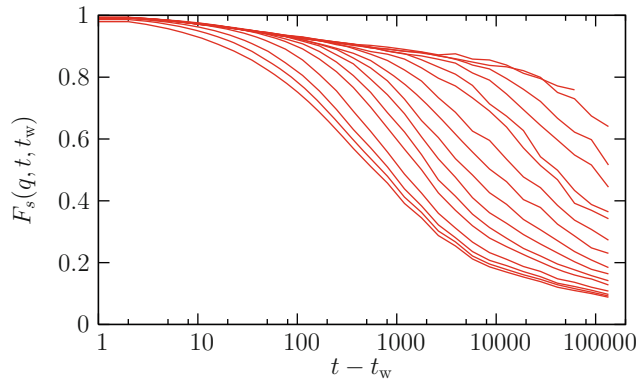
A Statistical Mechanics Perspective on Glasses and Aging, Fig. 21 Aging dynamics in a Lennard-Jones glass-forming liquid at low temperature. The system is quenched at time $t_w = 0$ at low T, where the temperature is kept constant. Two-time self-intermediate scattering functions are then measured for 20 logarithmically spaced waiting times t_w from $t_w = 1$ to $t_w = 10^5$ (from left to right). The relaxation becomes slower when t_w increases: the system ages

walls between domains evolve in a random environment. In order to move they have to overcome free energy barriers. It is then assumed an activated dynamic scaling which states that the typical barrier to extend the domain from linear size $\ell(t_w)$ to, say, $2\ell(t_w)$ scales as ℓ^ψ, where ψ is some "barrier" exponent. Using the Arrhenius law to relate dynamics to barriers, one gets that aging corresponds to the logarithmic growth with time of spatially correlated domains, $\ell \sim (T \log t_w)^{1/\psi}$. A domain growth picture of aging in spin glasses can be directly confirmed by numerical simulations (Kisker et al. 1996), only indirectly by experiments.

Memory and Rejuvenation Effects

Since the complete history of a sample in the glass phase matters, there is no reason to restrain experimental protocols to the simple aging experiment mentioned above. Indeed, experimentalists have investigated scores of more elaborated protocols that have revealed an incredibly rich, and sometimes quite unexpected, physics (Young 1998). We restrain ourselves here to a short discussion of memory and rejuvenation effects observed during temperature cycling experiments (Refregier et al. 1987) (one can imagine applying a magnetic field or a mechanical constraint, be they constant in time or sinusoidal, etc.). These two effects were

first observed in spin glasses, but the protocol was then repeated in many different materials, from polymers and organic liquids to disordered ferroelectrics. After several unsuccessful attempts, similar effects are now observed in numerical work as well (Berthier and Young 2005; Berthier and Bouchaud 2002). Recent results obtained from simulations of a three-dimensional glass-former exploring the spin-glass-like Gardner phase (Scalliet and Berthier 2019) are presented in Fig. 22.

There are three steps in temperature cycling experiments (Refregier et al. 1987). The first one is a standard aging experiment, namely a sudden quench from high to low temperature at time $t_w = 0$. The system then ages for a duration t_1 at constant temperature T_1. The system slowly relaxes toward equilibrium and its dynamics slows down: for our spin glass example (see Fig. 22) this is observed through the measurement of some dynamic susceptibility $\chi(t_w, \omega)$. Temperature is then suddenly shifted to $T_2 < T_1$ at time t_1. There, the material restarts aging (almost) as if the first step had not taken place. This is called "rejuvenation effect," because the system seems to forget it is already "old." At total time $t_1 + t_2$, temperature is then shifted back to its initial value T_1. Then, aging is found to proceed as a quasi-perfect continuation of the first step, as if the
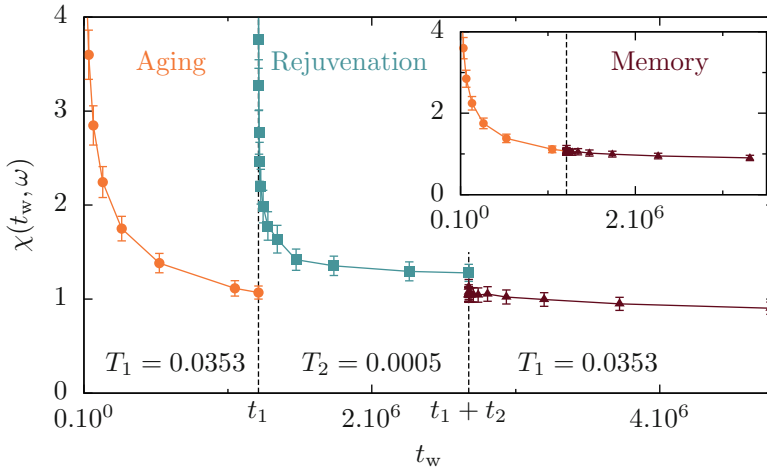
A Statistical Mechanics Perspective on Glasses and Aging, Fig. 22 Memory and rejuvenation effects obtained in the numerical simulation of a three-dimensional glass-former (Scalliet and Berthier 2019). There is a first aging step, $0 < t_w < 11$, during which the system slowly tries to reach thermal equilibrium at temperature T_1. The system "rejuvenates" in the second step at T_2, $t_1 < t < t_1 + t_2$, and it restart aging (rejuvenation). Finally in the third step, temperature is back to T_1, and memory of the first step is kept intact, as shown in the inset where relaxation during the second step of the experiment is taken away

second step had not taken place. The system has kept the "memory" of the first part of the experiment, despite the rejuvenation observed in the intermediate part. The memory effect becomes more spectacular when relaxation during the second step is removed, as in the inset of Fig. 22. The third relaxation appears indeed as a perfect continuation of the first one.

On top of being elegant and quite intriguing, such protocols are relevant because they probe more deeply the dynamics of aging materials, allowing one to ask more precise questions beyond the simplistic observation that "this material displays aging." Moreover, the observation of similar effects in many different glassy materials implies that these effects are intrinsic to systems with slow dynamics. Interesting also are the subtle differences observed from one material to the other.

Several experimental, numerical and theoretical papers have been devoted to this type of experiments, and these effects are not "mysterious" anymore (see Barrat et al. (2004)). A clear link between memory effects and typical lengthscales over which the slow dynamics takes place has been established. Because lengthscales depend so sensitively on timescales and on the working temperature, experiments performed at two different temperatures typically probe very different lengthscales, allowing the system to store memory of its state at different temperatures over different lengthscales (Berthier and Bouchaud 2002; Bouchaud et al. 2001). In return, this link has been elegantly exploited to obtain a rather precise experimental estimate of dynamic lengthscales involved in the aging dynamics of spin glass materials (Bert et al. 2004), which seems to confirm the slow logarithmic growth law mentioned before.

Discussion of the rejuvenation effect is slightly more subtle. It is indeed not yet obvious that the effect as it is observed in computer simulations and reported, for example, in Fig. 22, is exactly similar to the one observed in experiments. The difficulty comes from the fact that some seemingly innocuous details of the experimental protocol, such as the necessary use in experiments of finite cooling rates, in fact play a crucial role and influence the physics so that direct comparison between experiments and simulations is difficult. In numerical work, rejuvenation can be attributed to a gradual change with temperature of the nature

of spatial correlations between spins that develop with time (Berthier and Young 2005; Berthier and Bouchaud 2002). More drastic changes are predicted to occur in disordered systems as a result of the chaotic evolution with temperature of the metastable states in a spin glass (so-called chaos effect (Bray and Moore 1987)), which could also be responsible for the observed rejuvenation effect (Jönsson et al. 2004).

Mean-Field Aging and Effective Temperatures
Theoretical studies of mean-field glassy models have provided important insights into the aging dynamics of both structural and spin glasses (Cugliandolo and Kurchan 1993, 1994). Although such models are defined in terms of spin degrees of freedom interacting via infinite-ranged interactions, the deep connections between them and the mode-coupling theory of the glass transition make them serious candidates to investigate glassy states in general, not only thermodynamic properties at thermal equilibrium but also non-equilibrium aging dynamics. Despite their often reported "simplicity," it took several years to derive a proper asymptotic solution of the long-time dynamics for a series of mean-field spin glasses (see Cugliandolo in Barrat et al. (2004)). These results have then triggered an enormous activity (Crisanti and Ritort 2003) encompassing theoretical, numerical, and also experimental work trying to understand further these results, and to check in more realistic systems whether they have some reasonable range of applicability beyond mean-field.

This large activity, by itself, easily demonstrates the broad interest of these results. More recently, the derivation of the static properties of liquids and glasses in large dimensions has renewed the interest in mean-field dynamic phenomena (Parisi et al. 2020). In particular, the dynamic equations governing the equilibrium properties of supercooled liquids have now been derived (Maimbourg et al. 2016; Kurchan et al. 2016) and their consequences are being explored (Manacorda et al. 2020). The study of the non-equilibrium (aging and sheared) dynamics is now under way (Agoritsas et al. 2018, 2019; Altieri et al. 2020).

In these mean-field models, thermal equilibrium is never reached, and aging proceeds by downhill motion in an increasingly flat free energy landscape (Kurchan and Laloux 1996), with subtle differences between spin glass and structural glass models. In both cases, however, time translational invariance is broken, and two-time correlation and response functions depend on both their temporal arguments. In fact, the exact dynamic solution of the equations of motion for time correlators displays behaviors in strikingly good agreement with the numerical results reported in Fig. 21.

In these systems, the equations of motion in the aging regime involve not only temporal correlations, but also time-dependent response functions. At thermal equilibrium, response and correlation are not independent, since the fluctuation-dissipation theorem (FDT) relates both quantities. In aging systems, there is no reason to expect the FDT to hold and both quantities carry, at least in principle, distinct physical information. Again, the asymptotic solution obtained for mean-field models quantitatively establishes that the FDT does not apply in the aging regime. Unexpectedly, the solution also shows that a generalized form of the FDT holds at large waiting times (Cugliandolo and Kurchan 1993). This is defined in terms of the two-time connected correlation function for some generic observable $A(t)$,

$$C(t, t_{\mathrm{w}}) = \langle A(t)A(t_{\mathrm{w}})\rangle - \langle A(t)\rangle\langle A(t_{\mathrm{w}})\rangle, \quad (42)$$

with $t \geq t_{\mathrm{w}}$, and the corresponding two-time (impulse) response function

$$R(t, t_{\mathrm{w}}) = T\frac{\delta\langle A(t)\rangle}{\delta h(t_{\mathrm{w}})}\Bigg|_{h=0}. \quad (43)$$

Here h denotes the thermodynamically conjugate field to the observable A so that the perturbation to the Hamiltonian (or energy function) is $\delta E = -hA$, and angled brackets indicate an average over initial conditions and any stochasticity in the dynamics. Note that we have absorbed the temperature T in the definition of the response,

for convenience. The associated generalized FDT reads then

$$R(t, t_w) = X(t, t_w) \frac{\partial}{\partial t_w} C(t, t_w), \qquad (44)$$

with $X(t, t_w)$ the so-called fluctuation-dissipation ratio (FDR). At equilibrium, correlation and response functions are time translation invariant, depending only on $\tau = t - t_w$, and equilibrium FDT imposes that $X(t, t_w) = 1$ at all times. A parametric fluctuation-dissipation (FD) plot of the step response or susceptibility

$$\chi(t, t_w) = \int_{t_w}^{t} dt' R(t, t'), \qquad (45)$$

against

$$\Delta C(t, t_w) = C(t, t) = C(t, t_w), \qquad (46)$$

is then a straight line with unit slope. These simplifications do not occur in nonequilibrium systems. But the definition of an FDR through Eq. (44) becomes significant for aging systems (Cugliandolo and Kurchan 1993, 1994). In mean-field spin glass models the dependence of the FDR on both temporal arguments is only through the correlation function,

$$X(t, t_w) \sim X(C(t, t_w)), \qquad (47)$$

valid at large waiting times, $t_w \rightarrow \infty$. For mean-field structural glass models, the simplication (47) is even more spectacular since the FDR is shown to be characterized by only two numbers instead of a function, namely $X \sim 1$ at short times (large value of the correlator) corresponding to a quasi-equilibrium regime, with a crossover to a nontrivial number, $X \sim X^{\infty}$ for large times (small value of the correlator). This implies that parametric FD plots are simply made of two straight lines with slope 1 and X^{∞}, instead of the single straight line of slope 1 obtained at equilibrium.

Since any kind of behavior is in principle allowed in nonequilibrium situations, getting such a simple, equilibrium-like structure for the FD relations is a remarkable result. This immediately led

to the idea that aging systems might be characterized by an effective thermodynamic behavior and the idea of quasi-equilibration at different timescales (Cugliandolo et al. 1997). In particular, generalized FD relations suggest to define an effective temperature, as

$$T_{eff} = \frac{T}{X(t, t_w)}, \qquad (48)$$

such that mean-field glasses are characterized by a unique effective temperature, $T_{eff} = T/X^{\infty}$ It is thought of as the temperature at which slow modes are quasi-equilibrated. One finds in general that $0 < X^{\infty} < 1$, such that $T_{eff} > T$, as if the system had kept some memory of its high temperature initial state.

The name "temperature" for the quantity defined in Eq. (48) is not simply the result of a dimensional analysis but has a deeper, physically appealing meaning that is revealed by asking the following questions. How does one measure temperatures in a many-body system whose relaxation involves well-separated timescales? What is a thermometer (and a temperature) in a far from equilibrium aging material? Answers are provided in Cugliandolo et al. (1997), and Kurchan (2005) both for mean-field models and for additional toy models with multiple relaxation timescales. The idea is to couple an additional degree of freedom, such as a harmonic oscillator, $x(t)$, which plays the role of the thermometer operating at frequency w, to an observable of interest $A(t)$ via a linear coupling, $-\lambda x(t) A(t)$. Simple calculations show then that the thermometer "reads" the following temperature,

$$\frac{1}{2} K_B T_{meas}^2 = \frac{1}{2} \omega^2 \langle x^2 \rangle = \frac{\omega C'(\omega, t_w)}{2 \chi''(\omega, t_w)}, \qquad (49)$$

where $C'(\omega, t_w)$ is the real part of the Fourier transform of Eq. (42), and $\chi(\omega, t_w)$ the imaginary part of the Fourier transform of Eq. (43), with $h = \lambda x$. The relation (49) indicates that the bath temperature is measured, $T_{meas} = T$, if the frequency is high and FDT is satisfied, while $T_{meas} = T_{eff} > T$ if the frequency is slow enough to be tuned to that of the slow relaxation in the aging

material. The link between the FDR in Eq. (44) and the effective temperature measured in Eq. (49) was numerically confirmed in the computer simulation of a glassy molecular liquid in Berthier and Barrat (2002a).

More generally, relaxation in glassy systems occurs in well-separated time sectors (Cugliandolo and Kurchan 1994); it is then easy to imagine that each sector could be associated with an effective temperature (Kurchan 2005). A thermodynamic interpretation of effective temperatures has also been put forward, relating them to the concept of replica symmetry breaking (Franz et al. 1998). Interestingly, the full-step or one-step replica symmetry breaking schemes needed to solve the static problem in these models have a counterpart as the FDR being a function or a number, respectively, in the aging regime. Moreover, we note that these modern concepts are related to, but make much more precise, older ideas of quasi-equilibrium and fictive temperatures in aging glasses (Struik 1977).

Taken together, these results make the mean-field description of aging very appealing, and they nicely complement the mode-coupling/RFOT description of the equilibrium glass transition described above. Moreover, they have set the agenda for a large body of numerical and experimental work, as reviewed in Crisanti and Ritort (2003). In Fig. 23 we present recent numerical data obtained in an aging silica glass (Berthier 2007b), presented in the form of a parametric response-correlation plot. The measured correlation functions are the self-part of the intermediate scattering functions defined in Eq. (5), while the conjugated response functions quantify the response of particle displacements to a spatially modulated field conjugated to the density. Plots for silicon and oxygen atoms at different ages are presented. They seem to smoothly converge toward a two-straight line plot, as obtained in mean-field models (note, however, that this could be just a pre-asymptotic, finite "t_w" effect). Moreover, the second, nontrivial part of the plot is characterized by a slope that appears to be independent of the species, and of the wavevector chosen to quantify the dynamics, in agreement with the idea of a unique asymptotic value of the

FDR, possibly related to a well-defined effective temperature.

Beyond Mean-Field: Real Space

Despite successful results, such as those shown in Fig. 23, the broader applicability of the mean-field scenario of aging dynamics remains still unclear. While some experiments and simulations indeed seem to support the existence of well-behaved effective temperatures (Grigera and Israeloff 1999; Abou and Gallet 2004; Wang et al. 2006), other studies also reveal the limits of the mean-field scenario. Experiments have for instance reported anomalously large FDT violations associated with intermittent dynamics (Bellon et al. 2001; Bellon and Ciliberto 2002; Buisson et al. 2003a, b), while theoretical studies of model systems have also found non-monotonic or even negative response functions (Talbot et al. 2003; Nicodemi 1999; Krzkala 2005; Depken and Stinchcombe 2005), and ill-defined or observable-dependent FDRs (Fielding and Sollich 2002). In principle, these discrepancies with mean-field predictions are to be expected, since there are many systems of physical interest in which the dynamics are not of mean-field type, displaying both activated processes and spatial heterogeneity.
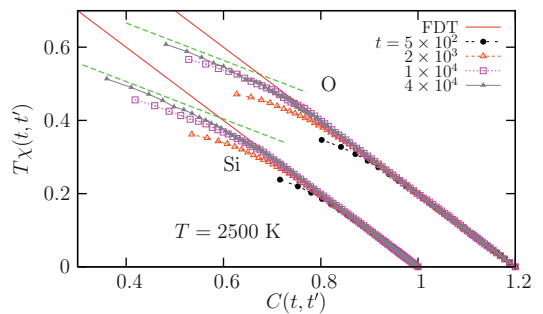
A Statistical Mechanics Perspective on Glasses and Aging, Fig. 23 Parametric correlation-response plots measured in the aging regime of a numerical model for a silica glass, SiO_2 (Berthier 2007b). The plots for both species smoothly converges toward a two-straight line plot of slope 1 at short times (large C values), and of slope $X^\infty \approx 0.51$ at large times (small values of C), yielding an effective temperature of about $T_{eff} = T/X^\infty \approx 4900$ K. Note that the glass transition temperature of SiO_2 is 1446 K

It is thus an important task to understand from the theoretical point of view when the mean-field concept of an FDR-related effective temperature remains viable. However, theoretically studying the interplay between relevant dynamic lengthscales and thermally activated dynamics in the nonequilibrium regime of disordered materials is clearly a challenging task. Nevertheless, this problem has been approached in different ways, as we briefly summarize in this subsection.

A first class of system that displays aging and spatial heterogeneity is given by coarsening systems. The paradigmatic situation is that of an Ising ferromagnetic model (with a transition at T_c) suddenly quenched in the ferromagnetic phase at time $t_w = 0$. For $t_w > 0$, domains of positive and negative magnetizations appear and slowly coarsen with time. The appearance of domains that grow with time proves the presence of both aging and heterogeneity.

The case where the quench is performed down to $T < T_c$ is well understood. The system becomes scale invariant (Bray 1994), since the only relevant lengthscale is the growing domain size, $\ell(t_w)$. Correlation functions display aging, and scale invariance implies that $C(t, t_w) \sim f(\ell(t)/\ell(t_w))$. Response functions can be decomposed into two contributions (Barrat 1998; Berthier et al. 1999): one part stems from the bulk of the domains and behaves as the equilibrium response, and a second one from the domain walls and becomes vanishingly small in the long time limit, where $\ell(t_w) \to \infty$ and the density of domain walls vanishes. This implies that for coarsening systems in $d \geq 2$, one has $X^\infty = 0$, or equivalently an infinite effective temperature, $T_{eff} = \infty$. The case $d = 1$ is special because $T_c = 0$ and the response function remains dominated by the domain walls, which yields the nontrivial value $X^\infty = 1/2$ (Godréche and Luck 2000; Lippiello and Zannetti 2000).

Another special case has retained attention. When the quench is performed at $T = T_c$, there is no more distinction between walls and domains and the above argument yielding $X^\infty = 0$ does not hold. Instead one studies the growth of critical fluctuations with time, with $\xi(t_w) \tilde{t_w}^{1/z}$ the correlation length at time t_w, where z is the dynamic exponent. Both correlation and response functions become nontrivial at the critical point (Godreche and Luck 2000). It proves useful in that case to consider the dynamics of the Fourier components of the magnetization fluctuations, $C_q(t, t_w) = \langle m_q(t)m_{-q}(t_w) \rangle$, and the conjugated response $R_q(t, t_w) = \frac{\delta \langle m_q(t) \rangle}{\delta h_{-q}(t_w)}$. From Eq. (44) a wavevector-dependent FDR follows, $X_q(t, t_w)$, which has interesting properties (Mayer et al. 2003) (see (Calabrese and Gambassi 2005) for a review).

In dimension $d = 1$, it is possible to compute $X_q(t, t_w)$ exactly in the aging regime at $T = T_c = 0$. An interesting scaling form is found, and numerical simulations performed for $d > 1$ confirm its validity:

$$X_q(t, t_w) = \chi(q^2 t_w), \qquad (50)$$

where the scaling function $\chi(x)$ is $\chi(x \to \infty) \to 1$ at small lengthscale, $q\xi \gg 1$, and $\chi(x \to 0) \to 1/2$ (in $d = 1$) at large distance, $q\xi \ll 1$; recall that $z = 2$ in that case.

Contrary to mean-field systems where geometry played no role, here the presence of a growing correlation lengthscale plays a crucial role in the off-equilibrium regime since $\xi(t_w)$ allows one to discriminate between fluctuations that satisfy the FDT at small lengthscale, $X_q \sim 1$, and those at large lengthscale which are still far from equilibrium, $0 < X_q \sim X^\infty < 1$. These studies suggest therefore that generalized fluctuation-dissipation relations in fact have a strong lengthscale dependence – a result which is not predicted by mean-field approaches.

Another interesting result is that the FDT violation for global observables (i.e., those at $q = 0$) takes a particularly simple form, since the introduction of a single number is sufficient, the FDR at zero wavevector, $X_{q = 0}(t, t_w) = X^\infty = 1/2$ (in $d = 1$). This universal quantity takes nontrivial values in higher dimension, for example, $X^\infty \approx 0.34$ is measured in $d = 2$ (Mayer et al. 2003). This shows that the study of global rather than local quantities makes the measurement of X^∞ **much** easier. Finally, having a nontrivial value of X^∞ **for** global observables suggests that the

possibility to define an effective temperature remains valid, but it has become a more complicated object, related to global fluctuations on large lengthscale.

Kinetically constrained spin models represent a second class of non-mean-field systems whose off-equilibrium has been thoroughly studied recently (Léonard et al. 2007). This is quite a natural thing to do since these systems have local, finite ranged interactions, and they combine the interesting features of being defined in terms of (effective) microscopic degrees of freedom, having local dynamical rules, and displaying thermally activated and heterogeneous dynamics.

The case of the Fredrickson-Andersen model, described in section "Theory of the Glass Transition," has been studied in great detail (Léonard et al. 2007), and we summarize the main results. Here, the relevant dynamic variables are the Fourier components of the mobility field, which also correspond in that case to the fluctuations of the energy density. Surprisingly, the structure of the generalized fluctuation-dissipation relation remains once more very simple. In particular, in dimension $d > 2$, one finds a scaling form similar to (50), $X_q(t, t_w) = \chi(q^2 t_w)$, with a well-defined limit at large distance $X_{q=0}(t, t_w) = X^\infty$. The deep analogy with critical Ising models stems from the fact that mobility defects in KCMs diffuse in a way similar to domain walls in coarsening Ising models. It is in fact by exploiting this analogy that analytic results are obtained in the aging regime of the Fredrickson-Andersen model (Mayer and Sollich 2007).

There is however a major qualitative difference between the two families of model. The (big!) surprise lies in the sign of the asymptotic FDR, since calculations show that (Mayer et al. 2006)

$$X^\infty = -3, d > 2. \tag{51}$$

In dimension $d = 1$, one finds $X_{q=0}(t, t_w) = f(t/t_w)$ with $X_{q=0}(t \to \infty, t_w) = \frac{3\pi}{16-6\pi} \approx -3.307$. Numerical simulations confirm these calculations. In Fig. 24, we show such a comparison between simulations (symbols) and theory (lines) in the case of the $d = 3$ Fredrickson-Andersen model

(Mayer et al. 2006). Fourier components of the mobility field yield parametric FD plots that follow scaling with the variable $q^2 t_w$, as a direct result of the presence of a growing lengthscale for dynamic heterogeneity, $\xi(t_w)\sqrt{t_w}$. Again, generalized fluctuation-dissipation relations explicitly depend on the spatial lengthscale considered, unlike in mean-field studies. In Fig. 24, the limit $q = 0$ corresponding to global observables is also very interesting since the plot is a pure straight line, as in equilibrium. Unlike equilibrium, however, the slope is not 1 but -3. A negative slope in this plot means a negative FDR, and therefore suggests a negative effective temperature, a very nonintuitive result at first sight.

Negative response functions in fact directly follows from the thermally activated nature of the dynamics of these models (Mayer et al. 2006). First, one should note that the global observable shown in Fig. 24 corresponds to fluctuations of the energy, $e(t_w)$, whose conjugated field is temperature. In the aging regime the system slowly drifts toward equilibrium. Microscopic moves result from thermally activated processes, corresponding to the local crossing of energy barriers. An infinitesimal change in temperature, $T \to T + \delta T$ with $\delta T > 0$, accelerates these barrier crossings and makes the relaxation dynamics faster. The energy response to a positive temperature pulse is therefore negative, $\delta e < 0$, which directly yields $\delta e/\delta T < 0$, which explains the negative sign of the FDR. This result does not hold in mean-field glasses, where thermal activation plays no role.

Finally, another scenario holds for local observables in some KCMs when kinetic constraints are stronger, such as the East model (Léonard et al. 2007) or a bidimensional triangular plaquette model (Jack et al. 2006b). Here, relaxation is governed by a hierarchy of energy barriers that endow the systems with specific dynamic properties. In the aging regime following a quench, in particular, the hierarchy yields an energy relaxation that arises in discrete steps which take place on very different timescales, reminiscent of the "time sectors" encountered in mean-field spin glasses. Surprisingly, it is found that to each of these discrete relaxations one can
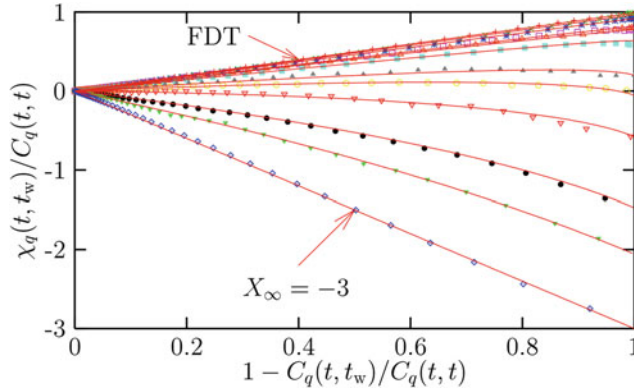
A Statistical Mechanics Perspective on Glasses and Aging, Fig. 24 Parametric response-correlation plots for the Fourier components of the mobility field in the $d = 3$ Fredrickson-Andersen model. Symbols are from simulations, lines from analytic calculations, and wavevectors decrease from top to bottom. The FDT is close to being satisfied at large q corresponding to local equilibrium. At larger distance deviations from the FDT are seen, with an asymptotic FDR which becomes negative. Finally, for energy fluctuations at $q = 0$ (bottom curve), the plot becomes a pure straight line of (negative!) slope -3, as a result of thermally activated dynamics

associate a well-defined (positive) value of the fluctuation-dissipation ratio, again reminiscent of the dynamics of mean-field spin glass models. Therefore, a physical picture seems to have some validity, even in models that are very far from the mean-field limit: in that picture, slow relaxation takes place on multiple timescales, with each timescale characterized by a different effective temperature.

Beyond Mean-Field: Energy Landscape

What the mean-field approach crucially lacks is the description of activated processes that allow the system to jump over larger and larger barriers at large times. One way to introduce this key effect is to study mean-field models at finite system size N. In fact, the mean field theory of aging is derived by first taking the limit $N \to \infty$ to study the dynamics on large but finite timescales. Instead, if one focuses on timescales that diverge exponentially with N, activated processes will occur. One can then analyze in a controlled way how jumping over barriers alters the mean-field dynamics.

This approach was pioneered numerically by Crisanti and Ritort (2000a; b, 2003), and more recently pursued further in (Baity-Jesi et al. 2018a, b; Billoire et al. 2005; Stariolo and Cugliandolo 2019). One of the most important outcomes of their study is to show the existence

of an effective temperature and its relation with the energy landscape, more precisely the complexity, even when barriers are crossed. The understanding of the dynamical evolution in this regime was reached recently by theoretical and rigorous analysis of the Random Energy Model (REM) in (Baity-Jesi et al. 2018a; Baity-Jesi et al. 2018b; Arous et al. 2002; Gayrard 2019). It was shown that when observing the dynamics on exponentially large (in N) timescales, activated processes lead to a dynamical evolution that can be mapped on the one of the trap model (Bouchaud 1992; Dyre 1987). Again, an interesting relation with the energy landscape emerges: the exponent of the trapping time power law describing aging dynamics at a given energy is directly linked to the slope of the configurational entropy at that energy. It is not yet clear whether this scenario goes beyond the REM and applies, for instance, to the Monte Carlo dynamics of the p-spin model. In this case the energy landscape is more complex and one needs to understand the interplay between energy and entropic barriers (Barrat and Mézard 1995; Cammarota and Marinari 2015, 2018).

To this end, a series of recent works focused on the organization in configuration space of the barriers that can be used to escape from a given minimum for the p-spin spherical model. By using

the Kac-Rice formalism, these works computed the entropy of the barriers at a given energy and at a certain distance from a given minimum (Ros et al. 2019) and obtained the dynamical instanton representing the escape from a given minimum.

Finally, another set of works performed a complementary study on finite size models of three dimensional supercooled liquids. The key idea was to focus on a size that is large enough to be representative of the bulk behavior and small enough to be able to study the dynamics in terms of energy landscape (Büchner and Heuer 1999; Doliwa and Heuer 2003; Heuer 2008). This led to the introduction of the notion of metabasins, a set of basins that corresponds to the same metastable state. A study of the dynamics in terms of energy barriers between metabasins was then performed. It showed in a very compelling way that the dynamics start to be activated even above the MCT cross-over in 3D systems (Doliwa and Heuer 2003; Denny et al. 2003). Interestingly, a strong relationship with the dynamics of the trap model was also found in this case (Heuer 2008).

All the results cited above provide valuable information and insights on activated dynamics. Interestingly, they show that relations between aging dynamics and energy landscape found within mean-field theory seem to hold more broadly. Many questions remain open and will hopefully be addressed in future work, such as understanding and characterizing the dynamical paths and the barrier crossings leading to relaxation during the aging regime.

Driven Glassy Materials

We have introduced aging phenomena with the argument that in a glass phase, the timescale to equilibrate becomes so long that the system always remembers its complete history. This is true in general, but one can wonder whether it is possible to invent a protocol where the material history could be erased, and the system "rejuvenated" (McKenna and Kovacs 1984). This concept has been known for decades in the field of polymer glasses, where complex thermomechanical histories are often used.

Let us consider an aging protocol where the system is quenched to low temperature at time $t_\mathbf{w} = 0$, but the system is simultaneously forced by an external mechanical constraint. Experimentally one finds that a stationary state can be reached, which explicitly depends on the strength of the forcing: a system which is forced more strongly relaxes faster than a material that is less solicited, a phenomenon called "shear-thinning." The material has therefore entered a driven steady state, where memory of its age is no longer present and the dynamics have become stationary: aging is stopped.

Many studies of these driven glassy states have been performed in recent years. These studies are relevant for the rheology of supercooled liquids and glasses, and the $T \ll T_g$ limit corresponds to studies of the plasticity of amorphous solids, a broad field in itself, see section "Rheology." In the colloidal world, such studies are also relevant for the newly-defined field of the rheology of "soft glassy materials." These materials are (somewhat tautologically) defined as those for which the nonlinear rheological behavior is believed to result precisely from the competition between intrinsically slow relaxation processes and an external forcing (Sollich et al. 1997; Ikeda et al. 2012). It is believed that the rheology of dense colloidal suspensions, foams, emulsions, binary mixtures, or even biophysical systems is ruled by such a competition, which represents a broad scope for applications.

From the point of view of statmech modeling, soft glassy rheology can be naturally studied from the very same angles as the glass transition itself. As such trap models (Sollich et al. 1997; Sollich 1998), mean-field spin glasses (Berthier et al. 2000), and the related mode-coupling theory approach (Miyazaki and Reichman 2002; Fuchs and Cates 2002) have been explicitly extended to include an external mechanical forcing. In all these cases, one finds that a driven steady state can be reached and aging is indeed expected to stop at a level that depends on the strength of the forcing. Many of the results obtained in aging systems about the properties of an effective temperature are also shown to apply in the driven case, as shown both theoretically (Berthier et al. 2000) and numerically (Berthier and Barrat 2002b). A most interesting aspect is that the

broad relaxation spectra predicted to occur in glassy materials close to a glass transition directly translate into "anomalous" laws both for the linear rheological behavior (seen experimentally in the broad spectrum of elastic, $G'(\omega)$ and loss, $G''(\omega)$, moduli), and the nonlinear rheological behavior (a strong dependence of the viscosity η upon the shear rate $\dot{\gamma}$).

Future Directions

The problem of the glass transition, already very exciting in itself, has ramifications well beyond the physics of supercooled liquids. Glassy systems figure among the even larger class of "complex systems." These are formed by a set of interacting degrees of freedom showing nontrivial emergent behavior: as a whole they exhibit properties that are not already encoded in the definition of the individual parts. As a consequence the study of glass-formers as statistical mechanics models characterized by frustrated interactions is a fertile ground to develop new concepts and techniques that will likely be applied to other physical, and more generally, scientific situations.

An example, already cited in this review, is the progress obtained in computer science and information theory (Bouchaud et al. 2011) using techniques originally developed for spin glasses and structural glasses. There is no doubt that progress will steadily continue in the future along these interdisciplinary routes. Concerning physics, glassiness is such a ubiquitous and, yet as we showed, rather poorly understood problem that many developments are very likely to take place in the next decade.

Instead of guessing future developments of the field (and then very likely be proven wrong), we prefer to list a few problems we would like to see solved in the next years.

- Is the glass transition related to a true phase transition? If yes, a static or a dynamic one? A finite or zero temperature one?
- Do RFOT theory, defects models, or frustration-based theory form the correct

starting points of "the" theory of the glass transition?
- Is MCT really a useful theory for the first decades of slowing down of the dynamics? Can one find direct evidence that an avoided MCT transition exists and controls the dynamics?
- What is the correct physical picture for the low temperature phase of glass-forming liquids and spin glasses?
- Are there general principles governing off-equilibrium dynamics, and in particular aging and sheared materials?
- Do non-disordered, finite-dimensional, and finite-range statmech model exist that display a thermodynamically stable amorphous phase at low temperature?

Finally, notice that we did not discuss possible interplays between glassiness, disorder, and quantum fluctuations. This is a very fascinating topic that has boomed in recent years; new phenomena such as Many-Body Localization (Nandkishore and Huse 2015) and Quantum Scars (Turner et al. 2018) have been discovered, revealing new facets of slow dynamics. Models of classical glasses, such as the KCMs and the p-spin models, found new applications in this arena (Pancotti et al. 2020; Facoetti et al. 2019).

Bibliography

Abou B, Gallet F (2004) Phys Rev Lett 93:160603

Adam G, Gibbs JH (1965) J Chem Phys 43:139

Adhikari AN, Capurso NA, Bingemann D (2007) J Chem Phys 127:114508

Agoritsas E, Biroli G, Urbani P, Zamponi F (2018) J Phys A Math Theor 51:085002

Agoritsas E, Maimbourg T, Zamponi F (2019) J Phys A Math Theor 52:144002

Albert S, Bauer T, Michl M, Biroli G, Bouchaud J-P, Loidl A, Lunkenheimer P, Tourbot R, Wiertel-Gasquet-C, Ladieu F (2016) Science 352:1308

Allen M, Tildesley D (1989) New York/Oxford, p 385

Altieri A, Biroli G, Cammarota C (2020) arXiv preprint arXiv:2005.05118

Anandkumar A, Ge R, Hsu D, Kakade SM, Telgarsky M (2014) J Mach Learn Res 15:2773

Angelani L, Paoluzzi M, Parisi G, Ruocco G (2018) Proc Natl Acad Sci 115:8700

Angelini MC, Biroli G (2017) Proc Natl Acad Sci 114:3328

Angelini TE, Hannezo E, Trepat X, Marquez M, Fredberg JJ, Weitz DA (2011) Proc Natl Acad Sci 108:4714

Angell CA (1995) Science 267:1924

Angell CA (1997) J Res Natl Inst Stand Technol 102:171

Antenucci F, Franz S, Urbani P, Zdeborová L (2019) Phys Rev X 9:011020

Appignanesi GA, Rodríguez Fris JA, Montani RA, Kob W (2006) Phys Rev Lett 96:057801

Arous GB, Bovier A, Gayrard V (2002) Phys Rev Lett 88:087201

Baity-Jesi M, Baños R, Cruz A, Fernandez LA, Gil-Narvion JM, Gordillo-Guerrero A, Iniguez D, Maiorano A, Mantovani F, Marinari E et al (2013) Phys Rev B 88:224416

Baity-Jesi M, Achard-de Lustrac A, Biroli G (2018a) Phys Rev E 98:012133

Baity-Jesi M, Biroli G, Cammarota C (2018b) J Stat Mech: Theory Exp 2018:013301

Baity-Jesi M, Sagun L, Geiger M, Spigler S, Arous GB, Cammarota C, LeCun Y, Wyart M, Biroli G (2019) J Stat Mech: Theory Exp 2019:124013

Bapst V, Keck T, Grabska-Barwińska A, Donner C, Cubuk ED, Schoenholz S, Obika A, Nelson A, Back T, Hassabis D et al (2020) Nat Phys 16:448

Barrat A (1998) Phys Rev E 57:3629

Barrat A, Mézard M (1995) J Phys I 5:941

Barrat J-L, Feigelman M, Kurchan J et al (2004) Slow relaxations and nonequilibrium dynamics in condensed matter 77. Springer, Berlin, Heidelberg, https://doi.org/10.1007/978-3-540-44835-8_5

Bässler H (1987) Phys Rev Lett 58:767

Bauer T, Lunkenheimer P, Loidl A (2013) Phys Rev Lett 111:225702

Bechinger C, Di Leonardo R, Löwen H, Reichhardt C, Volpe G, Volpe G (2016) Rev Mod Phys 88:045006

Bellon L, Ciliberto S (2002) Physica D 168:325

Bellon L, Ciliberto S, Laroche C (2001) EPL (Europhys Lett) 53:511

Bengtzelius U, Gotze W, Sjolander A (1984) J Phys C Solid State Phys 17:5915

Bennemann C, Donati C, Baschnagel J, Glotzer SC (1999) Nature 399:246

Berges J, Tetradis N, Wetterich C (2002) Phys Rep 363:223

Bert F, Dupuis V, Vincent E, Hammann J, Bouchaud J-P (2004) Phys Rev Lett 92:167203

Berthier L (2004) Phys Rev E 69:020201

Berthier L (2007a) Phys Rev E 76:011507

Berthier L (2007b) Phys Rev Lett 98:220601

Berthier L (2013) Phys Rev E 88. https://doi.org/10.1103/PhysRevE.88.022313

Berthier L (2014) Phys Rev Lett 112:220602

Berthier L, Barrat J-L (2002a) Phys Rev Lett 89:095702

Berthier L, Barrat J-L (2002b) J Chem Phys 116:6228

Berthier L, Biroli G (2011) Rev Mod Phys 83:587

Berthier L, Bouchaud J-P (2002) Phys Rev B 66:054404

Berthier L, Coslovich D (2014) Proc Natl Acad Sci 111:11668

Berthier L, Ediger MD (2016) Phys Today 69:40

Berthier L, Garrahan JP (2003) J Chem Phys 119:4367

Berthier L, Garrahan JP (2005) J Phys Chem B 109:3578

Berthier L, Jack RL (2015) Phys Rev Lett 114. https://doi.org/10.1103/PhysRevLett.114.205701

Berthier L, Kob W (2007) J Phys Condens Matter 19:205130

Berthier L, Kob W (2012) Phys Rev E:85. https://doi.org/10.1103/PhysRevE.85.011102

Berthier L, Kurchan J (2013) Nat Phys 9:310

Berthier L, Witten TA (2009) Phys Rev E 80:021502

Berthier L, Young A (2005) Phys Rev B 71:214429

Berthier L, Barrat J-L, Kurchan J (1999) Eur Phys J B-Condens Matter Complex Syst 11:635

Berthier L, Barrat J-L, Kurchan J (2000) Phys Rev E 61:5464

Berthier L, Chandler D, Garrahan JP (2004) EPL (Europhys Lett) 69:320

Berthier L, Biroli G, Bouchaud J-P, Cipelletti L, El Masri D, L'Hôte D, Ladieu F, Pierno M (2005) Science 310:1797

Berthier L, Biroli G, Bouchaud J-P, Kob W, Miyazaki K, Reichman D (2007a) J Chem Phys 126:184503

Berthier L, Biroli G, Bouchaud J-P, Kob W, Miyazaki K, Reichman DR (2007b) J Chem Phys 126:184504

Berthier L, Biroli G, Bouchaud J-P, Cipelletti L, van Saarloos W (2011a) Dynamical heterogeneities in glasses, colloids, and granular media, vol 150. OUP, Oxford

Berthier L, Jacquin H, Zamponi F (2011b) Phys Rev E 84:051103

Berthier L, Biroli G, Coslovich D, Kob W, Toninelli C (2012) Phys Rev E 86:031502

Berthier L, Charbonneau P, Jin Y, Parisi G, Seoane B, Zamponi F (2016a) Proc Natl Acad Sci 113:8397

Berthier L, Coslovich D, Ninarello A, Ozawa M (2016b) Phys Rev Lett 116. https://doi.org/10.1103/PhysRevLett.116.238002

Berthier L, Charbonneau P, Yaida S (2016c) J Chem Phys 144:024501

Berthier L, Flenner E, Szamel G (2017a) New J Phys 19:125006

Berthier L, Charbonneau P, Flenner E, Zamponi F (2017b) Phys Rev Lett 119:188002

Berthier L, Charbonneau P, Coslovich D, Ninarello A, Ozawa M, Yaida S (2017c) Proc Natl Acad Sci 114:11356

Berthier L, Ozawa M, Scalliet C (2019a) J Chem Phys 150:160902

Berthier L, Flenner E, Szamel G (2019b) J Chem Phys 150:200901

Berthier L, Biroli G, Bouchaud J-P, Tarjus G (2019c) J Chem Phys 150:094501

Berthier L, Biroli G, Charbonneau P, Corwin EI, Franz S, Zamponi F (2019d) J Chem Phys 151:010901

Berthier L, Flenner E, Fullerton CJ, Scalliet C, Singh M (2019e) J Stat Mech: Theory Exp 2019:064004

Berthier L, Charbonneau P, Kundu J (2019f) Phys Rev E 99. https://doi.org/10.1103/PhysRevE.99.031301

Berthier L, Charbonneau P, Ninarello A, Ozawa M, Yaida S (2019g) Nat Commun 10. https://doi.org/10.1038/s41467-019-09512-3

Berthier L, Charbonneau P, Kundu J (2020) Phys Rev Lett 125:108001

Bi D, Yang X, Marchetti MC, Manning ML (2016) Phys Rev X:6. https://doi.org/10.1103/Phys-RevX.6.021011

Billoire A, Giomi L, Marinari E (2005) EPL (Europhys Lett) 71:824

Binder K, Kob W (2011) Glassy materials and disordered solids: an introduction to their statistical mechanics. World Scientific

Binder K, Young AP (1986) Rev Mod Phys 58:801

Biroli G, Bouchaud J-P (2004) EPL (Europhys Lett) 67:21

Biroli G, Bouchaud J-P (2012) Structural glasses and supercooled liquids: theory, experiment, and applications. p 31

Biroli G, Cammarota C (2017) Phys Rev X 7:011011

Biroli G, Mézard M (2001) Phys Rev Lett 88:025501

Biroli G, Urbani P (2016) Nat Phys 12:1130

Biroli G, Urbani P (2018) SciPost Phys 4:020

Biroli G, Bouchaud J-P, Tarjus G (2005) J Chem Phys 123:044510

Biroli G, Bouchaud J-P, Miyazaki K, Reichman DR (2006) Phys Rev Lett 97:195701

Biroli G, Bouchaud J-P, Cavagna A, Grigera TS, Verrocchio P (2008) Nat Phys 4:771

Biroli G, Cammarota C, Tarjus G, Tarzia M (2014) Phys Rev Lett 112:175701

Biroli G, Rulquin C, Tarjus G, Tarzia M (2016) SciPost Phys 1. https://doi.org/10.21468/SciPostPhys.1.1.007

Biroli G, Cammarota C, Tarjus G, Tarzia M (2018a) Phys Rev B 98:174205

Biroli G, Cammarota C, Tarjus G, Tarzia M (2018b) Phys Rev B 98:174206

Boattini E, Marín-Aguilar S, Mitra S, Foffi G, Smallenburg F, Filion L (2020) arXiv preprint arXiv:2003.00586

Bouchaud J-P (1992) J Phys I 2:1705

Bouchaud J-P, Biroli G (2004) J Chem Phys 121:7347

Bouchaud J-P, Biroli G (2005) Phys Rev B 72:064204

Bouchaud J-P, Dupuis V, Hammann J, Vincent E (2001) Phys Rev B 65:024439

Bouchaud J-P, Mézard M, Dalibard J (2011) Complex systems: lecture notes of the les Houches Summer School 2006. Elsevier

Brambilla G, El Masri D, Pierno M, Berthier L, Cipelletti L, Petekidis G, Schofield AB (2009) Phys Rev Lett 102:085703

Bray A (1994) Adv Phys 43:357

Bray A, Moore M (1984) J Phys C Solid State Phys 17:L463

Bray A, Moore M (1987) Phys Rev Lett 58:57

Brito C, Wyart M (2009) J Chem Phys 131:149

Brito C, Lerner E, Wyart M (2018) Phys Rev X 8. https://doi.org/10.1103/PhysRevX.8.031050

Brun C, Ladieu F, LHôte D, Biroli G, Bouchaud J (2012) Phys Rev Lett 109:175702

Büchner S, Heuer A (1999) Phys Rev E 60:6507

Buisson L, Bellon L, Ciliberto S (2003a) J Phys Condens Matter 15:S1163

Buisson L, Ciliberto S, Garcimartin A (2003b) EPL (Europhys Lett) 63:603

Butler S, Harrowell P (1991) J Chem Phys 95:4454

Buttinoni I, Bialké J, Kümmel F, Löwen H, Bechinger C, Speck T (2013) Phys Rev Lett 110:238301

Calabrese P, Gambassi A (2005) J Phys A Math Gen 38:R133

Cammarota C (2013) EPL (Europhys Lett) 101:56001

Cammarota C, Biroli G (2012) Proc Natl Acad Sci 109:8850

Cammarota C, Biroli G (2013) J Chem Phys 138:12A547

Cammarota C, Marinari E (2015) Phys Rev E 92:010301

Cammarota C, Marinari E (2018) J Stat Mech: Theory Exp 2018:043303

Cammarota C, Seoane B (2016) Phys Rev B 94:180201

Cammarota C, Biroli G, Tarzia M, Tarjus G (2011) Phys Rev Lett 106:115705

Candelier R, Dauchot O, Biroli G (2009) Phys Rev Lett 102:1

Candelier R, Widmer-Cooper A, Kummerfeld JK, Dauchot O, Biroli G, Harrowell P, Reichman DR (2010a) Phys Rev Lett 105:135702. https://doi.org/10.1103/PhysRevLett.105.135702

Candelier R, Dauchot O, Biroli G (2010b) EPL (Europhys Lett) 92:24003

Cardenas M, Franz S, Parisi G (1999) J Chem Phys 110:1726

Castellana M, Decelle A, Franz S, Mézard M, Parisi G (2010) Phys Rev Lett 104:127206

Castellani T, Cavagna A (2005) J Stat Mech: Theory Exp 2005:P05012

Cavagna A (2009) Phys Rep 476:51

Cavagna A, Grigera TS, Verrocchio P (2007) Phys Rev Lett 98:187801

Cavagna A, Grigera TS, Verrocchio P (2012) J Chem Phys 136:204502

Chaikin PM, Lubensky TC, Witten TA (1995) Principles of condensed matter physics, vol 10. Cambridge University Press, Cambridge

Chakrabarty S, Karmakar S, Dasgupta C (2015) Sci Rep 5:12577

Chakrabarty S, Das R, Karmakar S, Dasgupta C (2016) J Chem Phys 145:034507

Chandler D, Garrahan JP, Jack RL, Maibaum L, Pan AC (2006) Phys Rev E 74:051501

Charbonneau P, Tarjus G (2013) Phys Rev E 87:042305

Charbonneau P, Corwin EI, Parisi G, Zamponi F (2012) Phys Rev Lett 109:205501

Charbonneau P, Kurchan J, Parisi G, Urbani P, Zamponi F (2014a) Nat Commun 5:1

Charbonneau P, Kurchan J, Parisi G, Urbani P, Zamponi F (2014b) J Stat Mech: Theory Exp 2014:P10009

Charbonneau P, Corwin EI, Parisi G, Zamponi F (2015) Phys Rev Lett 114:125504

Charbonneau P, Corwin EI, Parisi G, Poncet A, Zamponi F (2016a) Phys Rev Lett 117:045503

Charbonneau P, Dyer E, Lee J, Yaida S (2016b) J Stat Mech: Theory Exp 2016:074004

Charbonneau P, Kurchan J, Parisi G, Urbani P, Zamponi F (2017) Annu Rev Condens Matter Phys 8:265

Chaudhuri P, Berthier L, Kob W (2007) Phys Rev Lett 99:060604

Chaudhuri P, Berthier L, Sastry S (2010) Phys Rev Lett 104:165701

Chen Z, Sepúlveda A, Ediger M, Richert R (2013) J Chem Phys 138:12A519

Cheng Z, Zhu J, Chaikin PM, Phan S-E, Russel WB (2002) Phys Rev E 65:041405

Cohen MH, Grest G (1982) Phys Rev B 26:6313

Coslovich D (2011) Phys Rev E Stat Nonlinear Soft Matter Phys 83:1

Coslovich D, Pastore G (2007) J Chem Phys 127:124504

Coslovich D, Ozawa M, Berthier L (2018) J Phys Condens Matter 30:144004

Crauste-Thibierge C, Brun C, Ladieu F, Lhôte D, Biroli G, Bouchaud J-P (2010) Phys Rev Lett 104:165703

Crisanti A, Ritort F (2000a) EPL (Europhys Lett) 51:147

Crisanti A, Ritort F (2000b) EPL (Europhys Lett) 52:640

Crisanti A, Ritort F (2003) J Phys A Math Gen 36:R181

Cubuk ED, Schoenholz SS, Rieser JM, Malone BD, Rottler J, Durian DJ, Kaxiras E, Liu AJ (2015) Phys Rev Lett 114:1

Cubuk ED, Schoenholz SS, Kaxiras E, Liu AJ (2016) J Phys Chem B 120:6139. iSBN: 1520-5207 (Electronic) 1520-5207 (Linking)

Cubuk ED, Ivancic RJS, Schoenholz SS, Strickland DJ, Basu A, Davidson ZS, Fontaine J, Hor JL, Huang Y-R, Jiang Y, Keim NC, Koshigan KD, Lefever JA, Liu T, Ma X-G, Magagnosc DJ, Morrow E, Ortiz CP, Rieser JM, Shavit A, Still T, Xu Y, Zhang Y, Nordstrom KN, Arratia PE, Carpick RW, Durian DJ, Fakhraai Z, Jerolmack DJ, Lee D, Li J, Riggleman R, Turner KT, Yodh AG, Gianola DS, Liu AJ (2017) Science 358:1033. iSBN: 3487716170192

Cugliandolo LF, Kurchan J (1993) Phys Rev Lett 71:173

Cugliandolo LF, Kurchan J (1994) J Phys A Math Gen 27:5749

Cugliandolo LF, Kurchan J, Peliti L (1997) Phys Rev E 55:3898

D'Anna G, Grémaud G (2001) Nature 413:407

Dalle-Ferrier C, Thibierge C, Alba-Simionesco C, Berthier L, Biroli G, Bouchaud J-P, Ladieu F, L'Hôte D, Tarjus G (2007) Phys Rev E 76:041510

Darst RK, Reichman DR, Biroli G (2010) J Chem Phys 132:044510

Das SP, Mazenko GF (1986) Phys Rev A 34:2265

Dauchot O, Marty G, Biroli G (2005) Phys Rev Lett 95:265701

Debenedetti PG (1996) Metastable liquids: concepts and principles. Princeton University Press

Debenedetti PG, Stillinger FH (2001) Nature 410:259

DeGiuli E, Lerner E, Brito C, Wyart M (2014) Proc Natl Acad Sci 111:17054

Degiuli E, Lerner E, Wyart M (2015) J Chem Phys 142:164503

Denny RA, Reichman DR, Bouchaud J-P (2003) Phys Rev Lett 90:025503

Depken M, Stinchcombe R (2005) Phys Rev E 71:065102

Deseigne J, Dauchot O, Chaté H (2010) Phys Rev Lett 105:098001

Doliwa B, Heuer A (2003) Phys Rev E 67:030501

Donati C, Douglas JF, Kob W, Plimpton SJ, Poole PH, Glotzer SC (1998) Phys Rev Lett 80:2338

Donati C, Franz S, Glotzer SC, Parisi G (2002) J Non-Cryst Solids 307–310:215

Donev A, Torquato S, Stillinger FH, Connelly R (2004) J Appl Phys 95:989

Donev A, Torquato S, Stillinger FH (2005) Phys Rev E 71:011105

Downton MT, Kennett MP (2007) Phys Rev E 76:031502

Durian DJ (1995) Phys Rev Lett 75:4780

Dyre JC (1987) Phys Rev Lett 58:792

Dzero M, Schmalian J, Wolynes PG (2005) Phys Rev B 72:100201

Ediger MD (2000) Annu Rev Phys Chem 51:99

Ediger MD (2017) J Chem Phys 147:210901

Elmatad YS, Keys AS (2012) Phys Rev E Stat Nonlinear Soft Matter Phys 85:061502

Elmatad Y, Chandler D, Garrahan J (2009) J Phys Chem B 113:5563

Elmatad YS, Jack RL, Chandler D, Garrahan JP (2010) Proc Natl Acad Sci 107:12793

Facoetti D, Biroli G, Kurchan J, Reichman DR (2019) Phys Rev B 100:205108

Fernández L, Martín-Mayor V, Verrocchio P (2006) Phys Rev E 73:020501

Fielding S, Sollich P (2002) Phys Rev Lett 88:050603

Fisher DS (1986) Phys Rev Lett 56:416

Fisher DS, Huse DA (1986) Phys Rev Lett 56:1601

Flenner E, Berthier L, Charbonneau P, Fullerton CJ (2019) Phys Rev Lett 123:175501

Frank FC (1952) Proc R Soc Lond A Math Phys Sci 215:43

Franz S (2006) EPL (Europhys Lett) 73:492

Franz S, Parisi G (1997) Phys Rev Lett 79:2486

Franz S, Parisi G (1998) Physica A 23:317–339

Franz S, Parisi G (2000) J Phys Condens Matter 12:6335

Franz S, Parisi G (2013) J Stat Mech: Theory Exp 2013:P11012

Franz S, Mézard M, Parisi G, Peliti L (1998) Phys Rev Lett 81:1758

Franz S, Donati C, Parisi G, Glotzer SC (1999) Philos Mag B 79:1827. https://doi.org/10.1080/13642819908223066

Franz S, Mulet R, Parisi G (2002) Phys Rev E 65:021506

Franz S, Parisi G, Ricci-Tersenghi F, Rizzo T (2011) Eur Phys J E 34:1

Franz S, Parisi G, Ricci-Tersenghi F (2013) J Stat Mech: Theory Exp 2013:L02001

Franz S, Parisi G, Urbani P, Zamponi F (2015) Proc Natl Acad Sci 112:14539

Franz S, Parisi G, Sevelev M, Urbani P, Zamponi F (2017) SciPost Phys 2:019

Fredrickson GH, Andersen HC (1984) Phys Rev Lett 53: 1244

Fredrickson GH, Brawer SA (1986) J Chem Phys 84:3351

Fuchs M, Cates ME (2002) Phys Rev Lett 89:248304

Fullerton CJ, Berthier L (2017) EPL (Europhys Lett) 119: 36003

Fullerton CJ, Jack RL (2014) Phys Rev Lett 112:255701

Ganapathi D, Nagamanasa KH, Sood A, Ganapathy R (2018) Nat Commun 9:1

Garcia S, Hannezo E, Elgeti J, Joanny J-F, Silberzan P, Gov NS (2015) Proc Natl Acad Sci 112:15314

Gardner E (1985) Nucl Phys B 257:747

Garrahan JP (2002) J Phys Condens Matter 14:1571

Garrahan JP, Chandler D (2002) Phys Rev Lett 89:035704

Garrahan JP, Chandler D (2003) Proc Natl Acad Sci 100: 9710. tex.eprint: https://www.pnas.org/content/100/17/9710.full.pdf. tex.publisher: National Academy of Sciences

Garrahan JP, Jack RL, Lecomte V, Pitard E, van Duijvendijk K, van Wijland F (2007) Phys Rev Lett 98. https://doi.org/10.1103/Phys-RevLett.98.195702

Garrahan JP, Jack RL, Lecomte V, Pitard E, van Duijvendijk K, van Wijland F (2009) J Phys A Math Theor 42:075007

Gayrard V (2019) Probab Theory Relat Fields 174:501

Gazzillo D, Pastore G (1989) Chem Phys Lett 159:388

Gebremichael Y, Vogel M, Glotzer SC (2004) J Chem Phys 120:4415. https://doi.org/10.1063/1.1644539

Glarum SH (1960) J Chem Phys 33:639

Gleim T, Kob W, Binder K (1998) Phys Rev Lett 81:4404

Godréche C, Luck J (2000) J Phys A Math Gen 33:1151

Godreche C, Luck J (2000) J Phys A Math Gen 33:9141

Gokhale S, Nagamanasa KH, Ganapathy R, Sood A (2014) Nat Commun 5:4685

Gokhale S, Sood A, Ganapathy R (2016) Adv Phys 65:363

Goldstein M (1969) J Chem Phys 51:3728

Götze W (1999) J Phys Condens Matter 11:A1

Grigera TS, Israeloff N (1999) Phys Rev Lett 83:5038

Grigera TS, Parisi G (2001) Phys Rev E 63. https://doi.org/10.1103/PhysRevE.63.045102

Gross DJ, Mézard M (1984) Nucl Phys B 240:431

Guiselin B, Berthier L, Tarjus G (2020) arXiv preprint arXiv:2004.10555

Gutiérrez R, Garrahan JP (2016) J Stat Mech: Theory Exp 2016:074005

Gutiérrez R, Garrahan JP, Jack RL (2019) J Stat Mech: Theory Exp 2019:094006

Hallett JE, Turci F, Royall CP (2018) Nat Commun 9:1

Hansen J-P, McDonald IR (1990) Theory of simple liquids. Elsevier

Hartarsky I, Marêché L, Toninelli C (2019a) arXiv preprint arXiv:1904.09145

Hartarsky I, Martinelli F, Toninelli C (2019b) arXiv preprint arXiv:1910.06782

Hedges LO, Jack RL, Garrahan JP, Chandler D (2009) Science 323:1309

Henkes S, Fily Y, Marchetti MC (2011) Phys Rev E 84: 040301

Heuer A (2008) J Phys Condens Matter 20:373101

Hocky GM, Berthier L, Reichman DR (2014) J Chem Phys 141:224503

Hodge IM (1997) J Res Natl Inst Stand Technol 102:195

Hołyst R (2001) Physica A 292:255

Horbach J, Kob W (2001) Phys Rev E 64:041503

Hurley M, Harrowell P (1995) Phys Rev E 52:1694

Ikeda A, Berthier L, Sollich P (2012) Phys Rev Lett 109: 018301

Ikeda A, Berthier L, Biroli G (2013) J Chem Phys 138: 12A507

Ikeda H, Miyazaki K, Biroli G (2017a) EPL (Europhys Lett) 116:56004

Ikeda H, Zamponi F, Ikeda A (2017b) J Chem Phys 147: 234506

Isobe M, Keys AS, Chandler D, Garrahan JP (2016) Phys Rev Lett 117:1

Ivancic R, Cubuk E, Schoenholz S, Strickland D, Gianola D, Liu A (2017) Bull Am Phys Soc 62: B16–013

Jack RL, Berthier L (2012) Phys Rev E 85:021120

Jack RL, Berthier L (2016) J Chem Phys 144:244506

Jack RL, Fullerton CJ (2013) Phys Rev E 88:042304

Jack RL, Garrahan JP (2005) J Chem Phys 123:164508

Jack RL, Garrahan JP (2010) Phys Rev E 81:011111

Jack RL, Garrahan JP (2016) Phys Rev Lett 116. https://doi.org/10.1103/PhysRevLett.116.055702

Jack RL, Berthier L, Garrahan JP (2005) Phys Rev E 72: 016103

Jack RL, Mayer P, Sollich P (2006a) J Stat Mech: Theory Exp 2006:P03006

Jack RL, Berthier L, Garrahan JP (2006b) J Stat Mech: Theory Exp 2006:P12005

Jack RL, Hedges LO, Garrahan JP, Chandler D (2011) Phys Rev Lett 107. https://doi.org/10.1103/PhysRevLett.107.275702

Jaeger HM, Nagel SR, Behringer RP (1996) Rev Mod Phys 68:1259

Johari G (2000) J Chem Phys 112:7518

Jönsson P, Mathieu R, Nordblad P, Yoshino H, Katori HA, Ito A (2004) Phys Rev B 70:174402

Jung Y, Garrahan JP, Chandler D (2004) Phys Rev E 69: 061205

Kapteijns G, Ji W, Brito C, Wyart M, Lerner E (2019) Phys Rev E 99. https://doi.org/10.1103/Phys-RevE.99.012106

Karmakar S, Parisi G (2013) Proc Natl Acad Sci 110:2752

Karmakar S, Procaccia I (2011) arXiv preprint arXiv:1105.4053

Kauzmann W (1948) Chem Rev 43:219

Kearns KL, Ediger M, Huth H, Schick C (2010) J Phys Chem Lett 1:388

Kegel WK, van Blaaderen A (2000) Science 287:290

Keys AS, Abate AR, Glotzer SC, Durian DJ (2007) Nat Phys 3:260

Keys AS, Hedges LO, Garrahan JP, Glotzer SC, Chandler D (2011) Phys Rev X 1:1

Keys AS, Garrahan JP, Chandler D (2013) Proc Natl Acad Sci 110:4482

Keys AS, Chandler D, Garrahan JP (2015) Phys Rev E Stat Nonlinear Soft Matter Phys 92(1)

Khomenko D, Scalliet C, Berthier L, Reichman DR, Zamponi F (2020) Phys Rev Lett 124:225901

Kim K (2003) EPL (Europhys Lett) 61:790

Kirkpatrick TR, Thirumalai D (1987) Phys Rev Lett 58:2091

Kirkpatrick T, Wolynes P (1987a) Phys Rev A 35:3072

Kirkpatrick T, Wolynes P (1987b) Phys Rev B 36:8552

Kirkpatrick TR, Thirumalai D, Wolynes PG (1989) Phys Rev A 40:1045

Kisker J, Santen L, Schreckenberg M, Rieger H (1996) Phys Rev B 53:6418

Kivelson D, Kivelson SA, Zhao X, Nussinov Z, Tarjus G (1995) Physica A 219:27

Klongvessa N, Ginot F, Ybert C, Cottin-Bizonne C, Leocmach M (2019) Phys Rev Lett 123:248004

Kob W, Andersen HC (1993) Phys Rev E 48:4364

Kob W, Berthier L (2013) Phys Rev Lett 110:245702

Kob W, Coslovich D (2014) Phys Rev E 90:052305

Kob W, Donati C, Plimpton SJ, Poole PH, Glotzer SC (1997) Phys Rev Lett 79:2827

Kob W, Roldán-Vargas S, Berthier L (2012) Nat Phys 8:164

Krakoviack V (2010) Phys Rev E 82:061501

Krakoviack V (2011) Phys Rev E 84:050501

Krakoviack V (2014) J Chem Phys 141:104504

Krzakala F, Montanari A, Ricci-Tersenghi F, Semerjian G, Zdeborová L (2007) Proc Natl Acad Sci 104:10318

Krzkala F (2005) Phys Rev Lett 94:077204

Kurchan J (2005) Nature 433:222

Kurchan J, Laloux L (1996) J Phys A Math Gen 29:1929

Kurchan J, Parisi G, Zamponi F (2012) J Stat Mech: Theory Exp 2012:P10012

Kurchan J, Parisi G, Urbani P, Zamponi F (2013) J Phys Chem B 117:12979

Kurchan J, Maimbourg T, Zamponi F (2016) J Stat Mech: Theory Exp 2016:033210

Lačević N, Starr FW, Schrøder T, Glotzer S (2003) J Chem Phys 119:7372

Landes FP, Biroli G, Dauchot O, Liu AJ, Reichman DR (2020) Phys Rev E 101:010602

Larson RG (1999) The structure and rheology of complex fluids, vol 150. Oxford University Press, New York

Léonard S, Harrowell P (2010) J Chem Phys 133:244502

Léonard S, Mayer P, Sollich P, Berthier L, Garrahan JP (2007) J Stat Mech: Theory Exp 2007:P07017

Lerner E, Düring G, Wyart M (2013) Soft Matter 9:8252

Lerner E, Düring G, Bouchbinder E (2016) Phys Rev Lett 117:035501

Leutheusser E (1984) Phys Rev A 29:2765

Li Y-W, Xu W-S, Sun Z-Y (2014) J Chem Phys 140:124502

Li Y-W, Zhu Y-L, Sun Z-Y (2015) J Chem Phys 142:124507

Liao Q, Berthier L (2019) Phys Rev X 9:011049

Lin J, Lerner E, Rosso A, Wyart M (2014) Proc Natl Acad Sci 111:14382

Lipowski A, Johnston D, Espriu D (2000) Phys Rev E 62:3404

Lippiello E, Zannetti M (2000) Phys Rev E 61:3369

Liu AJ, Nagel SR (1998) Nature 396:21

Liu AJ, Nagel SR (2010) Annu Rev Condens Matter Phys 1:347

Lyubimov I, Ediger MD, de Pablo JJ (2013) J Chem Phys 139:144505

Maimbourg T, Kurchan J, Zamponi F (2016) Phys Rev Lett 116:015902

Malins A, Eggers J, Royall CP, Williams SR, Tanaka H (2013a) J Chem Phys 138:12A535

Malins A, Williams SR, Eggers J, Royall CP (2013b) J Chem Phys 139:234506

Manacorda A, Schehr G, Zamponi F (2020) J Chem Phys 152:164506

Mandal R, Bhuyan PJ, Rao M, Dasgupta C (2016) Soft Matter 12:6268

Mannelli SS, Biroli G, Cammarota C, Krzakala F, Urbani P, Zdeborová L (2020) Phys Rev X 10:011057

Mapes MK, Swallen SF, Ediger MD (2006) J Phys Chem B 110:507. https://doi.org/10.1021/jp0555955. PMID: 16471562

Marchetti MC, Joanny J-F, Ramaswamy S, Liverpool TB, Prost J, Rao M, Simha RA (2013) Rev Mod Phys 85:1143

Martinelli F, Morris R, Toninelli C (2019a) Commun Math Phys 369:761

Martinelli F, Toninelli C et al (2019b) Ann Probab 47:324

Marty G, Dauchot O (2005) Phys Rev Lett 94:015701

Matoz-Fernandez D, Martens K, Sknepnek R, Barrat J, Henkes S (2017) Soft Matter 13:3205

Mayer P, Sollich P (2007) J Phys A Math Theor 40:5823

Mayer P, Berthier L, Garrahan JP, Sollich P (2003) Phys Rev E 68:016116

Mayer P, Léonard S, Berthier L, Garrahan JP, Sollich P (2006) Phys Rev Lett 96:030602

McCullagh GD, Cellai D, Lawlor A, Dawson KA (2005) Phys Rev E 71:030102

McKenna G, Kovacs A (1984) Polym Eng Sci 24:1138

Menon N, Nagel SR (1995) Phys Rev Lett 74:1230

Mézard M, Montanari A (2006) J Stat Phys 124:1317

Mézard M, Parisi G (1999) Phys Rev Lett 82:747

Mézard M, Parisi G, Virasoro M (1987) Spin glass theory and beyond: an introduction to the replica method and its applications, vol 9. World Scientific

Miyazaki K, Reichman DR (2002) Phys Rev E 66:050501

Mizuno H, Shiba H, Ikeda A (2017) Proc Natl Acad Sci 114:E9767

Monasson R (1995) Phys Rev Lett 75:2847

Mongera A, Rowghanian P, Gustafson HJ, Shelton E, Kealhofer DA, Carn EK, Serwane F, Lucio AA, Giammona J, Campàs O (2018) Nature 561:401

Montanari A, Semerjian G (2006) J Stat Phys 125:23

Mossa S, Tarjus G (2006) J Non-Cryst Solids 352:4847

Nandi SK, Biroli G, Tarjus G (2016) Phys Rev Lett 116:145701

Nandkishore R, Huse DA (2015) Annu Rev Condens Matter Phys 6:15

Nelson DR (2002) Defects and geometry in condensed matter physics. Cambridge University Press

Ni R, Stuart MAC, Dijkstra M (2013) Nat Commun 4:1

Niblett S, de Souza VK, Jack R, Wales D (2018) J Chem Phys 149:114503

Nicodemi M (1999) Phys Rev Lett 82:3734

Ninarello AS (2017) Computer simulations of supercooled liquids near the experimental glass transition, PhD thesis, Montpellier

Ninarello A, Berthier L, Coslovich D (2017) Phys Rev X 7. https://doi.org/10.1103/PhysRevX.7.021039

Nishikawa Y, Hukushima K (2020) Phys Rev Lett 125: 065501

Noe F, Schutte C, Vanden-Eijnden E, Reich L, Weikl TR (2009) Proc Natl Acad Sci 106:19011. iSBN: 0027-8424

O'Hern CS, Langer SA, Liu AJ, Nagel SR (2002) Phys Rev Lett 88:075507

Ohern CS, Silbert LE, Liu AJ, Nagel SR (2003) Phys Rev E 68:011306

Ozawa M, Berthier L (2017) J Chem Phys 146:014502

Ozawa M, Ikeda A, Miyazaki K, Kob W (2018a) Phys Rev Lett 121:205501

Ozawa M, Berthier L, Biroli G, Rosso A, Tarjus G (2018b) Proc Natl Acad Sci 115:6656

Ozawa M, Parisi G, Berthier L (2018c) J Chem Phys 149: 154501

Ozawa M, Scalliet C, Ninarello A, Berthier L (2019) J Chem Phys 151:084504

Paeng K, Park H, Hoang DT, Kaufman LJ (2015) Proc Natl Acad Sci 112:4952

Pan AC, Garrahan JP, Chandler D (2005) Phys Rev E 72: 041106

Pancotti N, Giudice G, Cirac JI, Garrahan JP, Bañuls MC (2020) Phys Rev X 10:021051

Pardo L, Lunkenheimer P, Loidl A (2007) Phys Rev E 76: 030502

Paret J, Jack RL, Coslovich D (2020) J Chem Phys 152: 144502

Parisi G, Seoane B (2014) Phys Rev E 89:022309

Parisi G, Slanina F (2000) Phys Rev E 62:6554

Parisi G, Zamponi F (2010) Rev Mod Phys 82:789

Parisi G, Procaccia I, Rainone C, Singh M (2017) Proc Natl Acad Sci 114:5577

Parisi G, Urbani P, Zamponi F (2020) Theory of simple glasses: exact solutions in infinite dimensions. Cambridge University Press

Parmar ADS, Ozawa M, Berthier L (2020) Phys Rev Lett 125:085505

Pérez-Castañeda T, Rodríguez-Tinoco C, Rodríguez-Viejo J, Ramos MA (2014) Proc Natl Acad Sci 111:11275

Peters IR, Majumdar S, Jaeger HM (2016) Nature 532:214

Phan AD, Schweizer KS (2018) J Chem Phys 148:054502

Pinchaipat R, Campo M, Turci F, Hallett JE, Speck T, Royall CP (2017) Phys Rev Lett 119. https://doi.org/10.1103/PhysRevLett.119.028004

Pusey PN, VanMegen W (1986) Nature 320:340

Ràfols-Ribé J, Will P-A, Hänisch C, Gonzalez-Silveira M, Lenk S, Rodríguez-Viejo J, Reineke S (2018) Sci Adv 4:eaar8332

Rainone C, Urbani P (2016) J Stat Mech: Theory Exp 2016:053302

Rainone C, Urbani P, Yoshino H, Zamponi F (2015) Phys Rev Lett 114:015701

Refregier P, Vincent E, Hammann J, Ocio M (1987) J Phys 48:1533

Reinsberg SA, Qiu XH, Wilhelm M, Spiess HW, Ediger MD (2001) J Chem Phys 114:7299. https://doi.org/10.1063/1.1369160

Richard E, Montanari A (2014) Advances in neural information processing systems. pp 2897–2905

Richert R, Angell C (1998) J Chem Phys 108:9016

Ritort F, Sollich P (2003) Adv Phys 52:219

Rivoire O, Biroli G, Martin OC, Mézard M (2004) Eur Phys J B-Condens Matter Complex Syst 37:55

Rizzo T (2016) Phys Rev B 94:014202

Ronhovde P, Chakrabarty S, Hu D, Sahu M, Sahu K, Kelton K, Mauro N, Nussinov Z (2011) Eur Phys J E 34:105

Ronhovde P, Chakrabarty S, Hu D, Sahu M, Sahu KK, Kelton KF, Mauro NA, Nussinov Z (2012) Sci Rep 2:1

Ros V, Biroli G, Cammarota C (2019) EPL (Europhys Lett) 126:20003

Royall CP, Kob W (2017) J Stat Mech: Theory Exp 2017. https://doi.org/10.1088/1742-5468/aa4e92

Royall CP, Williams SR (2015) Phys Rep 560:1

Rulquin C, Urbani P, Biroli G, Tarjus G, Tarzia M (2016) J Stat Mech: Theory Exp 2016:023209

Russell EV, Israeloff N (2000) Nature 408:695

Russo J, Tanaka H (2015) Proc Natl Acad Sci 112:6920

Sagun L, Guney VU, Arous GB, LeCun YA (2014) arXiv preprint arXiv:1412.6615

Sausset F, Tarjus G, Viot P (2009) J Stat Mech: Theory Exp 2009:P04022

Scalliet C, Berthier L (2019) Phys Rev Lett 122:255502

Scalliet C, Berthier L, Zamponi F (2017) Phys Rev Lett 119:205501

Scalliet C, Berthier L, Zamponi F (2019a) Phys Rev E 99: 012107

Scalliet C, Berthier L, Zamponi F (2019b) Nat Commun 10:1

Scheidler P, Kob W, Binder K, Parisi G (2002) Philos Mag B 82:283

Schoenholz SS (2018) In: Journal of Physics: conference series, vol 1036. IOP Publishing, p 012021

Schoenholz SS, Cubuk ED, Sussman DM, Kaxiras E, Liu AJ (2015) Nat Phys 12:469

Schoenholz SS, Cubuk ED, Kaxiras E, Liu AJ (2016) Proc Natl Acad Sci 114:263

Schreck CF, Bertrand T, OHern CS, Shattuck M (2011) Phys Rev Lett 107:078301

Seif A, Grigera TS (2016) arXiv preprint arXiv:1611.06754

Sepúlveda A, Tylinski M, Guiseppi-Elie A, Richert R, Ediger M (2014) Phys Rev Lett 113:045901

Sethna JP, Shore JD, Huang M (1991) Phys Rev B 44:4943

Seyboldt R, Merger D, Coupette F, Siebenbürger M, Ballauff M, Wilhelm M, Fuchs M (2016) Soft Matter 12:8825

Sharp TA, Thomas SL, Cubuk ED, Schoenholz SS, Srolovitz DJ, Liu AJ (2018) Proc Natl Acad Sci 115:10943

Shi R, Tanaka H (2019) Sci Adv 5:eaav3194

Skoge M, Donev A, Stillinger FH, Torquato S (2006) Phys Rev E 74:041127

Sollich P (1998) Phys Rev E 58:738

Sollich P, Lequeux F, Hébraud P, Cates ME (1997) Phys Rev Lett 78:2020

Speck T (2019) J Stat Mech: Theory Exp 2019:084015

Stariolo DA, Cugliandolo LF (2019) EPL (Europhys Lett) 127:16002

Stevenson JD, Walczak AM, Hall RW, Wolynes PG (2008) J Chem Phys 129:194505

Struik L (1977) Polym Eng Sci 17:165

Swallen SF, Kearns KL, Mapes MK, Kim YS, McMahon RJ, Ediger MD, Wu T, Yu L, Satija S (2007) Science 315:353

Szamel G (2018) Phys Rev E 98. https://doi.org/10.1103/Phys-RevE.98.050601

Szamel G, Flenner E (2004) EPL (Europhys Lett) 67:779

Szamel G, Flenner E (2013) EPL (Europhys Lett) 101:66005

Talbot J, Tarjus G, Viot P (2003) J Phys A Math Gen 36:9009

Tarjus G, Kivelson D (1995) J Chem Phys 103:3071. https://doi.org/10.1063/1.470495

Tarjus G, Kivelson SA, Nussinov Z, Viot P (2005) J Phys Condens Matter 17:R1143

Tarzia M, Biroli G, Lefèvre A, Bouchaud J-P (2010) J Chem Phys 132:054501

Thalmann F, Dasgupta C, Feinberg D (2000) EPL (Europhys Lett) 50:54

Theurkauff I, Cottin-Bizonne C, Palacci J, Ybert C, Bocquet L (2012) Phys Rev Lett 108:268303

Tong H, Tanaka H (2018) Phys Rev X 8. https://doi.org/10.1103/PhysRevX.8.011041

Toninelli C, Biroli G, Fisher DS (2004) Phys Rev Lett 92:185504

Toninelli C, Wyart M, Berthier L, Biroli G, Bouchaud J-P (2005) Phys Rev E 71:041505

Toninelli C, Biroli G, Fisher DS (2006) Phys Rev Lett 96:035702

Turci F, Tarjus G, Royall CP (2017a) Phys Rev Lett 118:1

Turci F, Royall CP, Speck T (2017b) Phys Rev X 7. https://doi.org/10.1103/PhysRevX.7.031028

Turci F, Speck T, Royall CP (2018) Eur Phys J E 41. https://doi.org/10.1140/epje/i2018-11662-3

Turci F, Patrick Royall C, Speck T (2019) J Phys Conf Ser 1252:012012

Turner RM, Jack RL, Garrahan JP (2015) Phys Rev E 92. https://doi.org/10.1103/PhysRevE.92.022115

Turner CJ, Michailidis AA, Abanin DA, Serbyn M, Papić Z (2018) Nat Phys 14:745

Urbani P, Zamponi F (2017) Phys Rev Lett 118:038001

van Hemmen J, Morgenstern I (1987) In: Lecture notes in physics, vol 275. Springer, Berlin

van Meel JA, Charbonneau B, Fortini A, Charbonneau P (2009) Phys Rev E 80:061110

Vest J-P, Tarjus G, Viot P (2014) Mol Phys 112:1330

Vest J-P, Tarjus G, Viot P (2015) J Chem Phys 143:084505

Vila-Costa A, Ràfols-Ribé J, González-Silveira M, Lopeandia A, Abad-Muñoz L, Rodríguez-Viejo J (2020) Phys Rev Lett 124:076002

Wang P, Song C, Makse HA (2006) Nat Phys 2:526

Wang L, Ninarello A, Guan P, Berthier L, Szamel G, Flenner E (2019a) Nat Commun 10:1

Wang L, Berthier L, Flenner E, Guan P, Szamel G (2019b) Soft Matter 15:7018

Weeks ER, Crocker JC, Levitt AC, Schofield A, Weitz DA (2000) Science 287:627

Weeks ER, Crocker JC, Weitz DA (2007) J Phys Condens Matter 19:205131

Whitelam S, Garrahan JP (2004) J Phys Chem B 108:6611

Whitelam S, Berthier L, Garrahan JP (2004) Phys Rev Lett 92:185705

Whitelam S, Berthier L, Garrahan JP (2005) Phys Rev E 71:026128

Widmer-Cooper A, Harrowell P (2006) Phys Rev Lett 96:185701

Williams I, Turci F, Hallett JE, Crowther P, Cammarota C, Biroli G, Royall CP (2018) J Phys Condens Matter 30:094003

Wolynes PG (2009) Proc Natl Acad Sci

Wolynes PG, Lubchenko V (2012) Structural glasses and supercooled liquids: theory, experiment, and applications. Wiley

Wuttke J, Petry W, Pouget S (1996) J Chem Phys 105:5177

Wyart M (2010) EPL (Europhys Lett) 89:64001

Wyart M (2012) Phys Rev Lett 109:125502

Wyart M, Cates ME (2017) Phys Rev Lett 119. https://doi.org/10.1103/PhysRevLett.119.195501

Wyart M, Nagel SR, Witten TA (2005) EPL (Europhys Lett) 72:486

Xia X, Wolynes PG (2000) Proc Natl Acad Sci 97:2990. tex.eprint: https://www.pnas.org/content/97/7/2990.full.pdf. tex.publisher: National Academy of Sciences

Yaida S, Berthier L, Charbonneau P, Tarjus G (2016) Phys Rev E 94. https://doi.org/10.1103/Phys-RevE.94.032605

Yamamoto R, Onuki A (1998) Phys Rev E 58:3515

Yeo J, Moore M (2012) Phys Rev E 86:052501

Yoshino H, Zamponi F (2014) Phys Rev E 90:022302

Young AP (1998) Spin glasses and random fields, vol 12. World Scientific

Zdeborová L, Krzakala F (2016) Adv Phys 65:453

Zhu L, Brian C, Swallen S, Straus P, Ediger M, Yu L (2011) Phys Rev Lett 106:256103